

UNCLASSIFIED

SECURITY CLASSIFICATION OF THIS PAGE (When Data Entered)

REPORT DOCUMENTATION PAGE		READ INSTRUCTIONS BEFORE COMPLETING FORM	
1. REPORT NUMBER ONR CR 168-007-1	2. GOVT ACCESSION NO.	3. RECIPIENT'S CATALOG NUMBER	
4. TITLE AND SUBTITLE AN EVALUATION OF DIRECT CURRENT ELECTROMAGNETIC PROPULSION IN SEAWATER,		5. STATE OF REPORT & PERIOD COVERED Final Report, Jan-May 1979,	
6. AUTHOR George T. Hummert		7. PERFORMING ORG. REPORT NUMBER 79-9B2-EMSUB-R1	
8. PERFORMING ORGANIZATION NAME AND ADDRESS Westinghouse Electric Corporation R&D Center, 1310 Beulah Road Pittsburgh, PA 15235		9. CONTRACT OR GRANT NUMBER(s) N00014-78-C-0667/ New	
10. CONTROLLING OFFICE NAME AND ADDRESS Office of Naval Research 800 North Quincy St. Arlington, VA 22217		11. PROGRAM ELEMENT, PROJECT, TASK AREA & WORK UNIT NUMBERS 62332N, RF32-391-801, NR168-007	
12. MONITORING AGENCY NAME & ADDRESS (if different from Controlling Office) DCAFMA, Pittsburgh 1610-S-Federal Bldg, 1000 Liberty Avenue Pittsburgh, PA 15222		13. REPORT DATE August, 1979	
14. DISTRIBUTION STATEMENT (of this Report) Approved for public release; distribution unlimited.		15. NUMBER OF PAGES 73	
16. DISTRIBUTION STATEMENT (of the abstract entered in Block 20 - if different from Report) 16 F37311		17. SECURITY CLASS (of this report) Unclassified	
18. SUPPLEMENTARY NOTES 17 RF32312101		19. DECLASSIFICATION DOWNGRADING SCHEDULE	
20. KEY WORDS (Continue on reverse side if necessary and identify by block number) propulsion, electromagnetic, thrust, submarines, submersible, seawater, conductivity, drag, direct, currents			
21. ABSTRACT (Continue on reverse side if necessary and identify by block number) Electromagnetic seawater thrusters may be classified in one of three general categories: internal duct dc, external field dc, and peristaltic ac. Inter- nal duct dc thruster offers the advantages of low magnetic field leakage, simple construction, and potentially high reliability. The most efficient internal duct configuration consists of a converging inlet nozzle and a straight discharge duct. Ideal efficiency calculations based on the one- dimensional Bernoulli equation show that thrusters should be designed with			

DD FORM 1 JAN 73 1473

EDITION OF 1 NOV 65 IS OBSOLETE

UNCLASSIFIED

SECURITY CLASSIFICATION OF THIS PAGE (When Data Entered)

UNCLASSIFIED

SECURITY CLASSIFICATION OF

PAGE (When Data Entered)

Block 20 Continued:

→ large cross-sectional areas and operate at low discharge velocities. In practice, this may be accomplished by using multiple thruster ducts. Conductivity enhancement, high magnetic fields, and long electrodes also improve efficiency.

While the magnetic field-volume requirements for thruster capable of propelling full-size (2000 ton displacement) submarines appears beyond the present technology, it may be feasible to use superconducting magnets to build high efficiency, internal duct thruster capable of maneuvering small (<10 ton displacement) submersibles. ←

277-1-\*

Accession For	
N113 GRA&I	
L-113	
Unprocessed	
Justification	
By	
Distribution	
Availability	
Dist.	Available for special
A	

UNCLASSIFIED

SECURITY CLASSIFICATION OF THIS PAGE (When Data Entered)

AN EVALUATION OF DIRECT CURRENT ELECTROMAGNETIC  
PROPULSION IN SEAWATER

G. T. Hummert  
Electrotechnology Department

ABSTRACT

Electromagnetic seawater thrusters may be classified in one of three general categories: internal duct dc; external field dc, and peristaltic ac. Internal duct dc thrusters offer the advantages of low magnetic field leakage, simple construction, and potentially high reliability. The most efficient internal duct configuration consists of a converging inlet nozzle and a straight discharge duct. Ideal efficiency calculations based on the one-dimensional Bernoulli equation show that thrusters should be designed with large cross-sectional areas and operate at low discharge velocities. In practice, this may be accomplished by using multiple thruster ducts. Conductivity enhancement, high magnetic fields, and long electrodes also improve efficiency.

While the magnetic field-volume requirements for thruster capable of propelling full-size (2000 ton displacement) submarines appears beyond the present technology, it may be feasible to use superconducting magnets to build high efficiency, internal duct thruster capable of maneuvering small (~10 ton displacement) submersibles.

## TABLE OF CONTENTS

	Page
ABSTRACT . . . . .	1
NOMENCLATURE . . . . .	111
1.0 INTRODUCTION . . . . .	1
2.0 CONCLUSIONS AND RECOMMENDATIONS . . . . .	3
3.0 BACKGROUND . . . . .	5
3.1 General Description . . . . .	5
3.2 Performance Calculations . . . . .	6
3.2.1 Measure of Performance . . . . .	7
3.2.2 Parameter Specification . . . . .	7
3.2.3 Range of Parameter Variation . . . . .	8
4.0 THRUSTER PERFORMANCE CALCULATIONS . . . . .	10
4.1 Thruster Model . . . . .	10
4.2 Assumptions . . . . .	11
4.3 Thruster Performance Equations . . . . .	12
4.3.1 Thrust and Velocity Relationships . . . . .	12
4.3.2 Pressure Relationships . . . . .	13
4.3.3 Electromagnetic Pressure . . . . .	14
4.3.4 Voltage and Current . . . . .	15
4.3.5 Efficiency . . . . .	15
4.3.6 Multiple Duct Performance . . . . .	17
4.4 Efficiency Plots . . . . .	19
4.5 Conductivity Enhancement: HCL Seeding . . . . .	19
4.6 Sensitivity of Efficiency to Magnetic Field Strength . . . . .	20
4.7 Power Requirements vs. Speed . . . . .	21
4.8 Efficiency as a Function of Interaction Parameter . . . . .	21
4.9 Performance as a Function of Aspect Ratio . . . . .	22
5.0 GAS EVOLUTION THROUGH ELECTROLYSIS . . . . .	23
6.0 PRELIMINARY DESIGN PROCEDURE . . . . .	24
REFERENCES . . . . .	26
APPENDIX A-1: Submersible Hull and Thruster Drag . . . . .	61
APPENDIX A-2: Electromagnetic Coupling to Conducting-Fluid Flow . . . . .	66
APPENDIX A-3: Computer Program Listing and Sample Print-Out . . . . .	68

# NOMENCLATURE

$K_s$	$= C_D A_s \rho / 2 = \text{constant of proportionality: } D = K_s v_s^2 \text{ (Nt / (m/s)}^2)$
$v_s$	$= \text{relative velocity between submerged body and water (m/s)}$
$v_{out}$	$= \text{discharge velocity (m/s)}$
$v_p$	$= \text{velocity in pumping region of duct (m/s)}$
$C_D$	$= \text{drag coefficient (dimensionless)}$
$v_p$	$= \text{velocity in pumping region of duct (m/s)}$
$A_s$	$= \text{effective drag cross-sectional area (m}^2)$
$\rho$	$= \text{density of water (kg/m}^3)$
$\sigma$	$= \text{electrical conductivity of water (mho/m)}$
$D$	$= \text{drag (newtons)}$
$T$	$= \text{thrust (newtons)}$
$J$	$= \text{duct electrical current density (amp/m}^2)$
$I$	$= \text{duct electrical current (amps)}$
$V$	$= \text{duct voltage (volts)}$
$L$	$= \text{electrode length (meters)}$
$B$	$= \text{duct magnetic field (tesla)}$
$b$	$= \text{one-half electrode spacing (m)}$
$a$	$= \text{one-half duct width along B-field direction (m)}$
$\alpha$	$= \text{aspect ratio} = b/a \text{ (dimensionless)}$
$A_p$	$= 4ab = \text{cross-sectional area of duct in pumping region (m}^2)$
$A_{out}$	$= \text{cross-sectional area of discharge (m}^2)$
$A_c$	$= \text{cross-sectional area of inlet cone}$



- $\dot{m}$  = mass flow rate thru duct (kg/s)
- $\eta$  =  $Tv_s/IV$  = efficiency (dimensionless)
- $k_1$  = derived parameter =  $v_p/v_s$  (dimensionless)
- $P_o$  = free-stream pressure ( $Nt/m^2$ )
- $P_z$  = nozzle pressure ( $Nt/m^2$ )
- $P_{in}$  = pressure at pump inlet ( $Nt/m^2$ )
- $\Delta P_z$  =  $P_z - P_o$  = pressure drop through nozzle ( $Nt/m^2$ )
- $\Delta P_{in}$  =  $P_o - P_{in}$  = inlet pressure drop ( $Nt/m^2$ )
- $\Delta P_p$  =  $P_z - P_{in}$  = pump head ( $Nt/m^2$ )
- $f$  = factor appearing in voltage, current and efficiency expressions (dimensionless)
- $N$  = interaction parameter (dimensionless)
- $W_f$  = fluid power (watts)
- $\eta_p$  = propulsive efficiency (dimensionless)
- $\eta_e$  = electrical efficiency (dimensionless)
- $\epsilon$  =  $v_p/v_s$  (dimensionless)

## 1.0 INTRODUCTION

This study was undertaken to investigate the practicality of internal duct, direct current electromagnetic propulsion of submersible ocean vessels, ranging from full size submarines down to small maneuverable underwater platforms. The scope of this study is limited to a broad overview of performance characteristics rather than detailed design considerations: the emphasis here is on rapid assessment of trade-offs between major design parameters, such as magnetic field intensity, electrode length and duct size. Performance and efficiency calculations do not, therefore, include minor hydrodynamic and magnetohydrodynamic (MHD) effects, and the resulting curves should be used for general comparisons and trade-off analyses. These curves, for instance, enable the reader to quickly determine overall thrust efficiency as a function of duct area, magnetic field strength, electrode length, and multiple ducting. This information is presented for each of three submersible classes: full, one-third, and one-tenth sizes corresponding to hull diameters of about 10, 3, and 1 meters, respectively.\* The assumed drag characteristics for these three sizes are given in Fig. 1.

As will be shown later, overall performance is a strong function of the magnetic field intensity, and the magnitude of field used for the performance curves given here ranges from conventional (0.5 T) to superconducting (5 T) excitation sources. The impact of conductivity enhancement via seeding with hydrochloric acid (HCl) is also presented along with estimates of the volume of evolved gases released by electrolysis at the electrode surfaces. Finally, duct dimensions are restricted to reasonable ranges of engineering capability, limited by the volume requirements for the magnetic field. It does not seem reasonable, for instance, to consider a thruster design that requires 10 Tesla (super-

---

\* See Appendix A-1 for a discussion of hull size, shape, displacement, and drag.

conducting excitation) throughout a duct interior of several hundred cubic meters. Duct dimensions, therefore, range from two to ten meters long and up to one square meter of cross-sectional area.



## 2.0 CONCLUSIONS AND RECOMMENDATIONS

Electromagnetic thrusters offer a silent, nearly undetectable means of submersible propulsion. Based upon efficiency calculations included in this study though, it seems unlikely that a practical thruster system could be developed for a full size (2000 ton, 10 m hull diameter) submarine. The chief reason for this conclusion lies in the difficulty of establishing high magnetic field intensities throughout the active pumping region contained between the electrodes. A reasonably efficient thruster cannot be designed and built until a superconducting dewar/winding capable of functioning reliably in a submersible environment has been demonstrated. Once this has been achieved, then efficiencies of ten percent or more may be possible for reduced hull sizes of one to three meters diameter, provided that speed is limited to approximately ten knots or less. It may be feasible to use electromagnetic propulsion for maneuvering small submersible platforms requiring either modest continuous thrust or occasional bursts of high thrust levels.

In general, efficiency may be improved by:

- minimizing thrust requirements.....small hulls operating at low velocities.
- using large areas, low velocity thrusters.....multiple thrust-ducts are the most practical way of achieving this objective without requiring excessive cross-sectional area per duct.
- operating at high magnetic fields.....preferably at field intensities much greater than that of conventional iron-copper magnetic circuits--hence, superconducting excitation is mandated.
- enhancing conductivity.....seeding seawater with a strong electrolyte such as hydrochloric acid has a pronounced

effect upon overall efficiency. The rate and duration of seeding is limited, of course, by on-board storage capacity.

Development of an electromagnetic thruster should proceed in several stages:

- Define the mission requirements -- range, speed, depth, hull drag, power source, and acceptable levels of magnetic leakage.
- Demonstrate the capability of establishing a high-intensity ( $\sim 5$  Tesla) magnetic field throughout a significant duct volume. This requires design and fabrication of a superconducting dewar/winding capable of functioning reliably in a submersible environment. One possible annular thruster configuration is shown in Figure 33 where a superconducting toroidal\* field winding establishes high fields in the pump annulus with relatively low leakage into the surrounding region.
- Construct and test a prototype thruster.
- For military applications, the possibility of detection should receive critical evaluation, and provision should be made to evaluate magnetic field leakage, hydrolysis, and chemical activity (such as pH shift due to seeding) as potential means of detection.

---

\* Large superconducting toroidal magnets have, in fact, been successfully used in radiotherapy.<sup>(9)</sup>

### 3.0 BACKGROUND

#### 3.1 General Description

Electromagnetic (EM) propulsion of sea vessels may be divided into three categories: internal duct dc; external field dc; and peristaltic ac induction. All three types of propulsion have been analyzed and discussed in the literature.<sup>(1-4)</sup> Here we present a brief description of these three.

The first type of thruster--internal duct dc--consists of electrodes mounted within a propulsion duct such that current (in the conducting fluid) established between the electrodes is perpendicular to a magnetic field established within the same region, but perpendicular to the direction of current flow. (See Fig. 2 for a pictorial diagram.) Interaction of current and magnetic field produces a mutually perpendicular pressure gradient or force directed along the duct axis. If the duct is open at either end, this gradient causes fluid flow and, hence, an axial reaction thrust. While in principle electromagnetic propulsion may be achieved quite easily by passing current between two electrodes located within a magnetic field, in practice the low value of electrical conductivity of seawater places a severe constraint on overall thrust efficiency that may be achieved.

The second type of thruster--external dc field--does not utilize thrust ducts. Instead, exterior electrodes are mounted along the hull and an external magnetic field is established such that interaction of electrode current and field produces external pressure gradients along the submersible's centerline, thereby creating propulsive thrust. Once again, though, the low conductivity of seawater limits ultimate thrust efficiency. A useful system requires superconducting excitation that establishes high magnetic fields throughout large volumes of water:

however, not only are such superconducting magnets expensive and difficult to build, but the resulting unshielded, easily detectible fields are most likely not suitable for military applications.

Finally, the third type of electromagnetic thruster--peristaltic ac induction--utilizes a flexible membrane to separate two fluid regions: one, an annular chamber containing a highly conducting fluid such as liquid metal; the other an inner cylindrical chamber open to the surrounding water. Radial ac magnetic fields induce circumferential ac currents in the outer (highly-conducting) annular chamber and these currents interacting with the induction fields generate pressure waves that impart axial motion to the conducting liquid. This, in turn, distorts the flexible membrane, thereby imparting axial motion to the water core. In short, traveling waves along the membrane squeeze the inner core, squirting water axially, thereby generating reaction thrust. While peristaltic induction may offer attractive efficiency and performance characteristics due to the high conductivity of the enclosed fluid (liquid metal), it does pose significant reliability and safety problems: the efficient liquid metals react chemically with most engineering materials--including water.

In summary, while all three types of electromagnetic propulsion pose significant technical problems, the internal duct design is simpler and probably more reliable than the others, and this work was commissioned specifically for a study of internal duct dc propulsion.

### 3.2 Performance Calculations

This section deals with specific items relating to performance evaluation, namely:

- choosing a primary measure of performance;
- separating the various interrelated parameters into dependent and independent variables;
- defining ranges of independent parameter variation.

### 3.2.1 Measure of Performance

Since many interrelated parameters enter into the performance calculations, we must decide upon the key or fundamental relationships that we wish to examine: ultimately, what are we interested in comparing? Useful thrust vs. input power at a fixed cruising speed? Or, cruising range vs. stored energy as a function of hull size? Or, maximum speed vs. electrode size as a function of magnetic field?

As mentioned earlier, internal duct E-M thrusters have an inherently low power conversion efficiency, and this is perhaps a most crucial measure of performance. Most of the results obtained in this study, therefore, are given in terms of ideal<sup>\*</sup> efficiency as speed curves for several hull sizes. Additional curves show the effects of conductivity enhancement (HCl seeding) as well as magnetic field intensity upon efficiency. Finally, the last curves show overall input power and thrust power as a function of speed for several hull sizes.

### 3.2.2 Parameter Specification

Clearly, we are not able to choose independent values for each of the interdependent parameters that influence performance. If, for example, we specify electrode voltage and current, then for a given duct size, the thrust requirement (hull drag) determines magnetic field intensity as a function of speed: all of these quantities cannot be selected independently. Mathematically, we cannot exceed the degrees of freedom that exist between the performance equations.

Our approach, therefore, has been to permit electrode voltage and current to remain unspecified--they are dependent variables whose values are determined as a consequence of other parameter selections. Since dc electrical power sources may be configured to match or nearly

---

<sup>\*</sup> Ideal in that electrolysis and hydrodynamic thruster losses are not included (see Sections 4.2, 4.9, and A-1). Magnetic excitation losses, either in terms of ohmic power dissipation (conventional magnet) or refrigeration power (superconducting magnet) are also not included in these calculations.



match most power requirements (e.g., 10 volts at 200 amps or 200 volts at 10 amps), this is a reasonably prudent engineering approach.\*

The following parameters are treated as independent variables and must be specified:

- magnetic field
- electrode length
- cross-sectional area of duct
- number of ducts
- fluid conductivity

### 3.2.3 Range of Parameter Variation

Lastly, the ranges of variation must be specified, and here again we are guided by practical engineering limitations rather than theoretical speculation. All five of the independent variables listed above are related in the sense that choosing one places practical constraints on the others. An extremely high, uniform magnetic field, for instance, cannot be established throughout a large volume. Duct dimensions must reflect this: we cannot seriously discuss duct lengths of hundreds of meters, nor can we consider cross-sectional areas greater than one or two square meters. The following ranges, therefore, were defined and specific calculations made for various combinations of these values:

<u>Variable</u>	<u>Range</u>
● Duct Area .....	0.25, 0.5, 1 square meters
● Electrode Length .....	2, 10 meters
● Magnetic Field .....	0.5, 2, 5 Tesla (2 to 5 T implies superconducting excitation)

---

\* It should be noted, however, that designing an actual thruster system may require several iterations wherein the thruster performance equations first determine an approximate power source; then actual power source terminal characteristics - such as would be available from various combinations of, say, submarine batteries - could be used for design modifications. An important part of this iteration would be variations in the aspect ratio, as discussed later in Section 4.9.



- Number of Ducts ..... 1, 4, 9, 16 (Each of the multiple ducts has the same cross-sectional area and electrode length. That is, one duct is not subdivided into multiple channels such that the total thrust area remains constant, but rather the total duct area increases by factors of 4, 9, and 16.)
- Conductivity ..... 4 mhos, the nominal conductivity of seawater. The effects of seeding with HCL were calculated by doubling the conductivity to 8 mhos. This corresponds to a 0.5% by weight solution of HCL.

#### 4.0 THRUSTER PERFORMANCE CALCULATIONS

##### 4.1 Thruster Model

Water-jet thrusters work on the principle of momentum conservation: an increase in stream momentum from intake to discharge produces a net reaction thrust. As shown in the pictorial sketch of Fig. 2, the electromagnetic thruster is composed of three sections: 1) converging inlet nozzle; 2) electrode-magnetic field region; 3) converging discharge nozzle. Definitions of the electrode (or pumping) region dimensions are also given in Fig. 2.

The converging inlet nozzle provides a smooth transition from the free-stream region immediately ahead of the intake to the internal pumping region, and if we assume that at a fixed uniform cruising speed,  $v_s^*$ , the inlet area is just large enough to provide the volumetric flow required, then no power will be expended drawing water into the inlet from ahead of the inlet plane. Matching the converging inlet opening to cruising speed also has the advantage of minimizing the thruster's displacement drag in that incident flow is directed into the duct, rather than around it.

The electrode or active pumping region consists of parallel electrodes mounted along the channel walls with a magnetic field established normal to the current-flow direction. The rectangular cross-sectional area,  $A_p$ , is assumed to be constant throughout the electrode region.

The third and last section of the thruster is the converging nozzle, which directs flow from the pumping region to a discharge orifice.

---

\* See Nomenclature for symbol definitions.

#### 4.2 Assumptions

In the calculations that follow, the following assumptions have been invoked unless otherwise noted:

- Thrust = velocity-squared drag

The thrust required to maintain a fixed speed is equal to total drag. Total hull drag, we assume, may be described by one equivalent drag coefficient that includes both frictional and displacement components. Total drag is then proportional to velocity squared times the cross-sectional area (see Fig. 1 for curves of drag vs. speed. Also see Appendix 1 for a comparison with more accurate drag calculations).

- Negligible thruster drag

Based upon a thruster design that utilizes a converging inlet nozzle, this is a reasonable assumption (see Appendix 1 for details).

- Negligible electrode-electrolysis losses (electrolysis voltage  $\ll$  pump voltage). The validity of this assumption depends to a large extent upon the aspect ratio, see Section 4.9.

- Nozzle inlet velocity = relative velocity between submersible and surrounding water

- Absence of cavitation within the inlet nozzle

A convergent inlet nozzle forces a static pressure drop with respect to the inlet or free stream pressure. Assuming no cavitation is equivalent to assuming that the submersible depth is great enough such that the absolute pressure at the pump inlet ( $P_{in}$ ) is greater than the vapor pressure of water (several psia).

### 4.3 Thruster Performance Equations

#### 4.3.1 Thrust and Velocity Relationships

(See Fig. 2 and the Nomenclature for symbol definitions.)

From the conservation of momentum, we have

$$\text{thrust} = \text{outlet momentum} - \text{inlet momentum}$$

or

$$T = \dot{m}(v_{\text{out}} - v_{\text{in}}) \quad (1)$$

where the main flow,  $\dot{m}$ , is given by

$$\dot{m} = \rho v_p A_p = \rho v_s A_{\text{in}} = \rho v_{\text{out}} A_{\text{out}} \quad (2)$$

Combining these two equations, we can express thrust as

$$T = \dot{m} v_p \left( \frac{A_p}{A_{\text{out}}} - \frac{v_s}{v_p} \right) = \rho A_p v_p^2 \left( \frac{A_p}{A_{\text{out}}} - \frac{v_s}{v_p} \right) \quad (3)$$

But thrust developed by the duct is equal to the submersible's drag force

$$D = (C_D A_s \rho / 2) v_s^2 = K_s v_s^2 \quad (4)$$

or

$$T = K_s v_s^2 \quad (5)$$

where  $K_s = C_D A_s \rho / 2$

Combining Eqs. (3) and (5), we get for  $k_1$  the ratio of internal duct velocity to inlet velocity

$$k_1 = \frac{v_p}{v_s} = \frac{A_{out}}{2A_p} \left\{ 1 + (1 + 4K_s / \rho A_{out})^{1/2} \right\} \quad (6)$$

Also, note that from Eq. (2),  $v_p A_p = v_s A_{in}$ , so that  $k_1 = A_{in}/A_p$  = ratio of inlet area to area of pumping region.

#### 4.3.2 Pressure Relationships (neglecting hydrodynamic losses)

##### Inlet

Applying the Bernoulli Equation, we have

$$P_o + 1/2 \rho v_s^2 = P_{in} + 1/2 \rho v_p^2 \quad (7)$$

Rearranging and using the pressure differential  $\Delta P_{in}$  yields

$$\Delta P_{in} = P_o - P_{in} = 1/2 \rho (v_p^2 - v_s^2)$$

or

$$\Delta P_{in} = 1/2 \rho v_p^2 (1 - (v_s/v_p)^2) \quad (8)$$

##### Exit Nozzle

Again, applying the Bernoulli Equation we have

$$P_z + 1/2 \rho v_p^2 = P_o + 1/2 \rho v_{out}^2 \quad (9)$$

then the nozzle pressure drop is

$$\Delta P_z = P_z - P_o = 1/2 \rho (v_{out}^2 - v_p^2)$$

or using Eq. (2) to express  $v_{out}$  in terms of  $v_p$ , we get

$$\Delta P_z = 1/2 \rho v_p^2 \left[ \left( \frac{A_p}{A_{out}} \right)^2 - 1 \right] \quad (10)$$

Pump

$$\text{pump head} = \Delta P_p = P_z - P_{in} = \Delta P_z + \Delta P_{in} \quad (11)$$

Substituting from Eqs. (8) and (10):

$$\Delta P_p = 1/2 \rho v_p^2 \left[ \left( \frac{A_p}{A_{out}} \right)^2 - \left( \frac{v_s}{v_p} \right)^2 \right] \quad (12)$$

But from Eq. (6),  $v_p = k_1 v_s$  and we can express the pump head in terms of the relative velocity,  $v_s$ :

$$\Delta P_p = 1/2 \rho v_s^2 \left[ k_1^2 \left( \frac{A_p}{A_{out}} \right)^2 - 1 \right] \quad (13)$$

This is the pump head or pressure differential that must be generated electromagnetically in order to sustain the relative velocity  $v_s$ . If the pump pressure satisfies this requirement, then thrust = drag at speed  $v_s$ .

#### 4.3.3 Electromagnetic Pressure

Neglecting electric and magnetic fringe effects near the electrode edges, we have:\*

$$\Delta P_p = JBL = \sigma BL \left( \frac{v}{2b} - v_p B \right) \quad (14)$$

---

\* See Appendix A-2 for a derivation of this equation.



#### 4.3.4 Voltage and Current

Substituting for  $\Delta P_p$  from Eq. (13) and solving for the electrode voltage,  $V$ , we get

$$V = \frac{\rho v_s^2 b f}{\sigma B L} + 2 B v_s k_1 b \quad (15)$$

where  $f = [(k_1 A_p / A_{out})^2 - 1]$ .

Now we can use Eqs. (13), (14), and (15) to solve for the current density,  $J$ , and hence the total current,  $I$  ( $= 2aIJ$ ):

$$I = 2aL\sigma \left( \frac{V}{2b} - v_p B \right)$$

$$I = \frac{a \rho v_s^2}{B} ((k_1 A_p / A_{out})^2 - 1)$$

or

$$I = a \rho v_s^2 f / B \quad (16)$$

where  $f$  is the dimensionless parameter given above.

#### 4.3.5 Efficiency

Pumping efficiency,  $\eta$ , is the ratio of thrust power to electrical input power

$$\eta = T v_s / IV \quad (17)$$

Substituting from Eqs. (5), (15), and (16), we have

$$\eta = 2K_s / [A_p \rho f k_1 (f / (2k_1^2 N) + 1)] \quad (18)$$

where again  $f = [(k_1 A_p / A_{out})^2 - 1]$  and we introduce the interaction parameter  $N$ , a measure of the interaction between electromagnetic and inertial body forces in the fluid, defined as

$$N = 0.5^2 L^2 v_p \quad (19)$$

Efficiency may also be expressed in terms of the propulsive and electrical efficiencies, which are defined, respectively, as

$$\eta_p = \frac{Tv}{W_f} \quad (20)$$

$$\eta_e = \frac{W_f}{I \cdot V} \quad (21)$$

where the fluid power,  $W_f = v_p \Delta P_p A_p$ .

Substituting from the previous expressions for these quantities, we have

$$\eta = \eta_p \cdot \eta_e \quad (22)$$

with

$$\eta_p = \frac{2}{k_1 A_p / A_{out} + 1} \quad (23)$$

$$\eta_e = \left[ 1 + \frac{1}{2N} \left( \frac{A_p}{A_{out}} \right)^2 - \frac{1}{k_1^2} \right]^{-1} \quad (24)$$

From Eq. (24) we note that efficiency increases as the nozzle discharge area  $A_{out}$  approaches the pump area,  $A_p$ . To maximize overall efficiency, then, we set  $A_{out} = A_p$ . This corresponds to the maximum cross-sectional discharge area consistent with no nozzle cavitation, and the governing equations become:

•• Velocity ratio:

$$k_1 \frac{v_p}{v_{gs}} = \frac{A_p}{A_p} \frac{A_n}{A_p} = (1/2) [1 + (1 + 4K_s / \rho A_p)^{1/2}] \quad (25)$$

- Electrode voltage:

$$V = 2Bv_s k_1 b (f/(2k_1^2 N) + 1) \quad (26)$$

where  $f = (k_1^2 - 1)$  and

$N$  = interaction parameter defined above.

- Electrode current:

$$I = a \rho v_s^2 f/B \quad (27)$$

- Efficiency:

$$\eta_p = 2/(k_1 + 1) \quad (28)$$

$$\eta_e = [1 + \frac{1}{2N} (1 - k_1^{-2})]^{-1}$$

where overall efficiency  $\eta = \eta_p \cdot \eta_e$ .

Equations (25) through (28) provide a basis for evaluating performance of a single duct propulsion system.

#### 4.3.6 Multiple Duct Performance

The single duct equations may be adapted to multiple duct analysis simply by altering the thrust coefficient,  $K_s$ . Let  $K'_s = K_s/n$  = thrust requirement for each of  $n$  ducts. Then we get the following multiple duct relationships:

- per duct velocity coefficient:

$$k'_1 = v'_p/v_s = (1/2) [1 + (1 + 4K'_s/\rho A'_p)^{1/2}] \quad (6')$$

where  $A'_p$  = area per duct

- electrode voltage:

$$V' = 2Bv_s k_1' b' (f' / (2k_1'^2 \cdot N') + 1) \quad (26')$$

$$\text{where } f' = k_1'^2 - 1, N' = \sigma B^2 L / \rho v_p'$$

- electrode current:

$$I' = a' \rho v_s^2 f' / B \quad (27')$$

- efficiency:

$$\eta' = [2 / (k_1' + 1)] \cdot [1 + (2N')^{-1} (1 + k_1'^{-2})]^{-1} \quad (28')$$

Suppose, then, that we compare the performance of  $n$  parallel ducts to a single duct where the combined parallel duct pumping area is equal to that of the single duct (that is,  $A_p' = A_p / \sqrt{n}$ ,  $a' = a / \sqrt{n}$ ,  $b' = b / \sqrt{n}$ ) then:

$$k_1' = k_1, f' = f, N' = N$$

$$I' = I / \sqrt{n}, V' = V \sqrt{n}$$

$$\eta' = \eta$$

And we see that there is no change in efficiency. If, however, we retain the same area per duct, but add  $n$  parallel ducts ( $A_p' = A_p$ ,  $a' = a$ ,  $b' = b$ ) then the velocity ratio  $k_1'$  is given by:

$$k_1' = (1/2) [1 + (1 + 4K_s / \rho n A_p)^{1/2}] \quad (29)$$

In this case,  $k_1' < k_1$ , due to the " $n$ " factor appearing in the denominator. Also, we find  $f' < f$  and  $N' > N$ . Substituting these inequalities into Eq. (28'), we find that the multiple duct efficiency increases ( $\eta' > \eta$ ). Thus, increasing the total thrust area by adding

parallel ducts decreases the inlet-to-pump velocity ratio and increases efficiency.

#### 4.4 Efficiency Plots

Efficiency plots based upon Eq. (28') are given in Figs. 3 to 26, where calculated, ideal efficiencies (based upon the assumptions discussed earlier) are plotted as a function of submersible velocity,  $v_s$ . Each plot contains a set of curves obtained using drag characteristics for three hull sizes, as given in Fig. 1. For each hull size, single duct efficiency is plotted along with several curves showing the effect of four, nine, and sixteen multiple ducts. The figures are arranged in three groups of eight, each group corresponding to ascending magnetic field intensities of 0.5, 2, and 5 Tesla, respectively. Within each group, electrode lengths of 2 and 10 meters are combined with duct areas of .25, .5, .75 and 1.0 square meters. As may be seen from the curves, efficiencies vary from less than .01 to over 99 percent. It must be emphasized that these plots are useful for comparing and indicating sensitivity of ideal performance to parameter variations--all of these combinations are not necessarily realistic. Sixteen thrusters, with a combined cross-sectional area of sixteen square meters propelling a one-meter diameter hull does not, for instance, represent a realistic configuration. But one such thruster propelling this size hull may be entirely feasible.

Not surprisingly, these plots show that efficiency improves as electrode length, magnetic field, duct area, and the number of ducts increase. Low thrust requirements due to less drag (smaller hull sizes) also improves efficiency.

#### 4.5 Conductivity Enhancement: HCl Seeding

As indicated by the performance equations derived in Section 4.3, electrical losses diminish and thrust efficiency increases as fluid conductivity increases. The conductivity of seawater, which has a

nominal value of about 4 mhos/m, increases significantly with the addition of a small percentage of hydrochloric acid (HCL). Neglecting possible increases in electrode corrosion rates, conductivity enhancement in a thruster may be accomplished by injecting HCL into the inlet nozzle where mixing and diffusion tends to create a uniform mixture prior to the electrode region. While from an efficiency consideration there is strong incentive to inject large amounts of HCL, the benefits of conductivity enhancement must be balanced against the limitations of solute storage capacity on board the submersible. As a compromise between these conflicting requirements, we have arbitrarily chosen a 0.5% solution (.14 molar concentration of HCL), which effectively doubles the bulk conductivity of seawater from 4 mhos/m to 8 mhos/m.<sup>(6)</sup> Figs. 27-29 show the effects of conductivity enhancement upon ideal efficiencies for full, third, and tenth size hulls, respectively. Note that the basic thruster-duct size ( $2 \text{ m} \times .25 \text{ m}^2$ ) is identical in all three cases, but that the number of ducts attached to each hull varies from: sixteen ducts, full-size hull; nine ducts, third-size hull; four ducts, tenth-size hull. These configurations are more representative of actual design possibilities than, say, a fixed number of ducts for all three sizes.

Seeding flow rates shown on the plots vary from 9400 gpm at 20 knots, full-size hull to 71 gpm at 2 knots, tenth-size hull. In general, efficiency increases somewhat less than the factor of two increase in conductivity.

#### 4.6 Sensitivity of Efficiency to Magnetic Field Strength

Ideal efficiencies for the three hull sizes and duct combinations (described in Section 4.5) are plotted in Fig. 30 for a fixed speed of 5 KTS and magnetic field variations from .5 to 5 Tesla. Although data for these plots are contained in the basic efficiencies curves given in Figs. 2 to 26, Fig. 30 more clearly illustrates the magnetic field dependence where an order of magnitude change in field intensity yields efficiency changes of nearly two orders of magnitude. As shown in the



figure, conventional excitation is limited to less than 2 Tesla due to saturation of ferromagnetic materials used in magnetic circuits.

#### 4.7 Power Requirements Vs. Speed

Total thrust power and electrical input power curves over a speed range of 2 to 20 knots are shown in Fig. 31 for the duct-hull combinations described in Section 4.5. These plots, which are based on a 2 T magnetic field intensity, underline the importance of low speed operation: doubling the cruising speed from 5 to 10 KTS, for instance, increases the total input power requirement by a factor of ten.

#### 4.8 Efficiency as a Function of Interaction Parameter

The electrical and propulsive efficiency expressions given by Eqs. 28 and 29 may be greatly simplified by substituting some typical values for the interaction parameter. Since the order of magnitude is determined mainly by the  $\sigma/\rho$  ratio ( $\approx 4 \cdot 10^{-4}$ ) in the expression  $N = \sigma B^2 h / \rho v_p$ , we can safely assume  $N \ll 1$ , or  $N$  is less than .01. And if the velocity ratio  $k_1$  is much greater than 1 ( $k_1 \gg 1$ ), then from Eqs. 28 and 29 the overall efficiency  $\eta < (.5) (2N)$  or  $\eta < N$ . That is, the efficiency is less than one percent. If, on the other hand, we assume  $k_1 = 1 + \epsilon$  where  $\epsilon \ll 1$  (that is, the velocity differential  $v_p - v_s \approx \epsilon v_s$ ), then

$$\eta_p' = \frac{2}{2 + \epsilon} = \frac{1}{1 + \epsilon/2} \approx 1 - \epsilon/2 \quad (30)$$

and

$$\eta_e' = \frac{1}{1 + (\epsilon/N)} \quad (31)$$

These expressions indicate that reasonable efficiencies may be achieved, provided that  $\epsilon$ , the velocity differential, is of the same order as the interaction parameter,  $N$ . This is illustrated by the curve in Fig. 32.

In addition to efficiency, though, a practical design must include other considerations such as: electrode voltage and current, and overall pump dimensions. While simply meeting the  $\epsilon = N$  criterion does not guarantee a practical design, the performance expressions discussed here do indicate the sensitivity of overall efficiency to the  $v_p/v_s$  ratio.

#### 4.9 Performance as a Function of Aspect Ratio

Although overall ideal efficiency is independent of aspect ratio, actual efficiency will depend to some extent on internal shape of the thruster ducts. This arises for two reasons:

- Viscous drag increases with wetted surface area. A square duct ( $\alpha=1$ ), therefore has minimum viscous drag. (See Appendix 1 for a detailed discussion of duct drag.)
- Electrolysis voltage remains nearly constant over a wide range of operating current densities.\* The ratio between this fixed voltage and the total electrode voltage, though, diminishes as the aspect ratio increases. That is, a duct cross section elongated in the direction of electrode separation requires a higher pump voltage and electrolysis losses become a small fraction of total electrical losses as the elongation increases.

Hence, we have two conflicting requirements, one for a unity aspect ratio in order to reduce viscous drag, the other for a high aspect ratio to minimize electrolysis losses. A careful trade-off analysis must be included in actual thruster designs.

A conventional copper-iron magnetic circuit will produce a more uniform field with reduced excitation losses as the aspect ratio increases. This, too, must be factored into the overall design.

---

\* The electrolysis potential at both the anodic and cathodic electrodes is  $\approx 2$  volts. Since this value is weakly dependent upon current density and strongly dependent on electro-chemical effects, it is realistic to assume a total electrolysis voltage of between five and ten volts.

## 5.0 GAS EVOLUTION THROUGH ELECTROLYSIS

Dissociation of water at the cathode discharges hydrogen gas along the electrode: two faradays of charge generates one mole (or 22.4 l of  $H_2$  at STP) so that:

$$Q_{H_2} = \text{hydrogen discharge rate} = 5.210^{-3} I_{kA} \text{ l/s} \quad (32)$$

This, of course, mixes with the thrust-exit stream of water and eventually bubbles to the surface. Using values for discharge flow and electrode currents associated, for example, with the full-hull size curves of Fig. 3, we have (at 20 KTS):

$$\text{thrust stream per duct} = 4.4 \times 10^3 \text{ l/s}$$

$$\text{electrode current/duct} = 104 \text{ kA}$$

then

$$Q_{H_2} = .54 \text{ l/s}$$

and we find an extremely low hydrogen-to-water volume ratio. Evolved hydrogen gas along the electrode surfaces should not hinder electrode performance, nor present a noticeable bubble or foam wake at the surface. Also, it may be possible to construct a porous electrode that captures the evolved gases. Final verification of these conclusions and possibilities must be made experimentally.

## 6.0 PRELIMINARY DESIGN PROCEDURE

Designing an electromagnetic thruster requires many iterations through the performance equations in order to balance efficiency, physical size and magnetic field intensity with desirable electrical characteristics. The following procedure is offered as a plausible design approach:

- (1) Using the known drag vs. speed requirements ( $K_s$ ) for a particular submersible and assuming a fixed number of thruster ducts of area  $A_p$ , find the velocity coefficient,  $k_1$  from Eq. 29. This determines the inlet-to-pump cross-sectional ratio ( $A_{in}/A_p$ ).
- (2) Using Eqs. 26', 27', and 28', calculate voltage, current, and efficiency at various combinations of the following parameters:
  - aspect ratio ( $\alpha$ )
  - pump length ( $L$ )
  - magnetic field ( $B$ )
  - velocity ( $v_s$ )
- (3) Repeat steps (1) and (2) over the range of interest for:
  - drag
  - cross-sectional area per thrust-duct
  - total number of thrusters

This procedure may be refined by including:

- duct drag (see Appendix A-1)
- electrolysis voltage (see Section 4.9)
- electromagnetic fringe effects
- inlet/outlet hydrodynamic losses

(These last two items should remain second order effects and are not pursued here.)

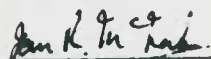
### ACKNOWLEDGMENTS

The author wishes to express his thanks to Dr. I. R. McNab for his helpful comments and notes; to Dr. S. K. Chow and Mr. E. Owen for their discussions; and to Mr. C. Alexion for his assistance in preparing computer plots as well as Appendix A-1.




G. T. Hummert  
Tribology & Magnetofluidynamics  
Electrotechnology Department

APPROVED: \_\_\_\_\_



I. R. McNab, Manager  
Tribology & Magnetofluidynamics  
Electrotechnology Department

APPROVED: \_\_\_\_\_



C. J. Mole, Manager  
Electrotechnology Department  
Chemical Sciences Division

#### REFERENCES

1. Doragh, R. A., "Magnetohydrodynamic Ship Propulsion Using Superconducting Magnets", Proc. Naval. Arch. and Marine Engineers Transactions, Vol. 71, p. 370, 1963.
2. Way, S., "Electromagnetic Propulsion for Cargo Submarines", AIAA/SNAME, Advanced Marine Vehicles Meeting, Norfolk, VA, May 22-24, 1967, AIAA Paper 67-363.
3. Neuringer, J. L., Migolsky, E., Turner, J. H., Haag, R. M., "Theoretical Investigation of a Peristaltic Magnetofluid Dynamic Induction Compressor-1", Journal of Ship Research, p. 56, March 1965.
4. Resler, E. L., "Magnetohydrodynamic Propulsion for Sea Vehicles", Seventh Symposium Naval Hydrodynamics, Rome, Italy, p. 1437, August, 1968.
5. Adamson, A. F., Lever, B. G., Stones, W. F., "The Production of Hypochlorite by Direct Electrolysis of Seawater: Electrode Materials and Design of Cells for the Process", J. App. Chemistry, Vol. 13, p. 483, 1963.
6. Weast, R. C., Ed., CRC Handbook of Chemistry and Physics, CRC Press, Inc., Cleveland, 1977, pg. D-218, 231, 252, 268.
7. Baumeister, T. and L. Marks, Standard Handbook for Mechanical Engineers, McGraw Hill Book Company, New York, 1961, pages 11/49.
8. Hughes, W. F. and Young, F. J., "The Electromagnetodynamics of Fluids", John Wiley & Sons, New York, 1966.
9. Stekly, Z. J., Lucas, E. J., Punchard, F. B., "A Large Toroidal Coil System for the Stanford Medical Pion Generator", Fifth International Conference on Magnet Technology (MT-5), Roma, Italy, April 21-25, 1975, pp. 419-423.



# COMPUTER PROGRAM

Record of Transmittal within Westinghouse

Westinghouse Research Laboratories

Date 9/19/79

\* To: Distribution List

This shipment contains:

The computer program SUBCAL  
(title)

and/or the following documents describing the above or other computer programs:

<u>Research</u> <u>No.</u>	<u>Author</u>	<u>Title</u>	<u>Proprietary</u> <u>Class</u>
79-9B2-EMSUB-R1	G. T. Hummert	An Evaluation of Direct Current Electromagnetic Propulsion in Seawater	2

If you wish to send this material outside of Westinghouse, you must obtain approval from the Supervisor, Computer Center. This approval will be in accordance with the policy set forth in Chairman's Letter No. 3 dated August 11, 1969. For purposes of this policy, the Research Laboratories considers this program to be in Class A.†  
(A, B, C, or D)

Sender G. T. Hummert  
Address 401-4C6 Phone 5717

\* One copy of this sheet must accompany every copy of the program or document transmitted outside the Research Labs. In addition, send one copy to E. J. Duckett, 801-3rd, and one to N.A. Mascia, 401-2B5.

† For definitions of classes, the sender is directed to Research Laboratories Operation Manual, Section 5.2.7. If assistance is needed, contact the Computer Center Supervisor, N.A. Mascia (WIN 236-7741).

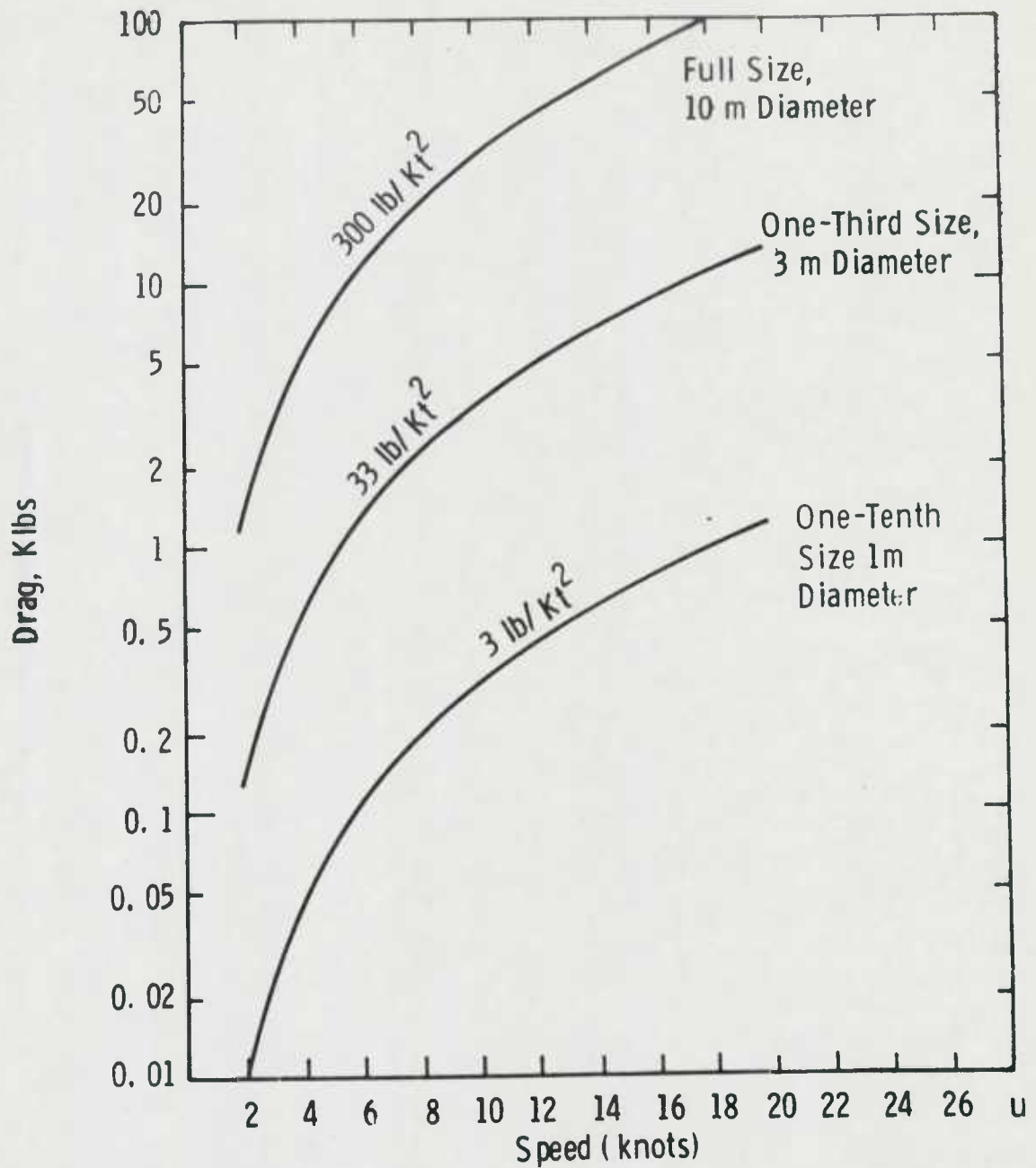


Fig. 1 — Drag characteristics used for performance calculations

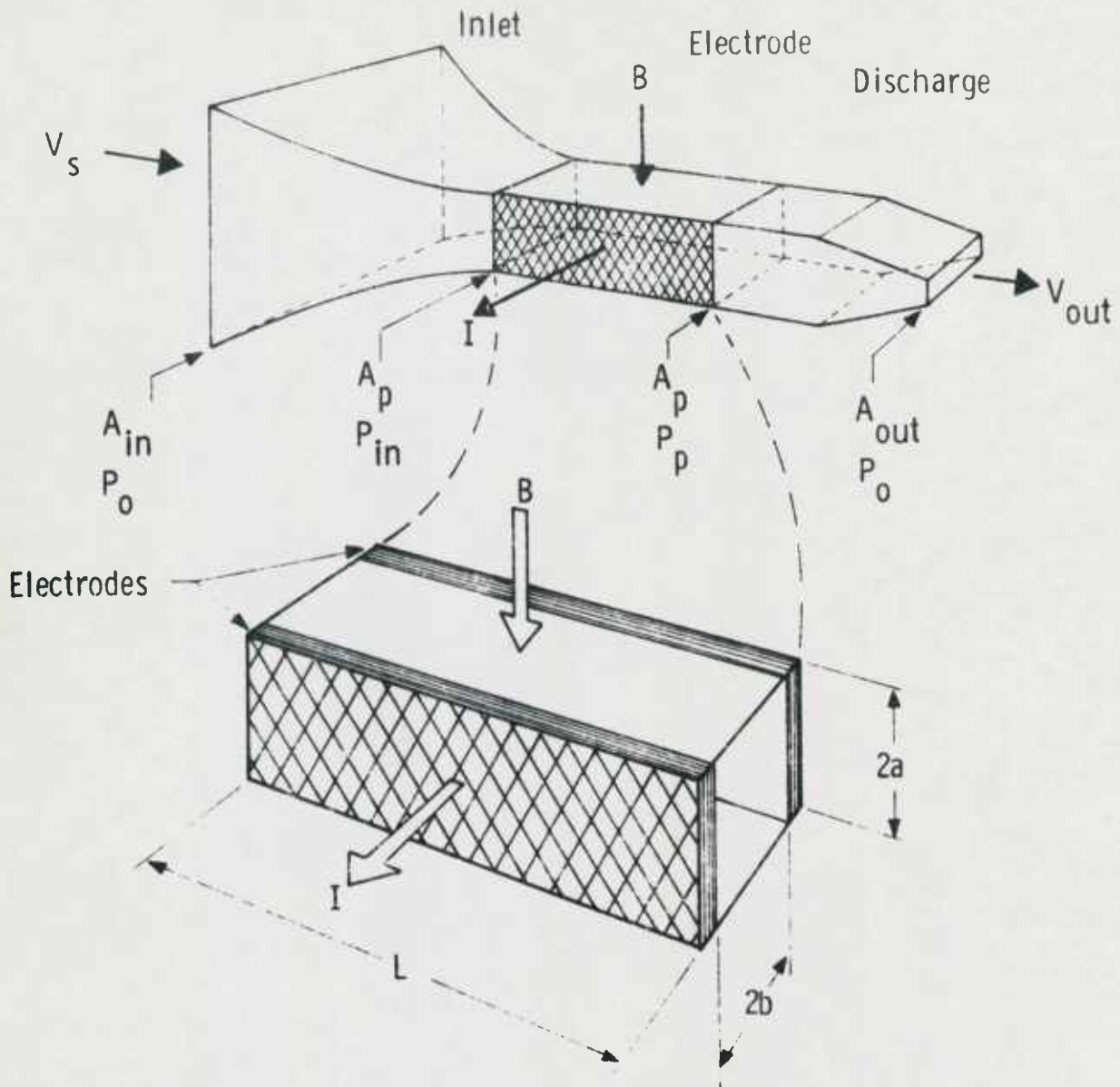


Fig. 2 — Pictorial diagram of internal duct thruster with converging inlet and outlet nozzles. Details of electrode region showing configuration used for duct analysis

FIGURE 3

# IDEAL EFFICIENCY VS SPEED SINGLE AND MULTIPLE DUCTS

MAGNETIC FIELD = 0.5 T  
EACH DUCT AREA = .25 SQ M  
ELECTRODE LENGTH = 2.0 M

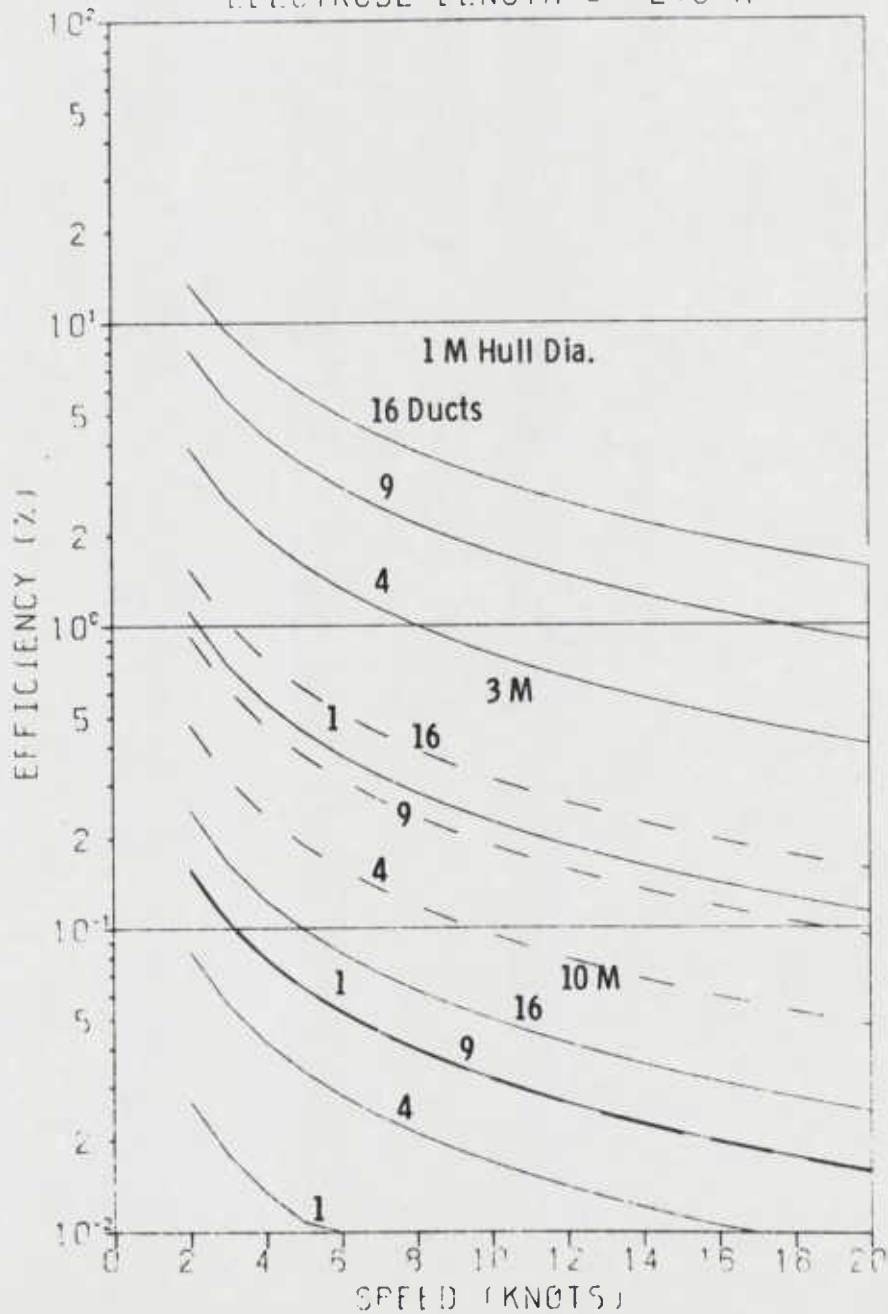


FIGURE 4

# IDEAL EFFICIENCY VS SPEED SINGLE AND MULTIPLE DUCTS

MAGNETIC FIELD = 0.5 T  
EACH DUCT AREA = .50 SQ M  
ELECTRODE LENGTH = 2.0 M

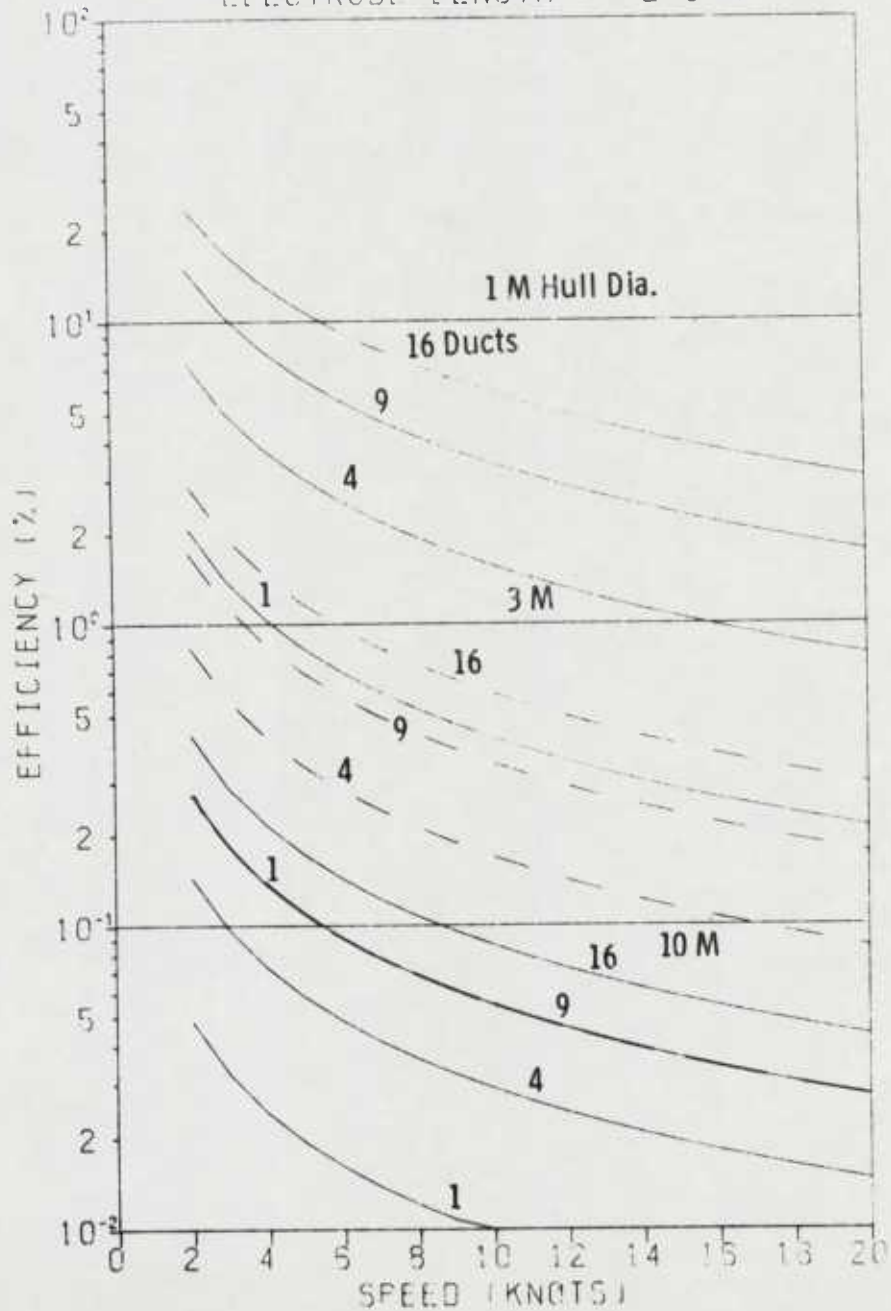


FIGURE 5

# IDEAL EFFICIENCY VS SPEED SINGLE AND MULTIPLE DUCTS

MAGNETIC FIELD = 0.5 T  
EACH DUCT AREA = .75 SQ M  
ELECTRODE LENGTH = 2.0 M

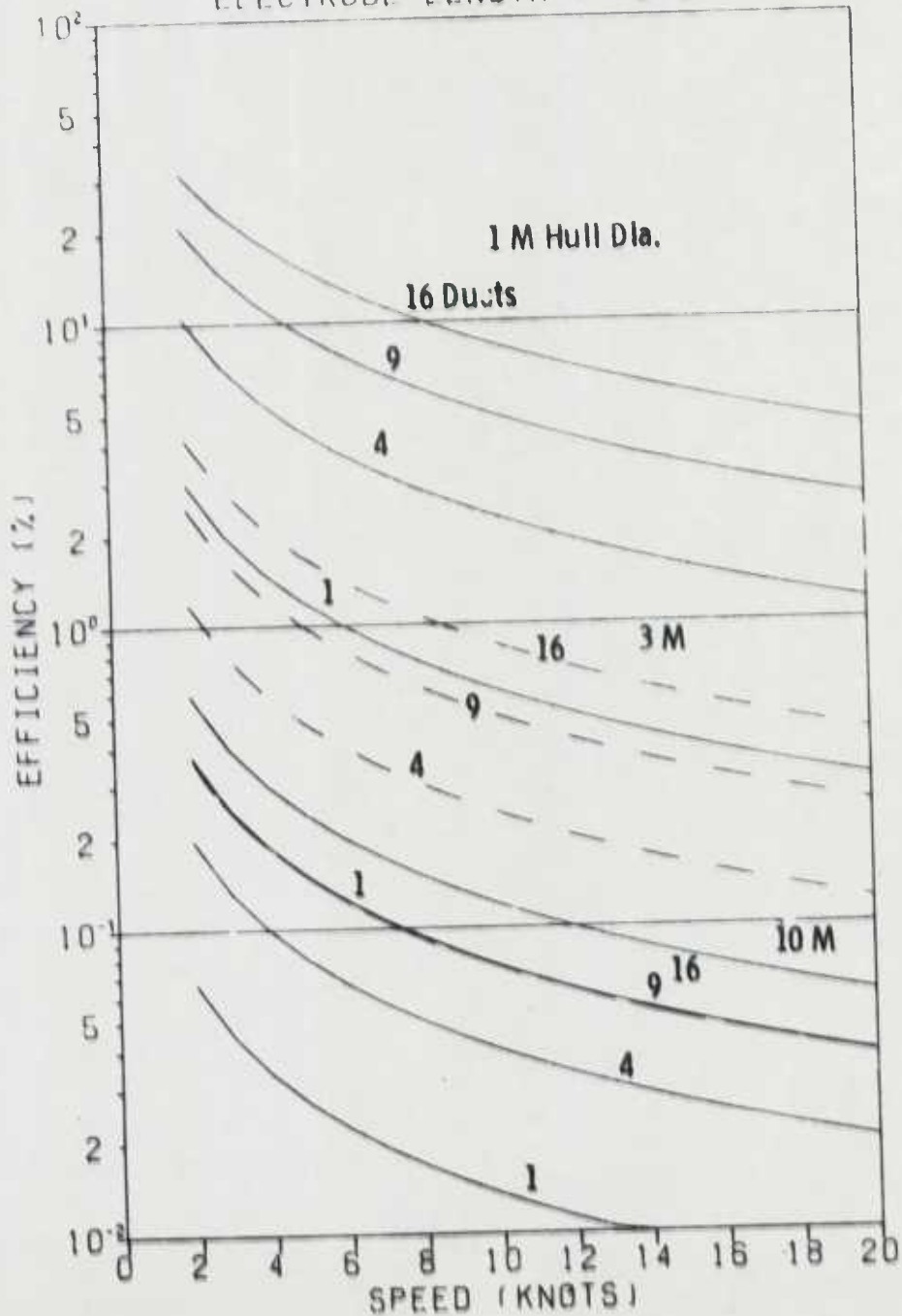




FIGURE 6

# IDEAL EFFICIENCY VS SPEED SINGLE AND MULTIPLE DUCTS

MAGNETIC FIELD = 0.5 T  
EACH DUCT AREA = 1.0 SQ M  
ELECTRODE LENGTH = 2.0 M

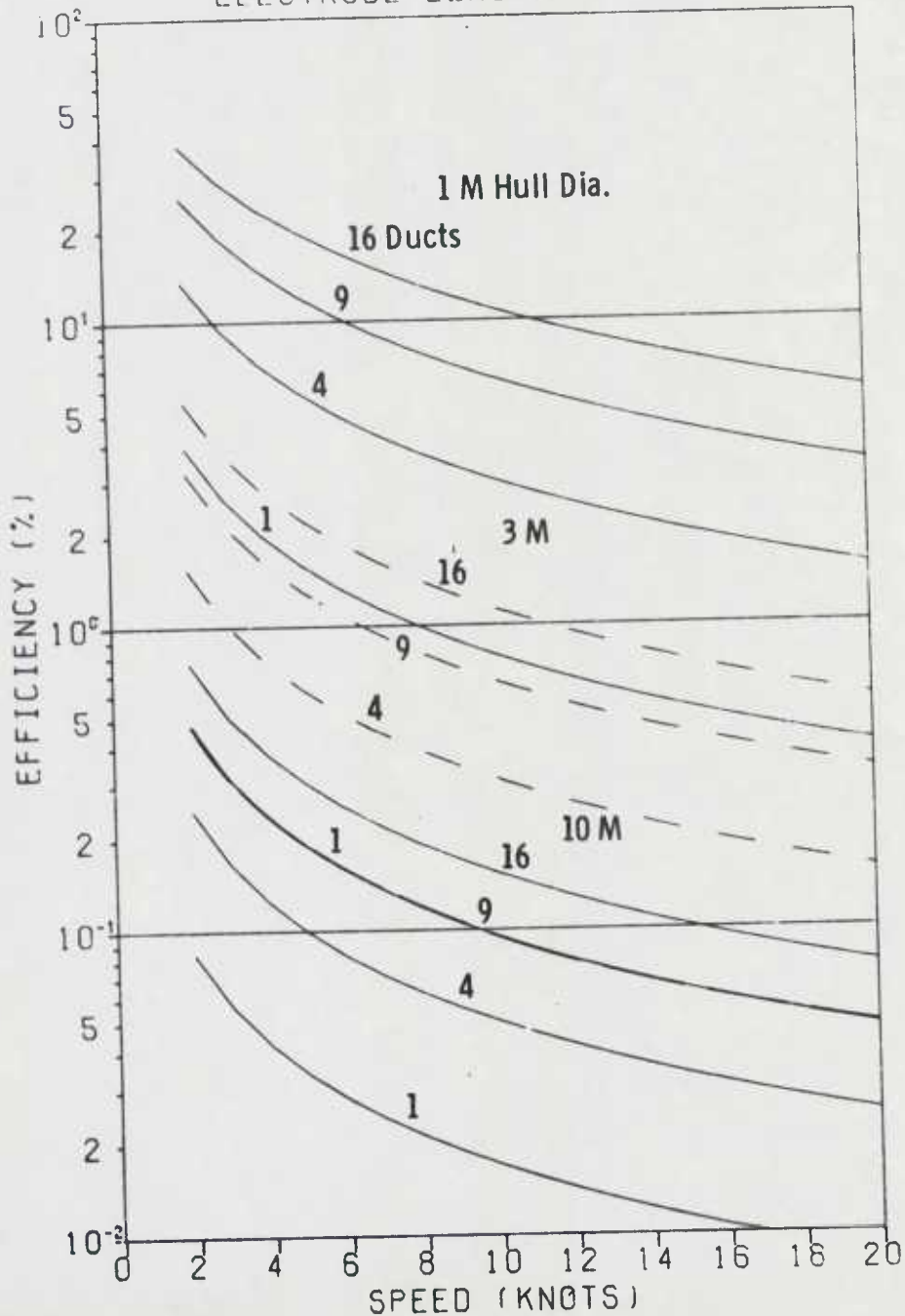


FIGURE 7

# IDEAL EFFICIENCY VS SPEED SINGLE AND MULTIPLE DUCTS

MAGNETIC FIELD = 0.5 T  
EACH DUCT AREA = .25 SQ M  
ELECTRODE LENGTH = 10.0 M

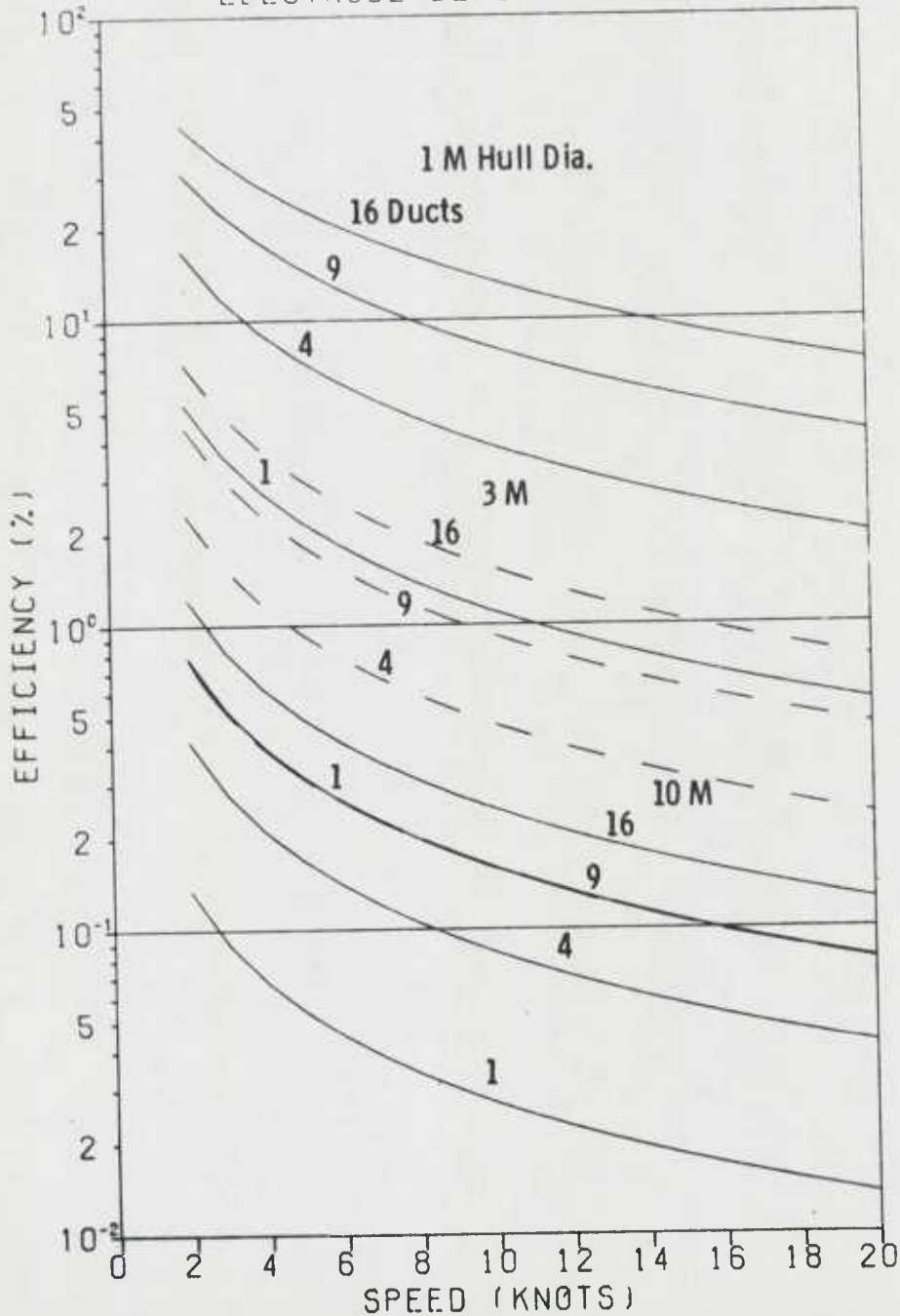


FIGURE 8

# IDEAL EFFICIENCY VS SPEED SINGLE AND MULTIPLE DUCTS

MAGNETIC FIELD = 0.5 T  
EACH DUCT AREA = .50 SQ M  
ELECTRODE LENGTH = 10.0 M

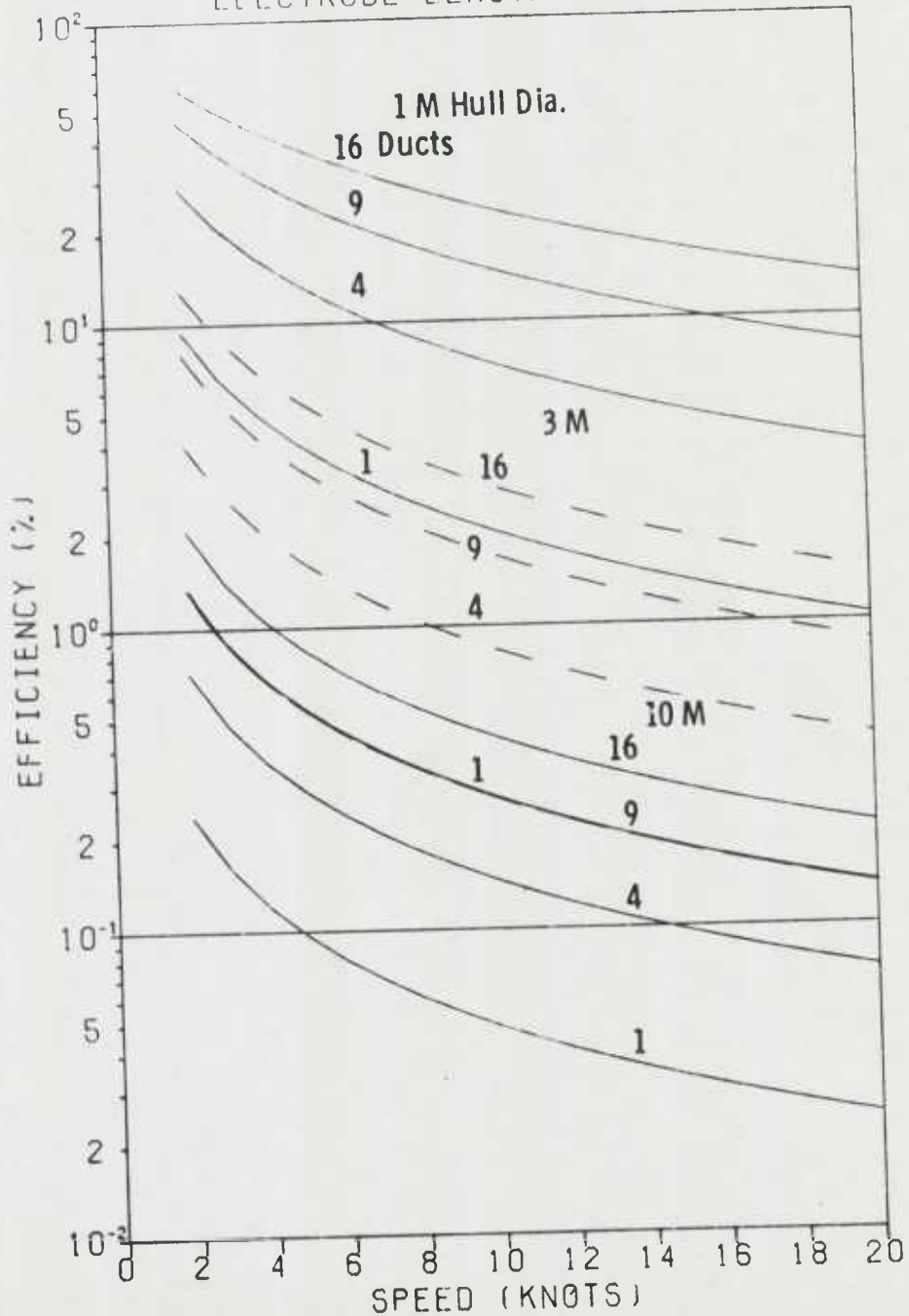


FIGURE 9

# IDEAL EFFICIENCY VS SPEED SINGLE AND MULTIPLE DUCTS

MAGNETIC FIELD = 0.5 T  
EACH DUCT AREA = .75 SQ M  
ELECTRODE LENGTH = 10.0 M

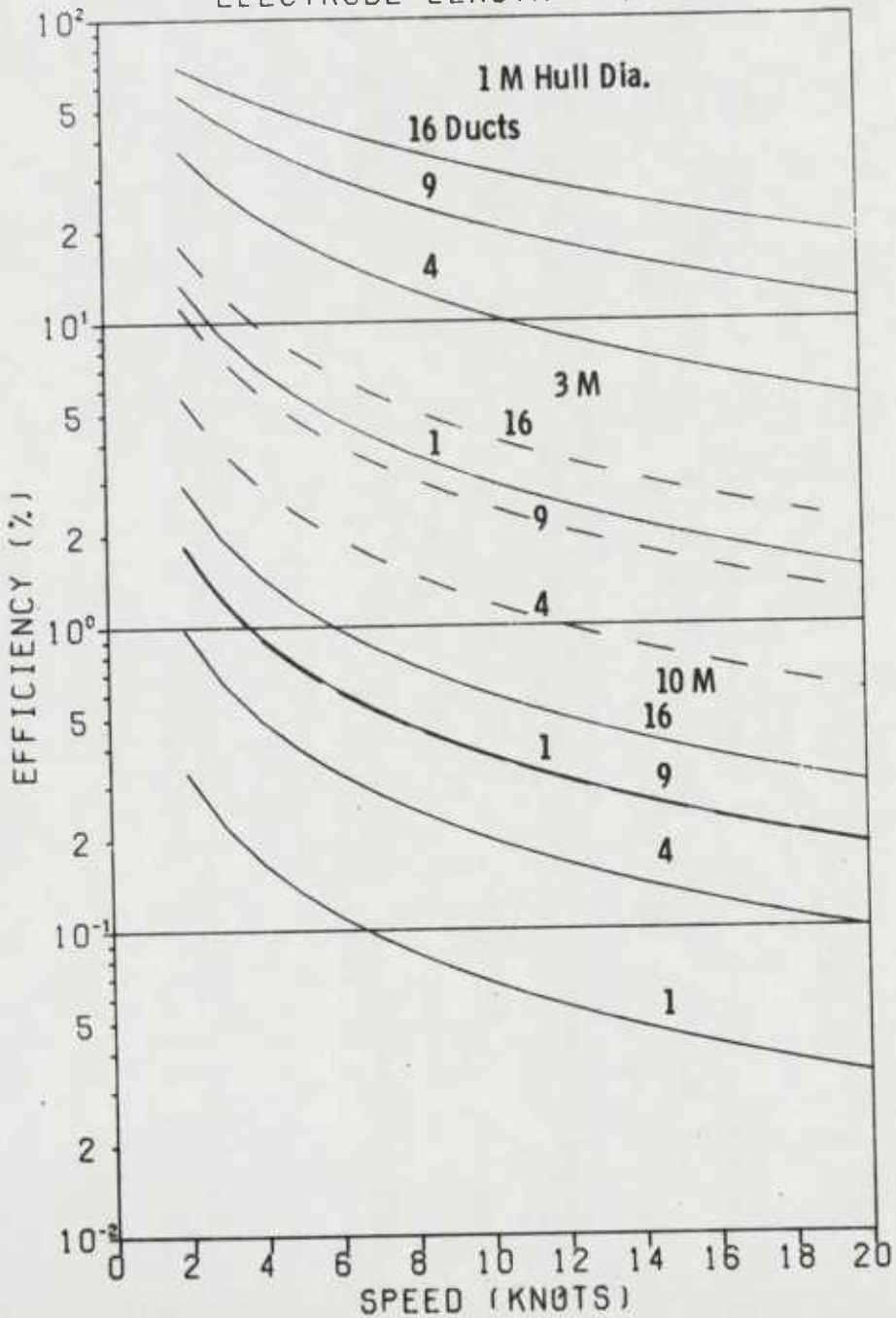


FIGURE 10

# IDEAL EFFICIENCY VS SPEED SINGLE AND MULTIPLE DUCTS

MAGNETIC FIELD = 0.5 T  
EACH DUCT AREA = 1.0 SQ M  
ELECTRODE LENGTH = 10.0 M

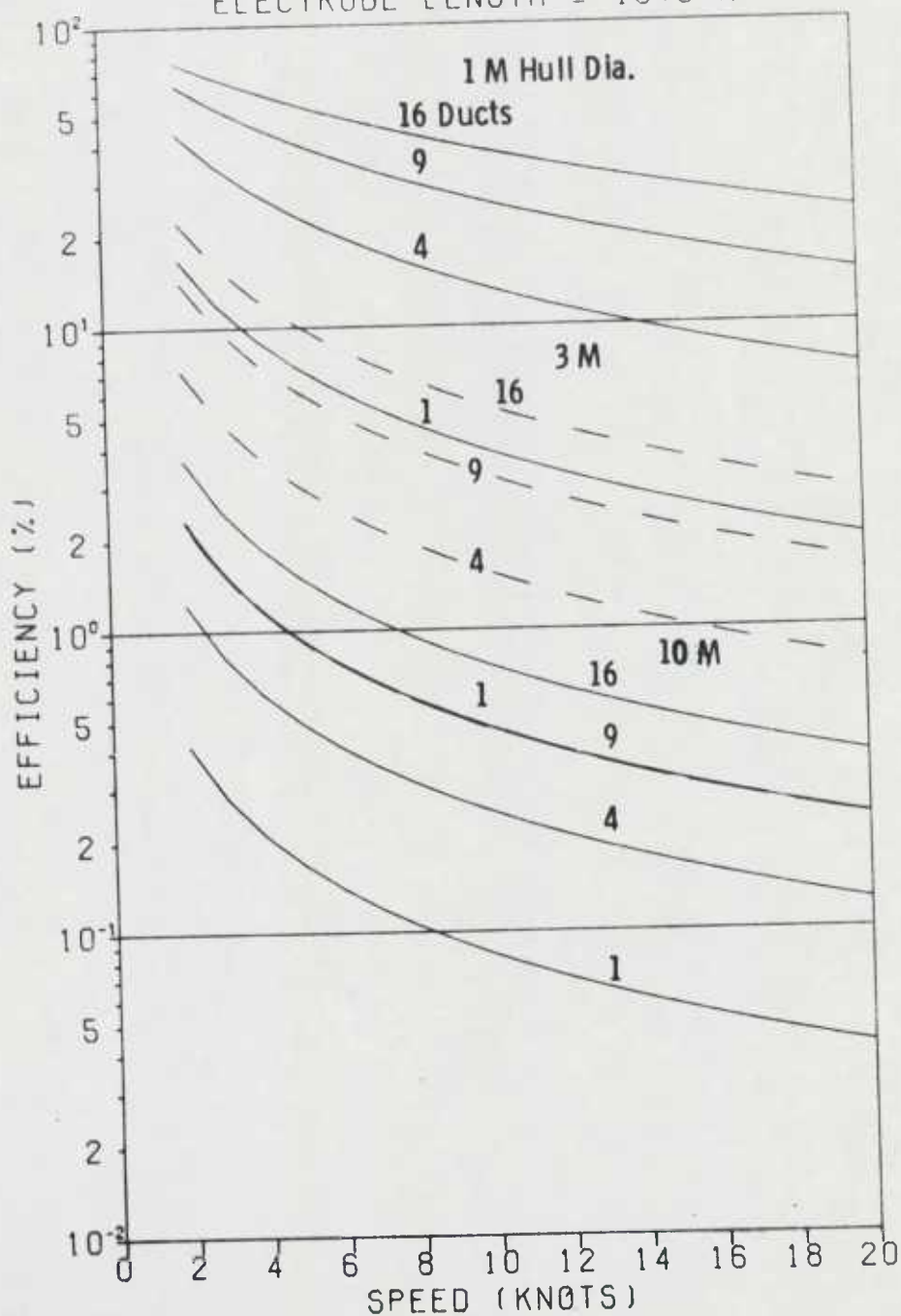


FIGURE 11

# IDEAL EFFICIENCY VS SPEED SINGLE AND MULTIPLE DUCTS

MAGNETIC FIELD = 2.0 T  
EACH DUCT AREA = .25 SQ M  
ELECTRODE LENGTH = 2.0 M

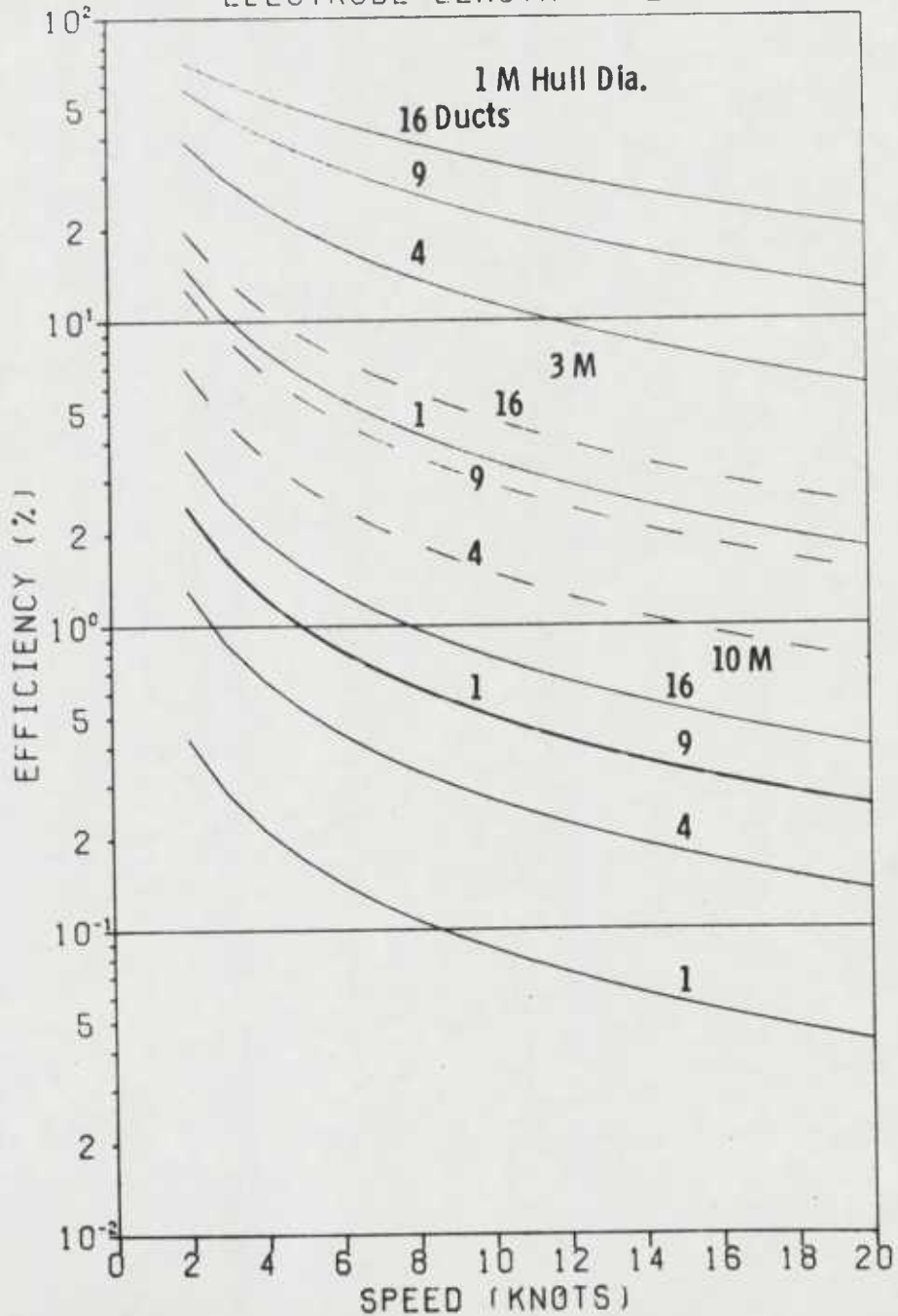




FIGURE 12

# IDEAL EFFICIENCY VS SPEED SINGLE AND MULTIPLE DUCTS

MAGNETIC FIELD = 2.0 T  
EACH DUCT AREA = .50 SQ M  
ELECTRODE LENGTH = 2.0 M

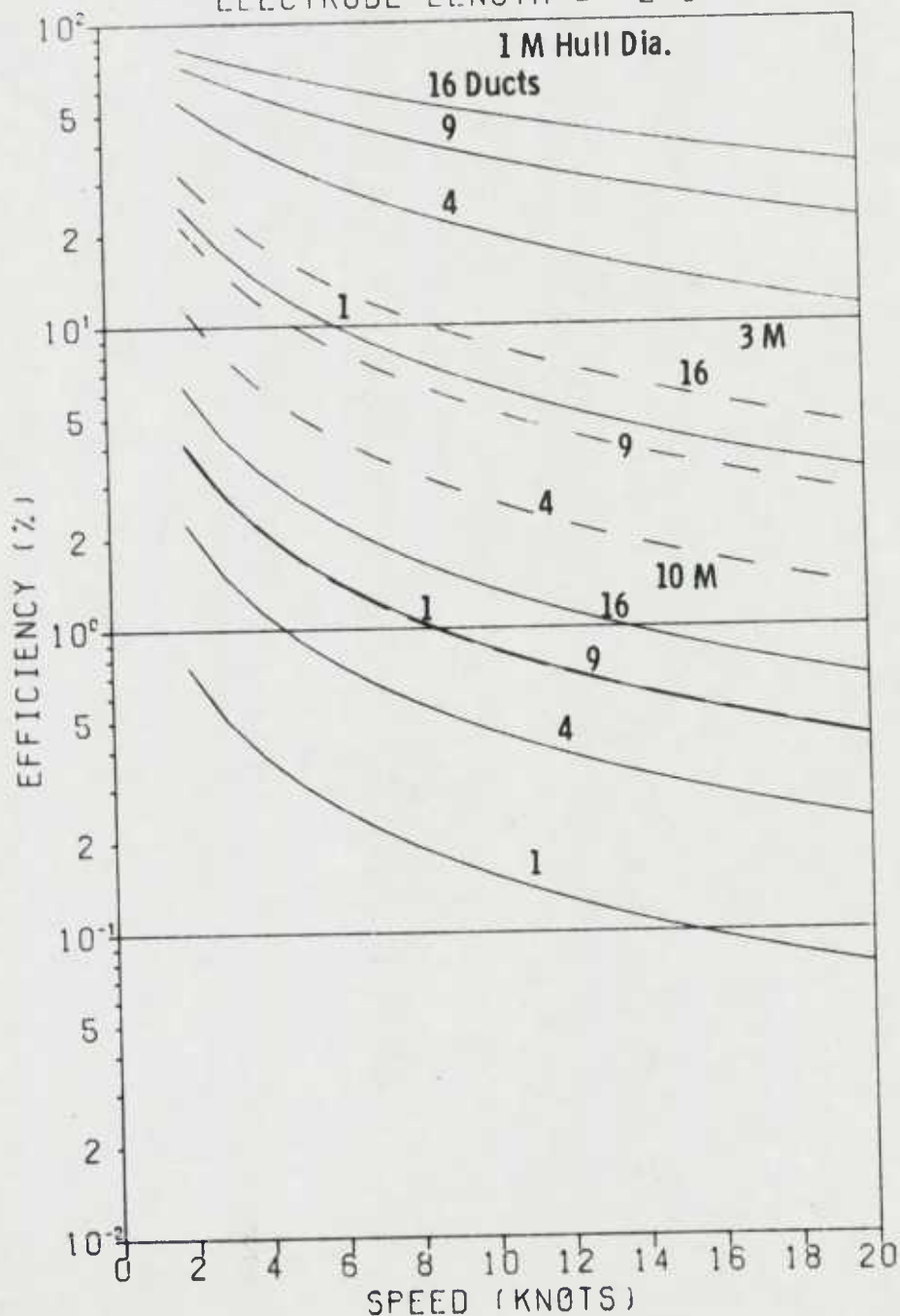


FIGURE 13

# IDEAL EFFICIENCY VS SPEED SINGLE AND MULTIPLE DUCTS

MAGNETIC FIELD = 2.0 T  
EACH DUCT AREA = .75 SQ M  
ELECTRODE LENGTH = 2.0 M

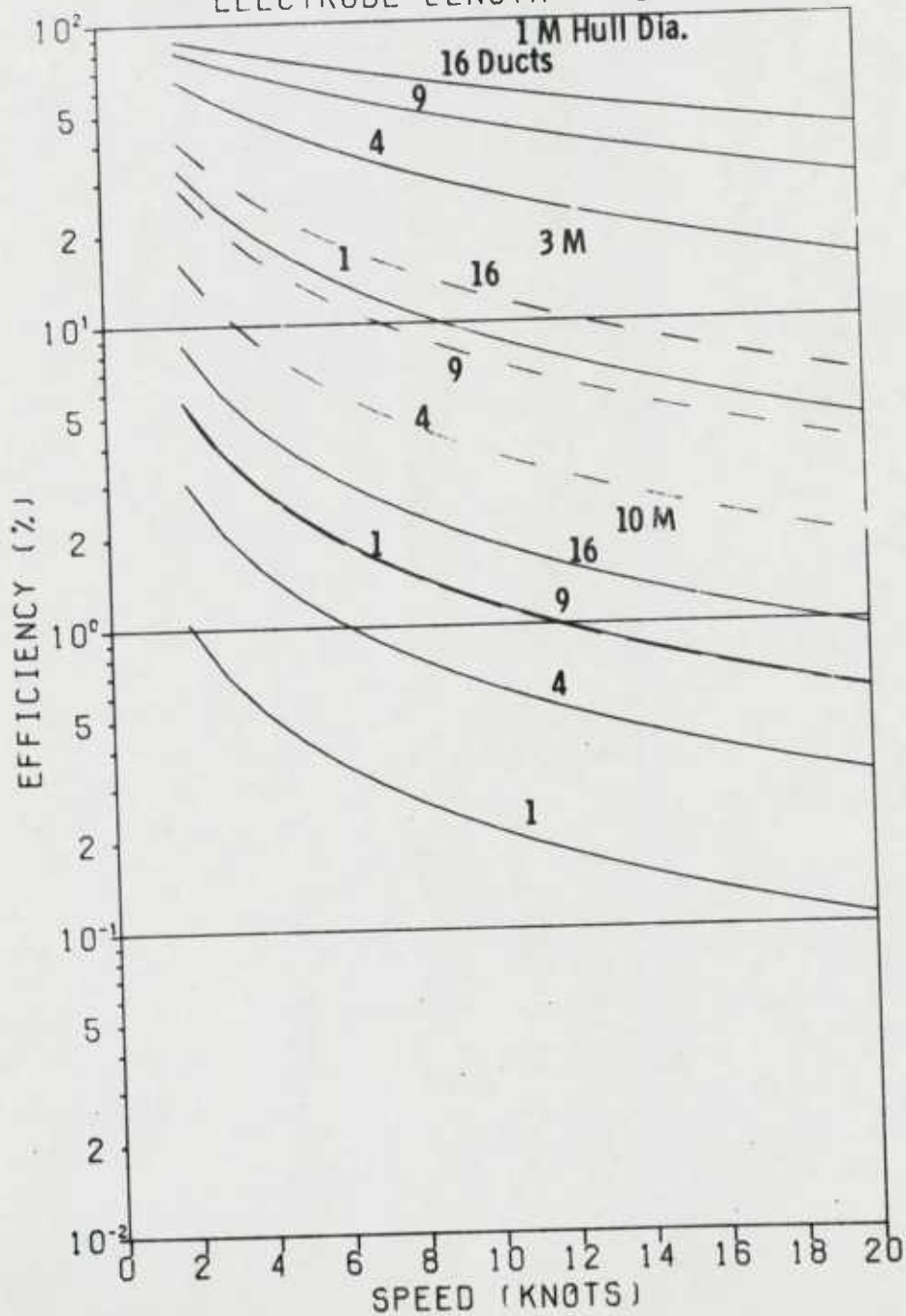


FIGURE 14

# IDEAL EFFICIENCY VS SPEED SINGLE AND MULTIPLE DUCTS

MAGNETIC FIELD = 2.0 T  
EACH DUCT AREA = 1.0 SQ M  
ELECTRODE LENGTH = 2.0 M

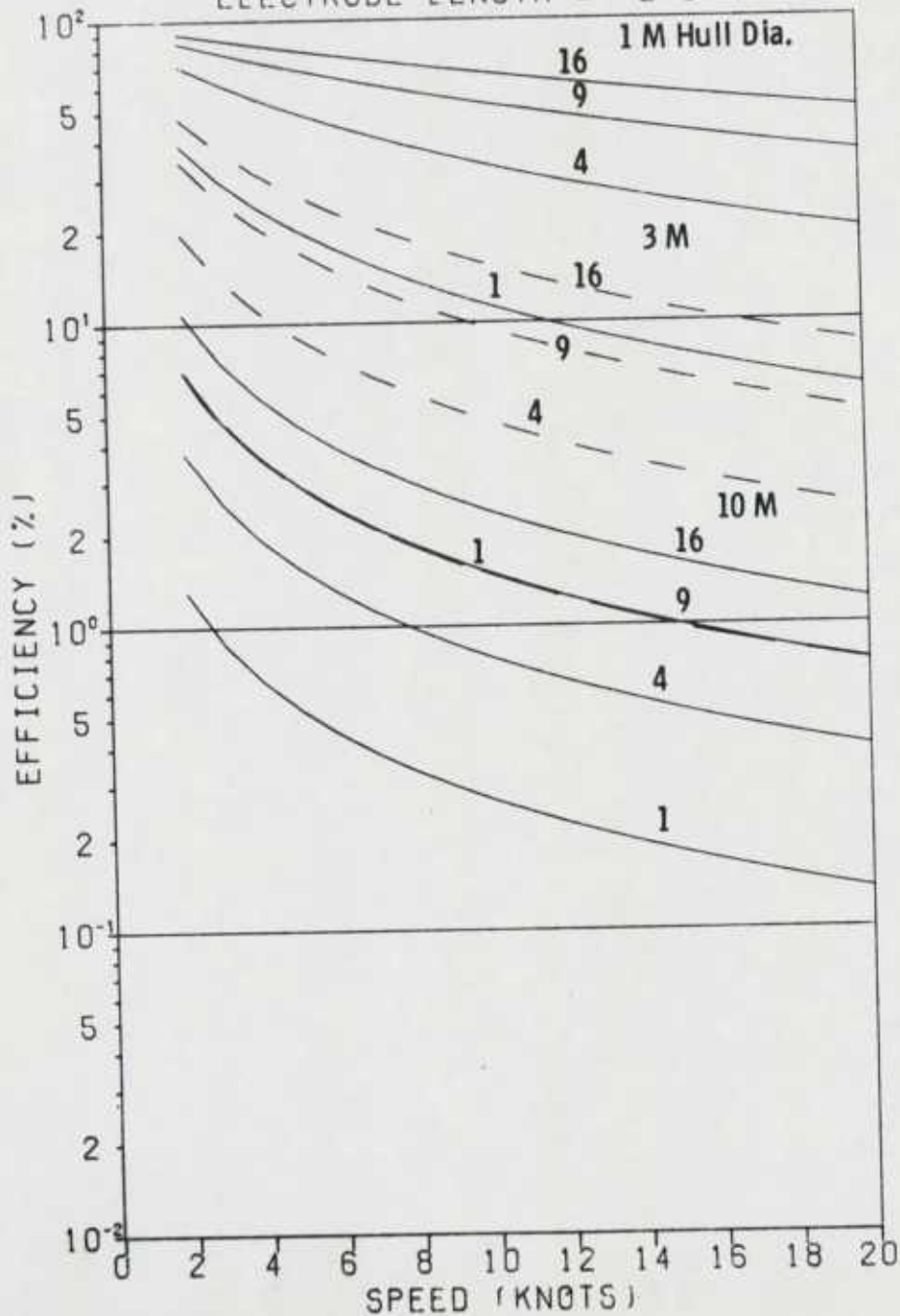


FIGURE 15

# IDEAL EFFICIENCY VS SPEED SINGLE AND MULTIPLE DUCTS

MAGNETIC FIELD = 2.0 T  
EACH DUCT AREA = .25 SQ M  
ELECTRODE LENGTH = 10.0 M

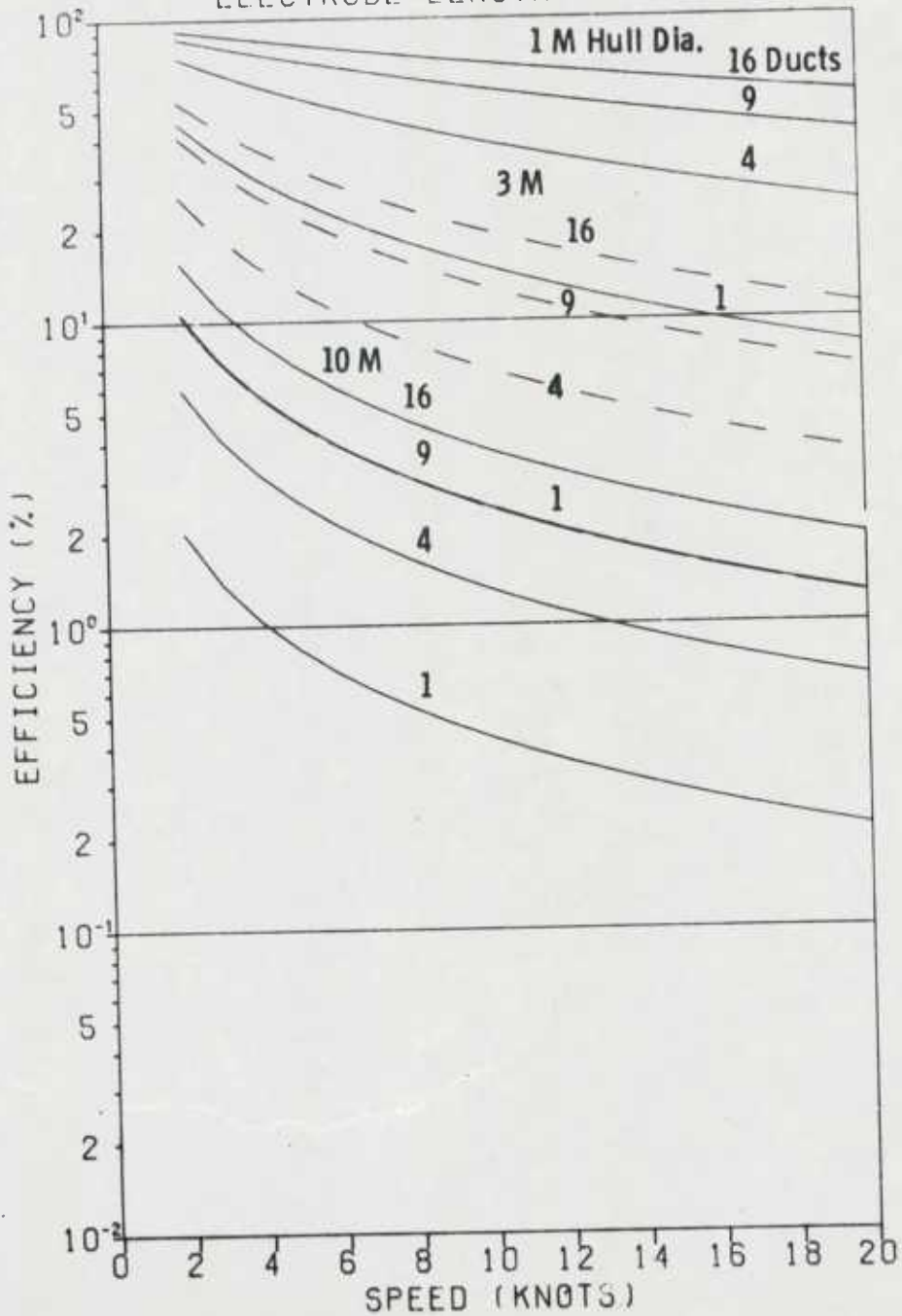


FIGURE 16

# IDEAL EFFICIENCY VS SPEED SINGLE AND MULTIPLE DUCTS

MAGNETIC FIELD = 2.0 T  
EACH DUCT AREA = .50 SQ M  
ELECTRODE LENGTH = 10.0 M

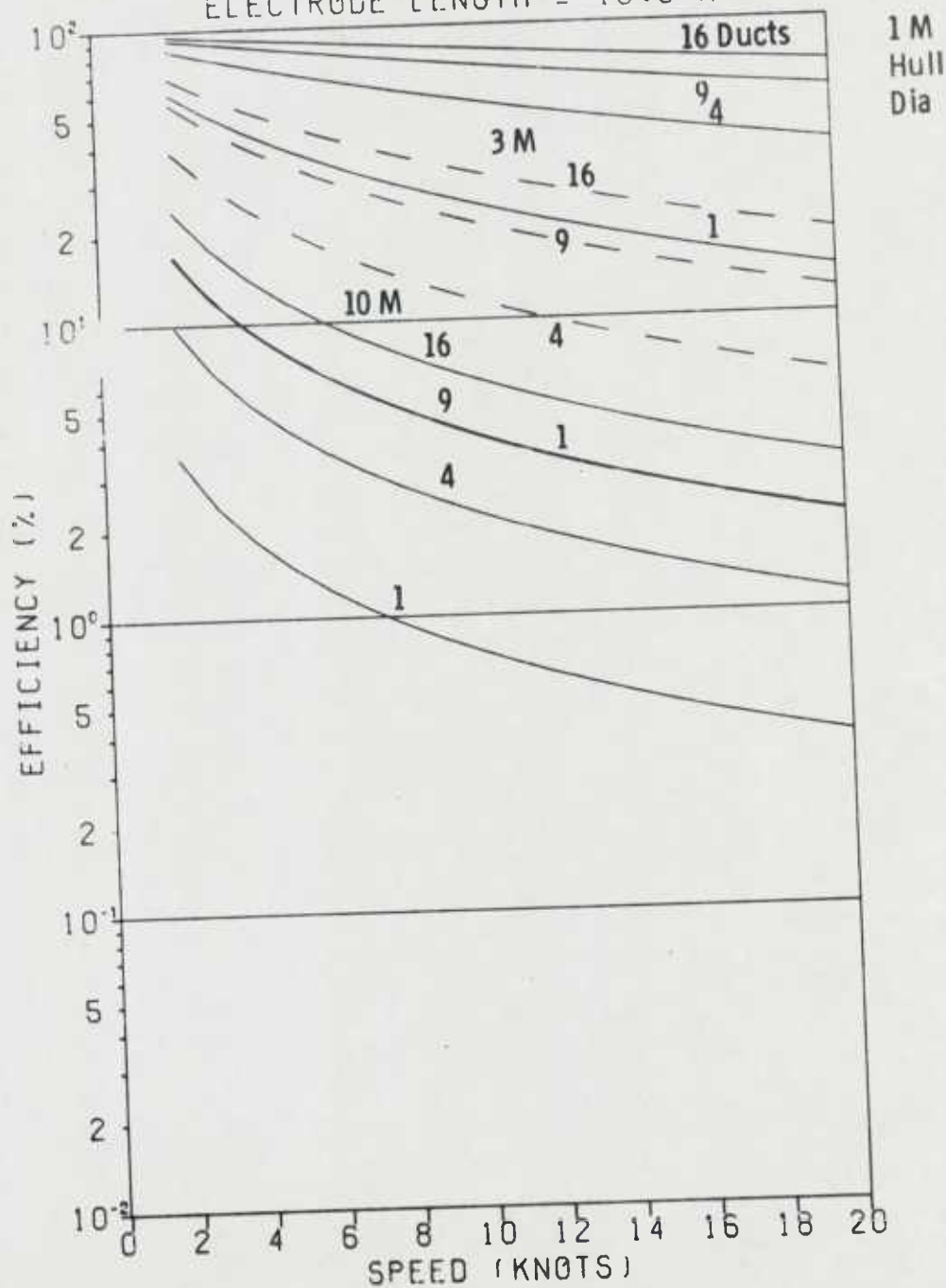


FIGURE 17

# IDEAL EFFICIENCY VS SPEED SINGLE AND MULTIPLE DUCTS

MAGNETIC FIELD = 2.0 T  
EACH DUCT AREA = .75 SQ M  
ELECTRODE LENGTH = 10.0 M

1 M Hull Dia.

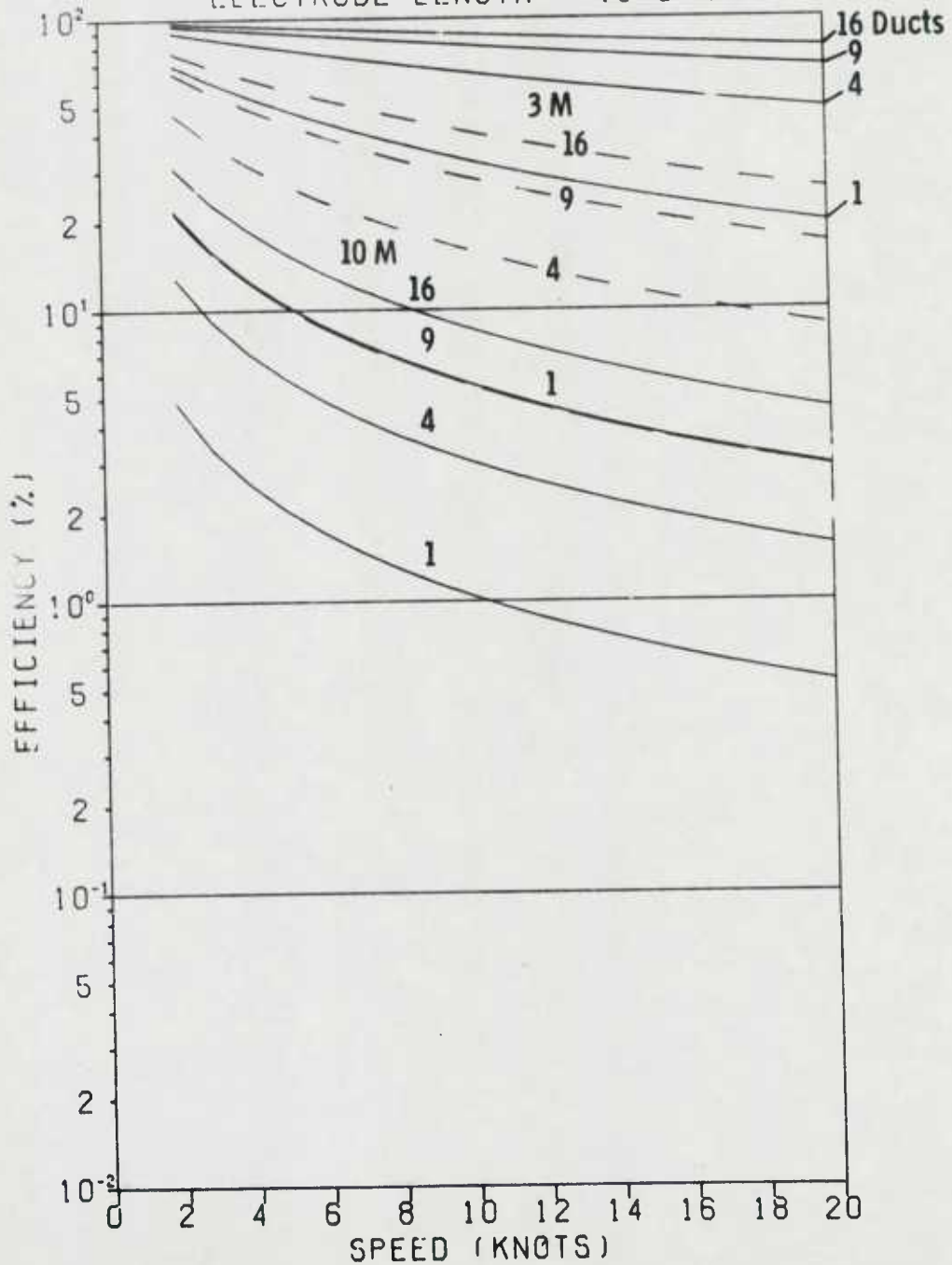




FIGURE 18

# IDEAL EFFICIENCY VS SPEED SINGLE AND MULTIPLE DUCTS

MAGNETIC FIELD = 2.0 T  
EACH DUCT AREA = 1.0 SQ M 1 M Hull Dia.  
ELECTRODE LENGTH = 10.0 M

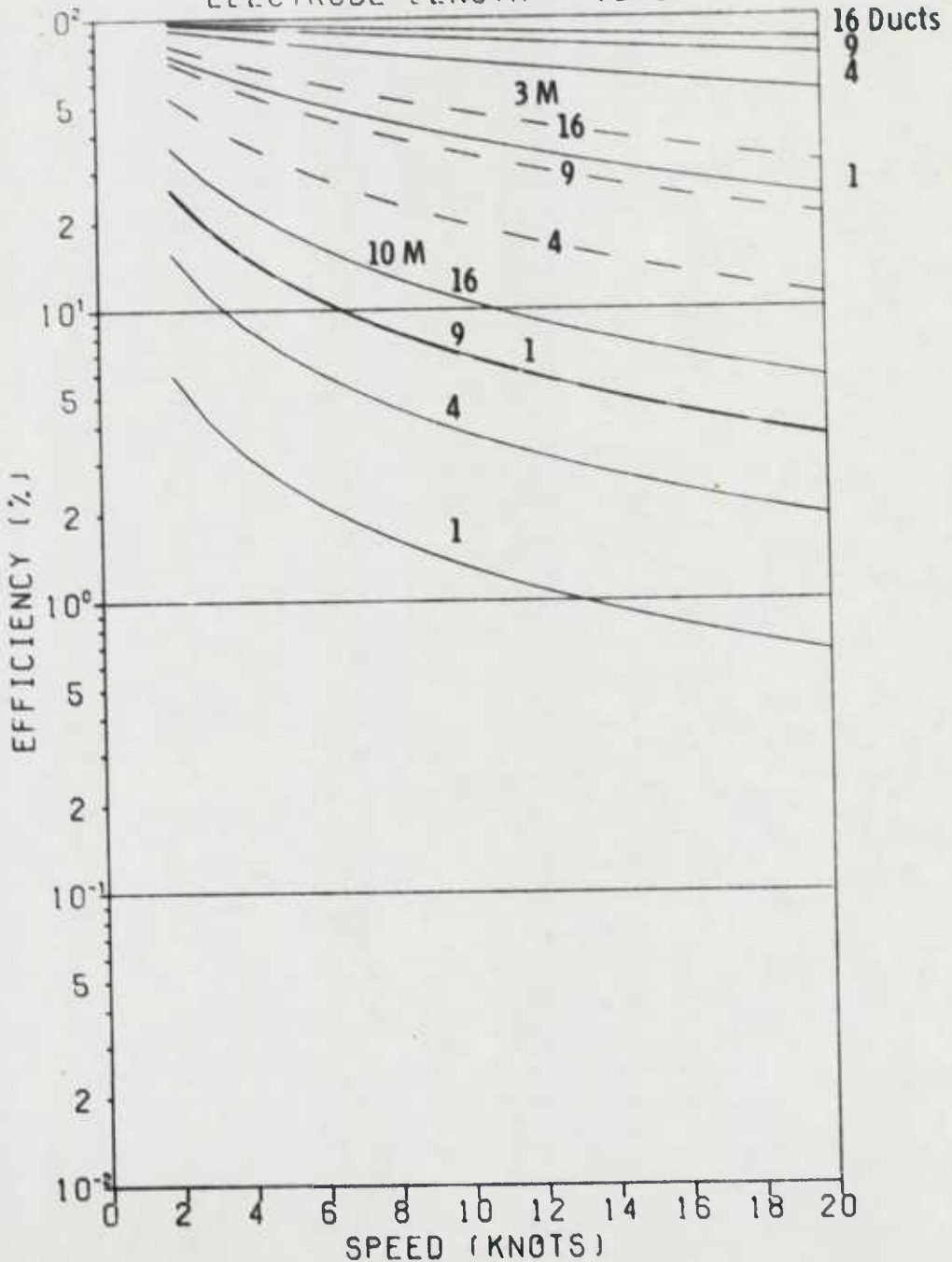


FIGURE 19

# IDEAL EFFICIENCY VS SPEED SINGLE AND MULTIPLE DUCTS

MAGNETIC FIELD = 5.0 T  
EACH DUCT AREA = .25 SQ M  
ELECTRODE LENGTH = 2.0 M

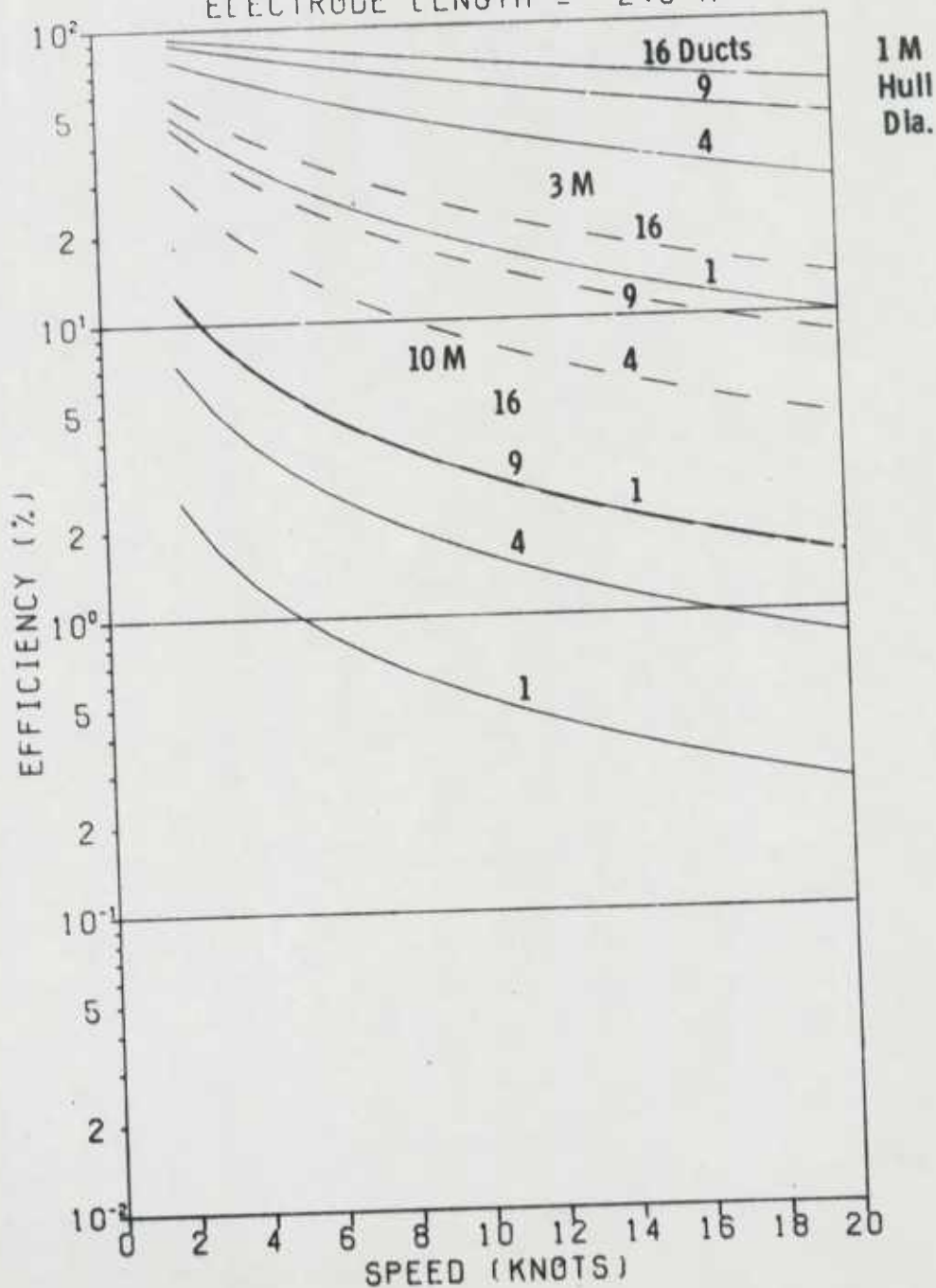


FIGURE 20

# IDEAL EFFICIENCY VS SPEED SINGLE AND MULTIPLE DUCTS

MAGNETIC FIELD = 5.0 T  
EACH DUCT AREA = .50 SQ M  
ELECTRODE LENGTH = 2.0 M

1 M  
Hull  
Dia.

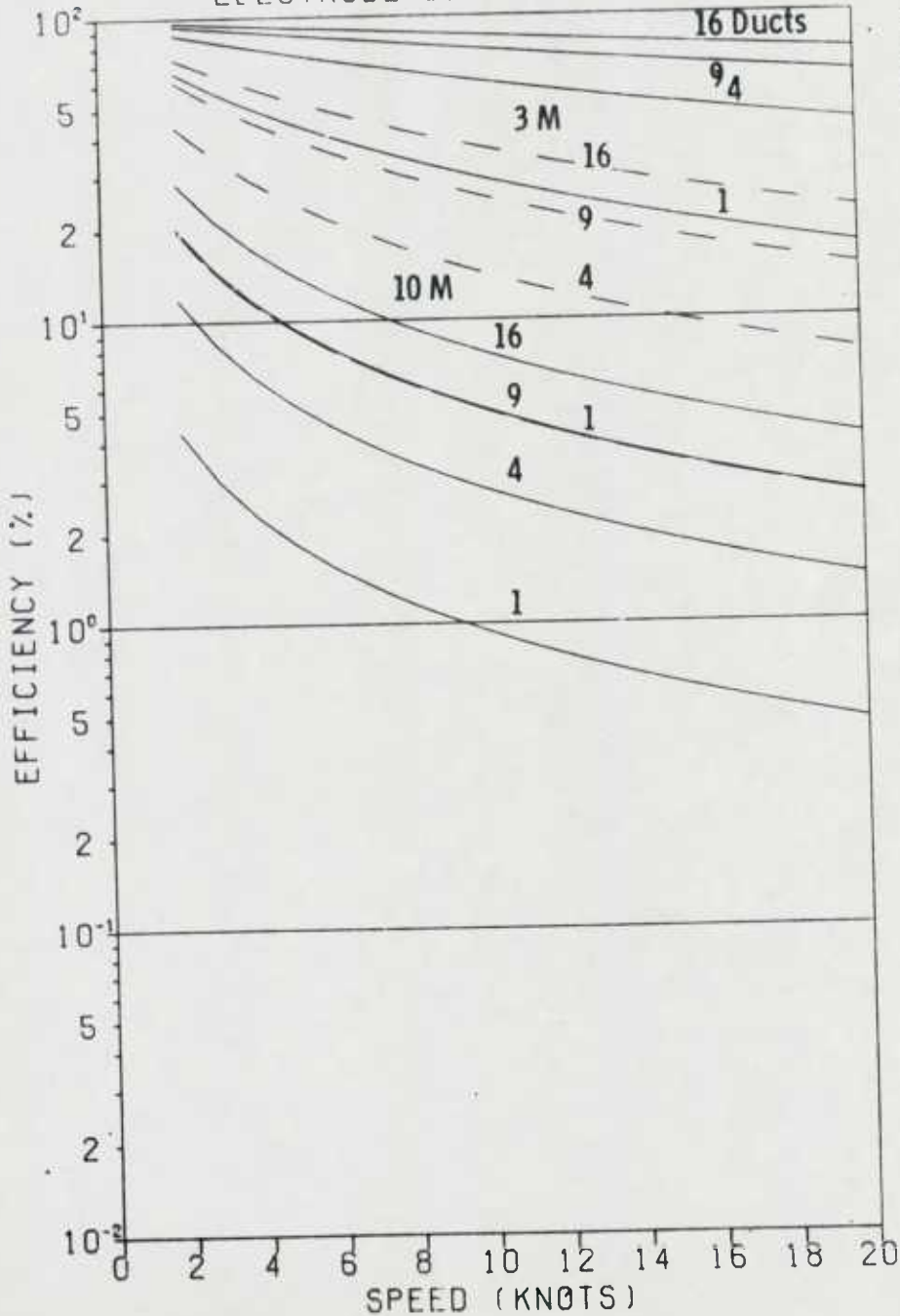


FIGURE 21

# IDEAL EFFICIENCY VS SPEED SINGLE AND MULTIPLE DUCTS

MAGNETIC FIELD = 5.0 T  
EACH DUCT AREA = .75 SQ M  
ELECTRODE LENGTH = 2.0 M 1 M Hull Diam.

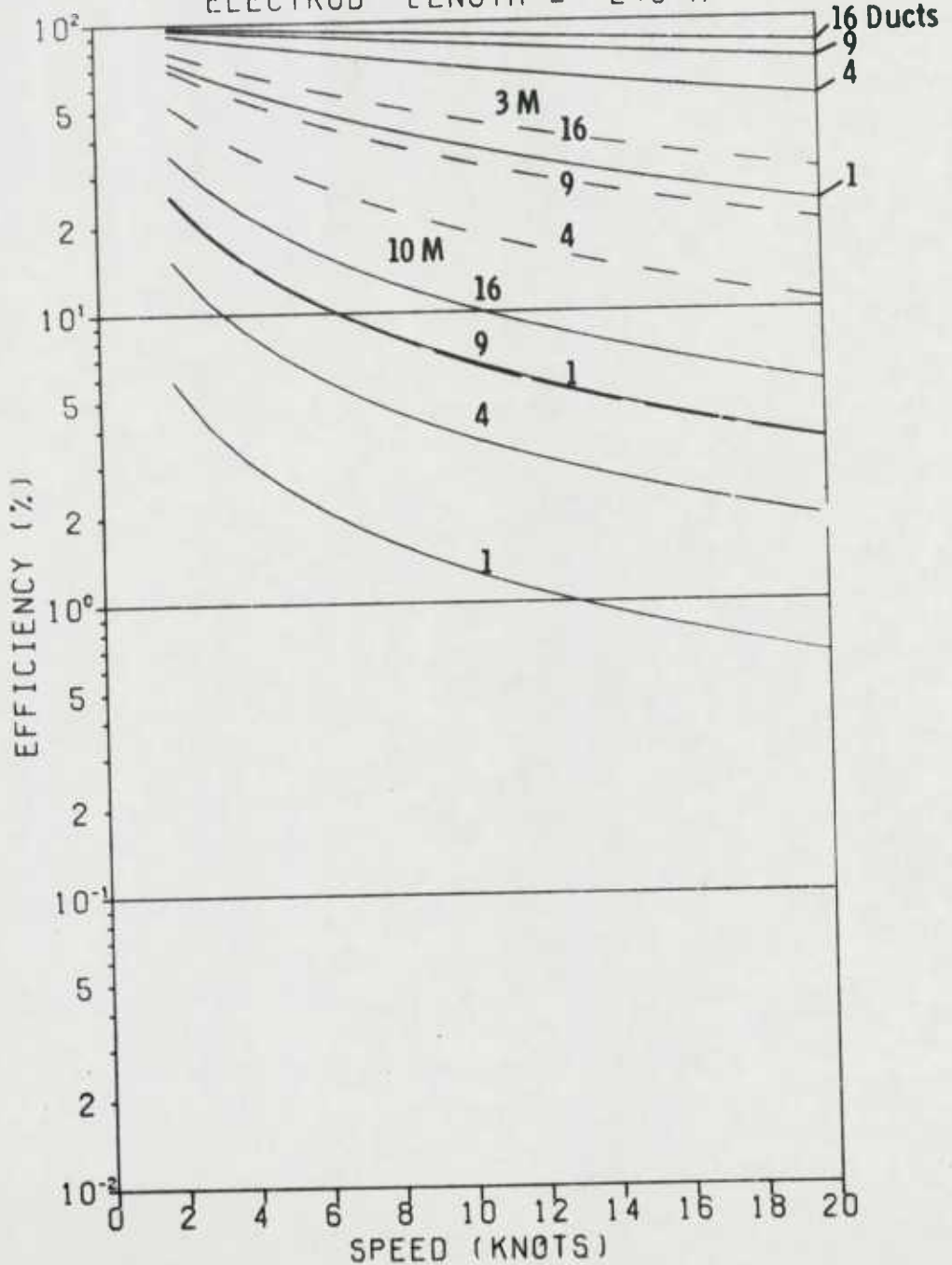


FIGURE 22

# IDEAL EFFICIENCY VS SPEED SINGLE AND MULTIPLE DUCTS

MAGNETIC FIELD = 5.0 T  
EACH DUCT AREA = 1.0 SQ M 1 M Hull Dia.  
ELECTRODE LENGTH = 2.0 M

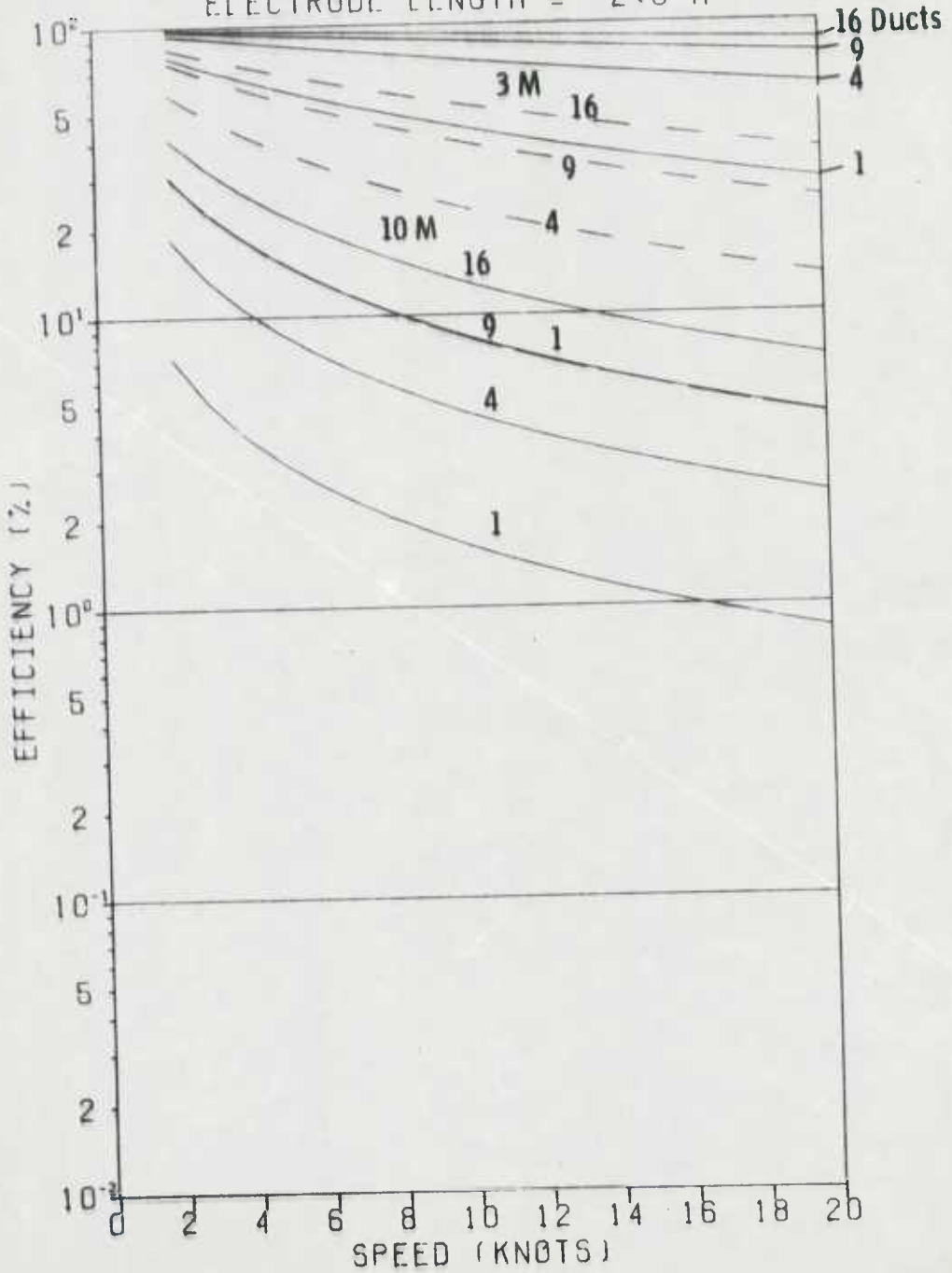


FIGURE 23

# IDEAL EFFICIENCY VS SPEED SINGLE AND MULTIPLE DUCTS

MAGNETIC FIELD = 5.0 T  
EACH DUCT AREA = .25 SQ M  
ELECTRODE LENGTH = 10.0 M

1 M Hull Dia.

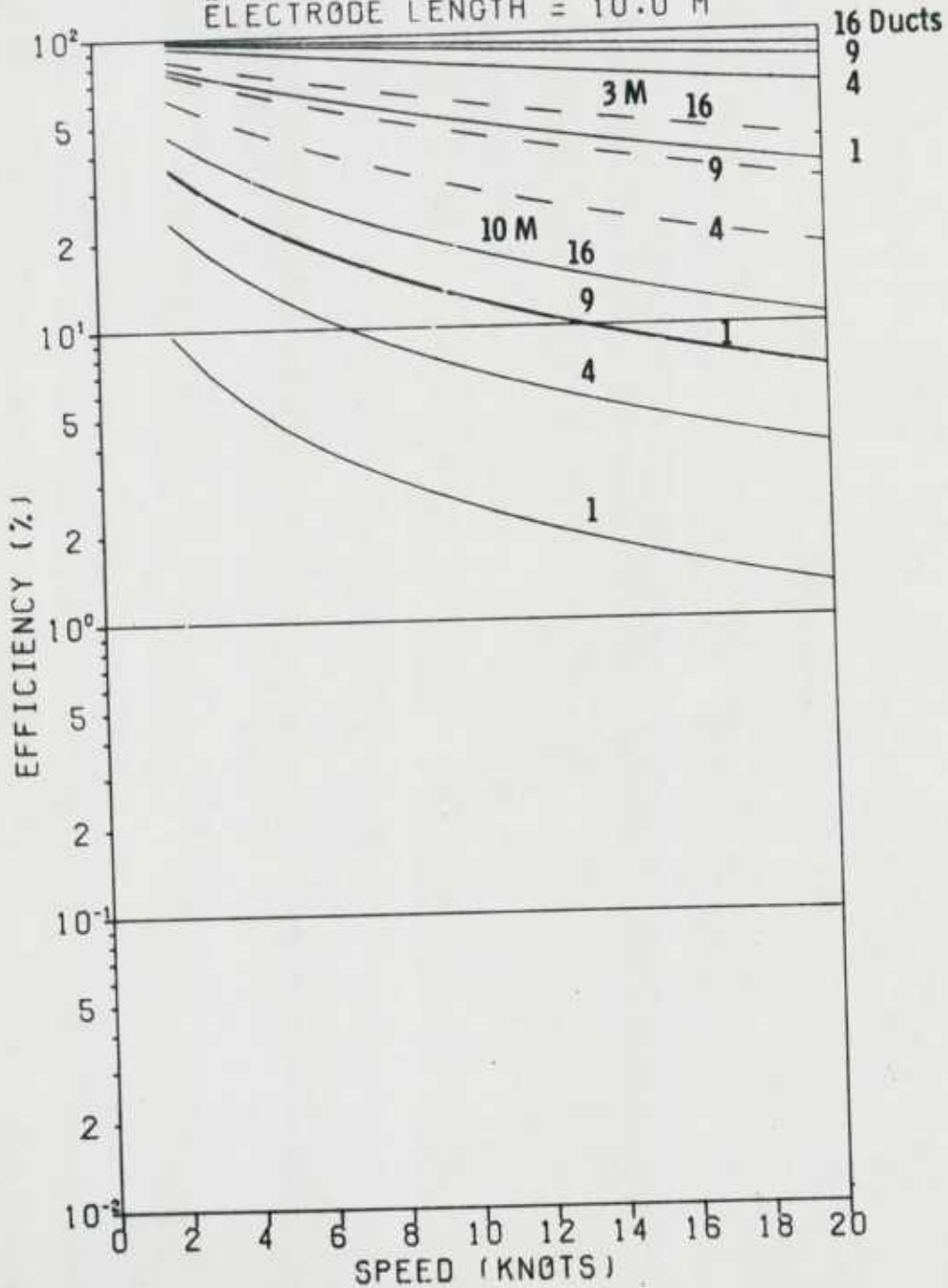




FIGURE 24

# IDEAL EFFICIENCY VS SPEED SINGLE AND MULTIPLE DUCTS

MAGNETIC FIELD = 5.0 T  
EACH DUCT AREA = .50 SQ M  
ELECTRODE LENGTH = 10.0 M

1 M Hull Dia.

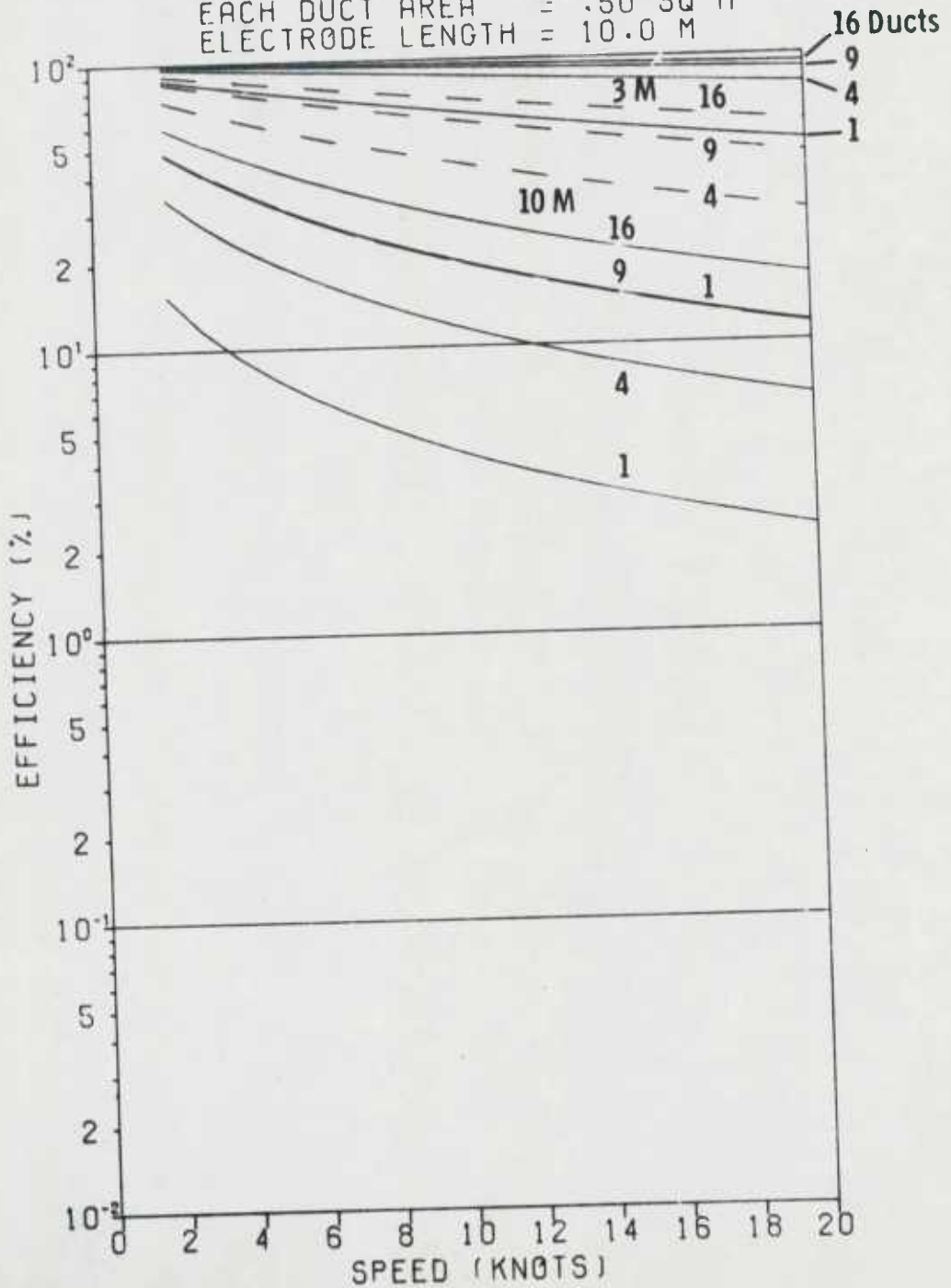


FIGURE 25

# IDEAL EFFICIENCY VS SPEED SINGLE AND MULTIPLE DUCTS

MAGNETIC FIELD = 5.0 T  
EACH DUCT AREA = .75 SQ M  
ELECTRODE LENGTH = 10.0 M

1 M Hull Dia.

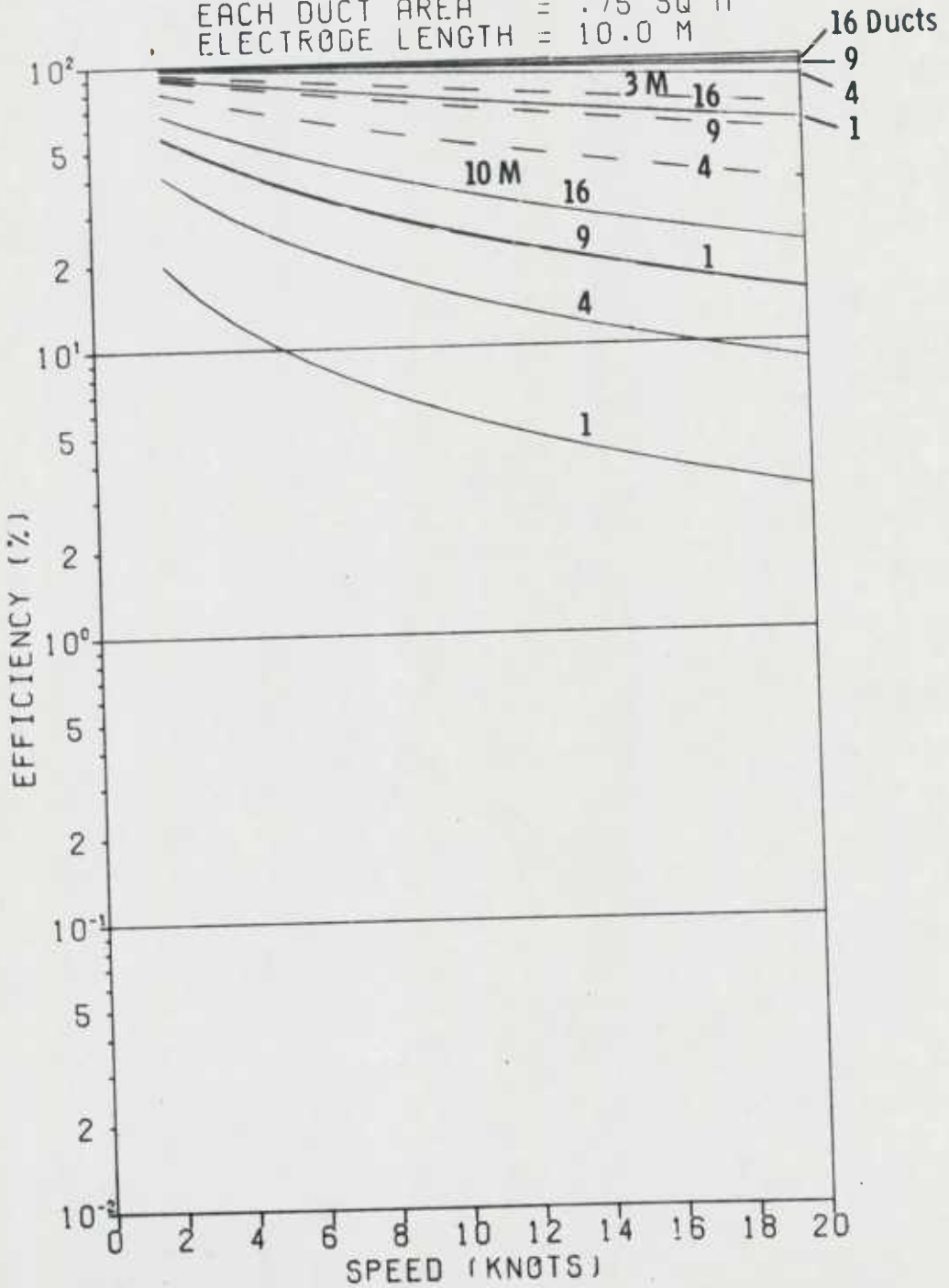
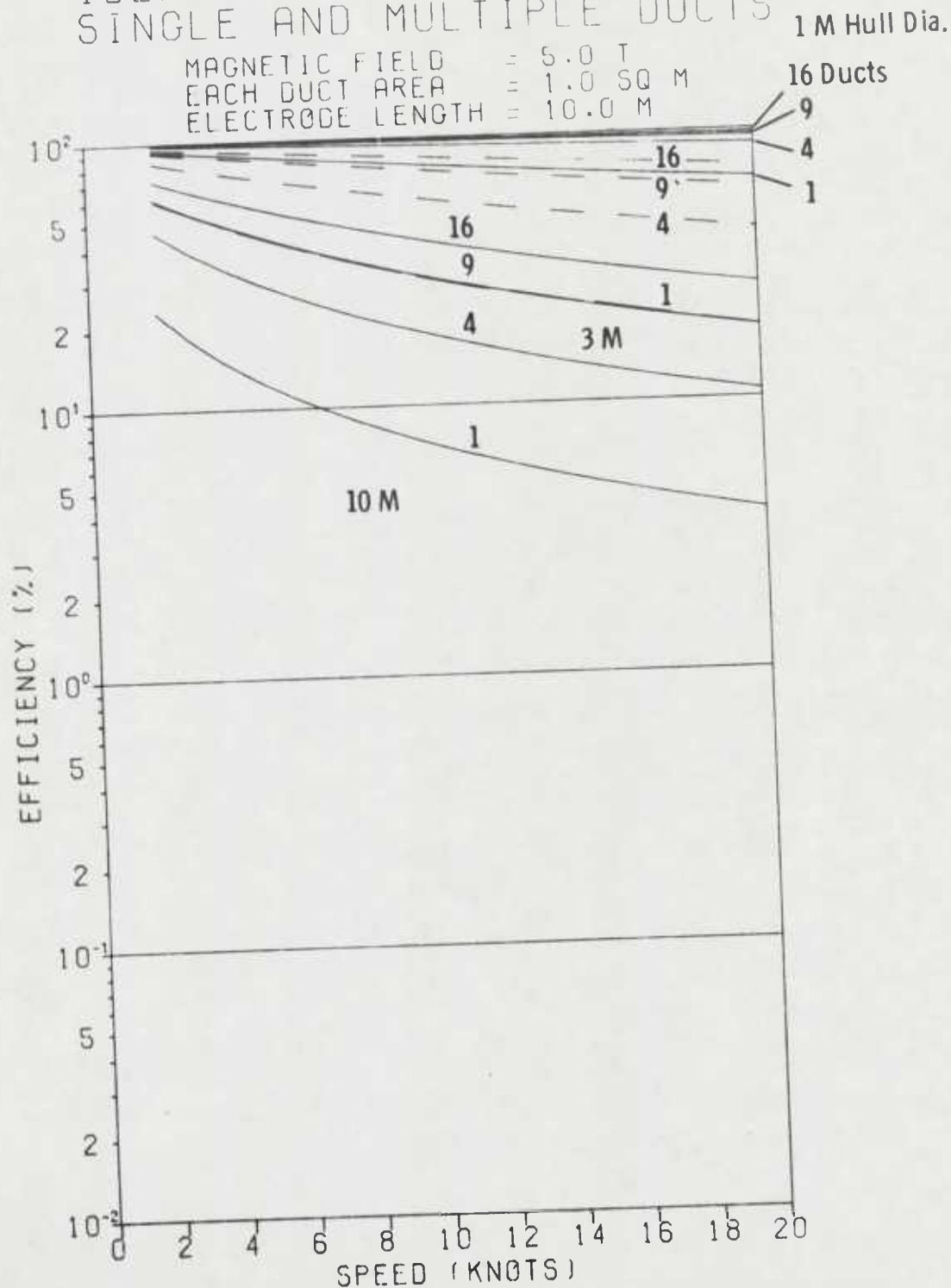


FIGURE 26

# IDEAL EFFICIENCY VS SPEED SINGLE AND MULTIPLE DUCTS



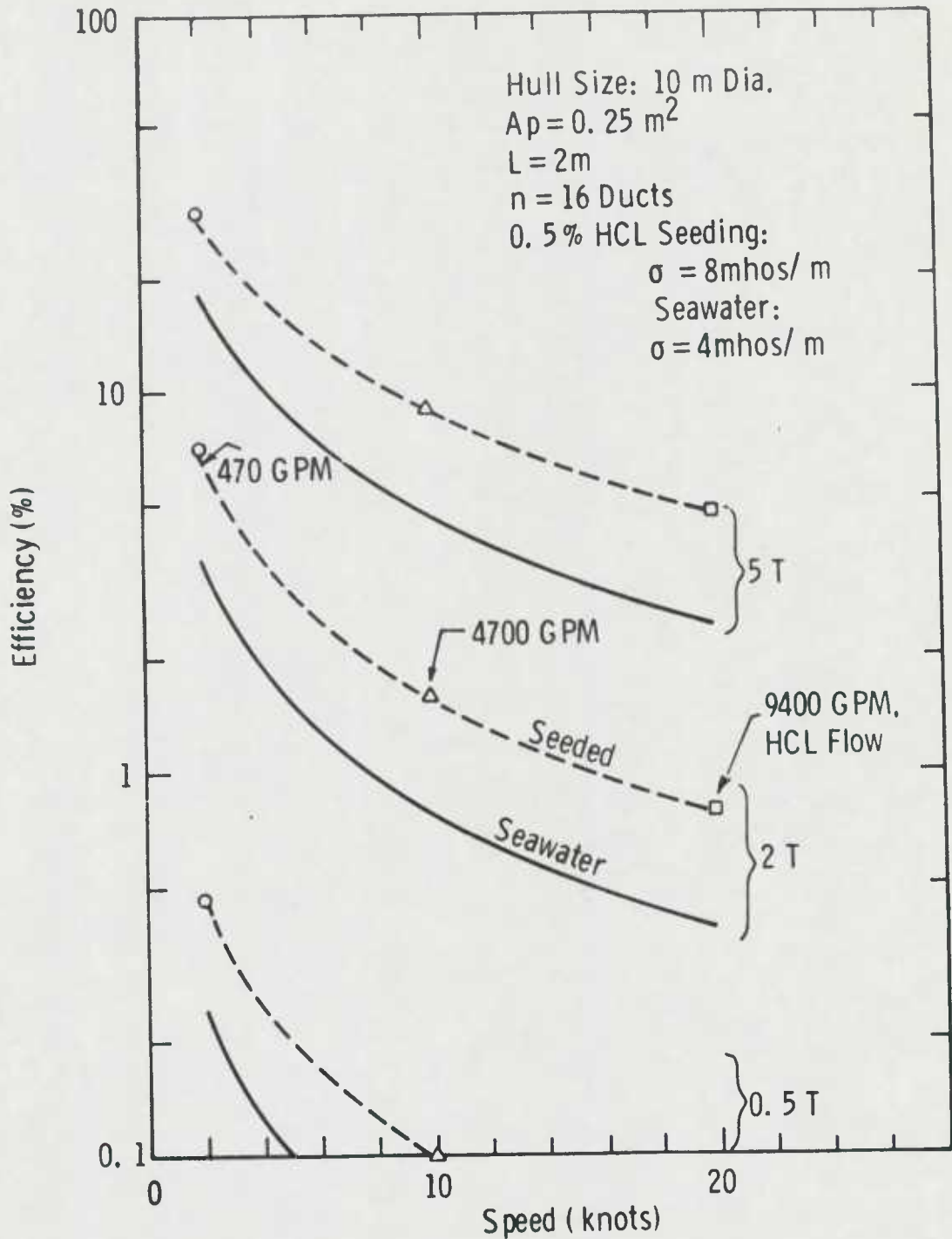


Fig.27 — Efficiency improvement via HCL seeding: full size hull

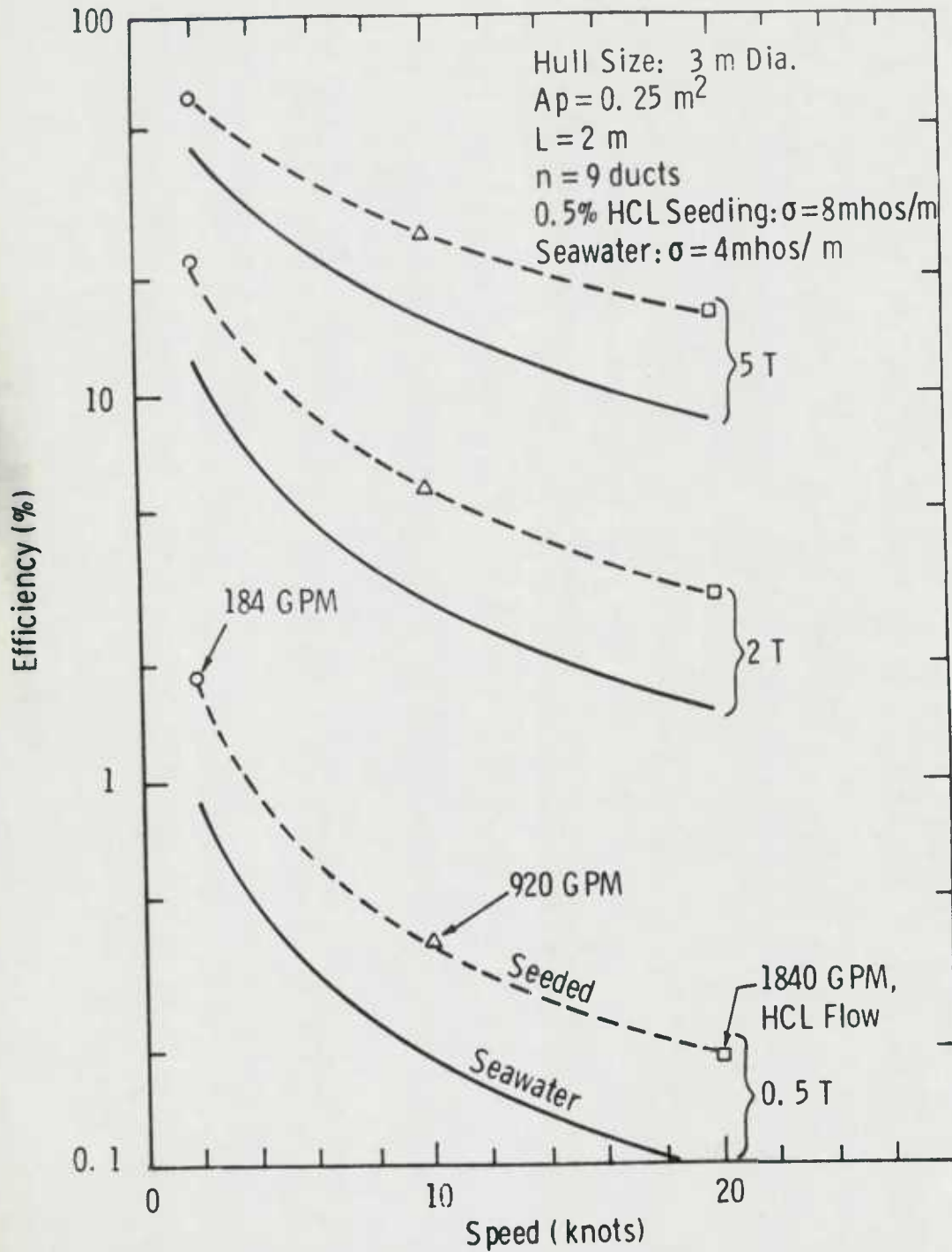


Fig. 28 — Efficiency improvement via HCL seeding: third-size hull

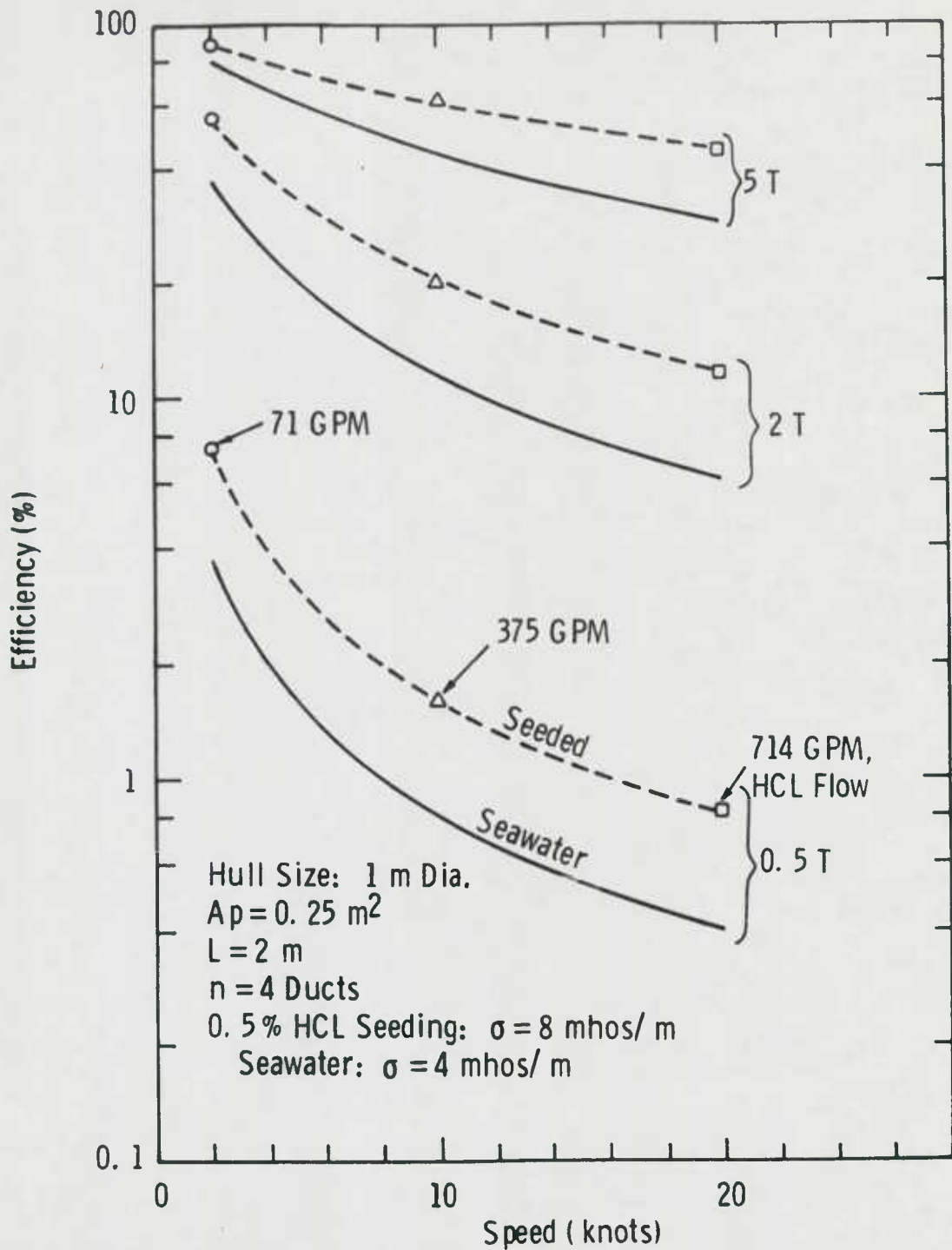


Fig. 29 — Efficiency improvement via HCL seeding: tenth-size hull



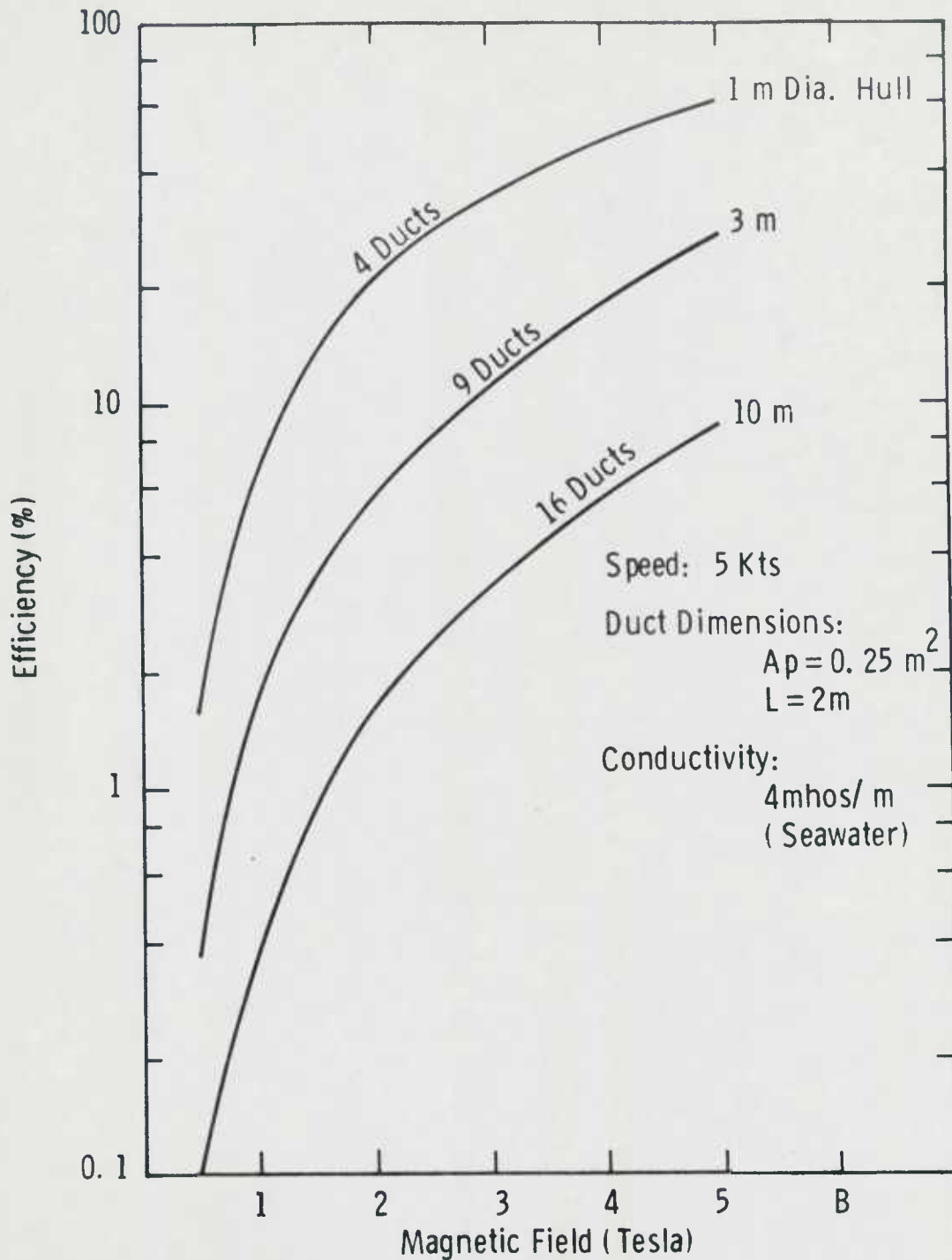


Fig. 30 — Ideal efficiency vs. magnetic field intensity for selected number of ducts & hull sizes

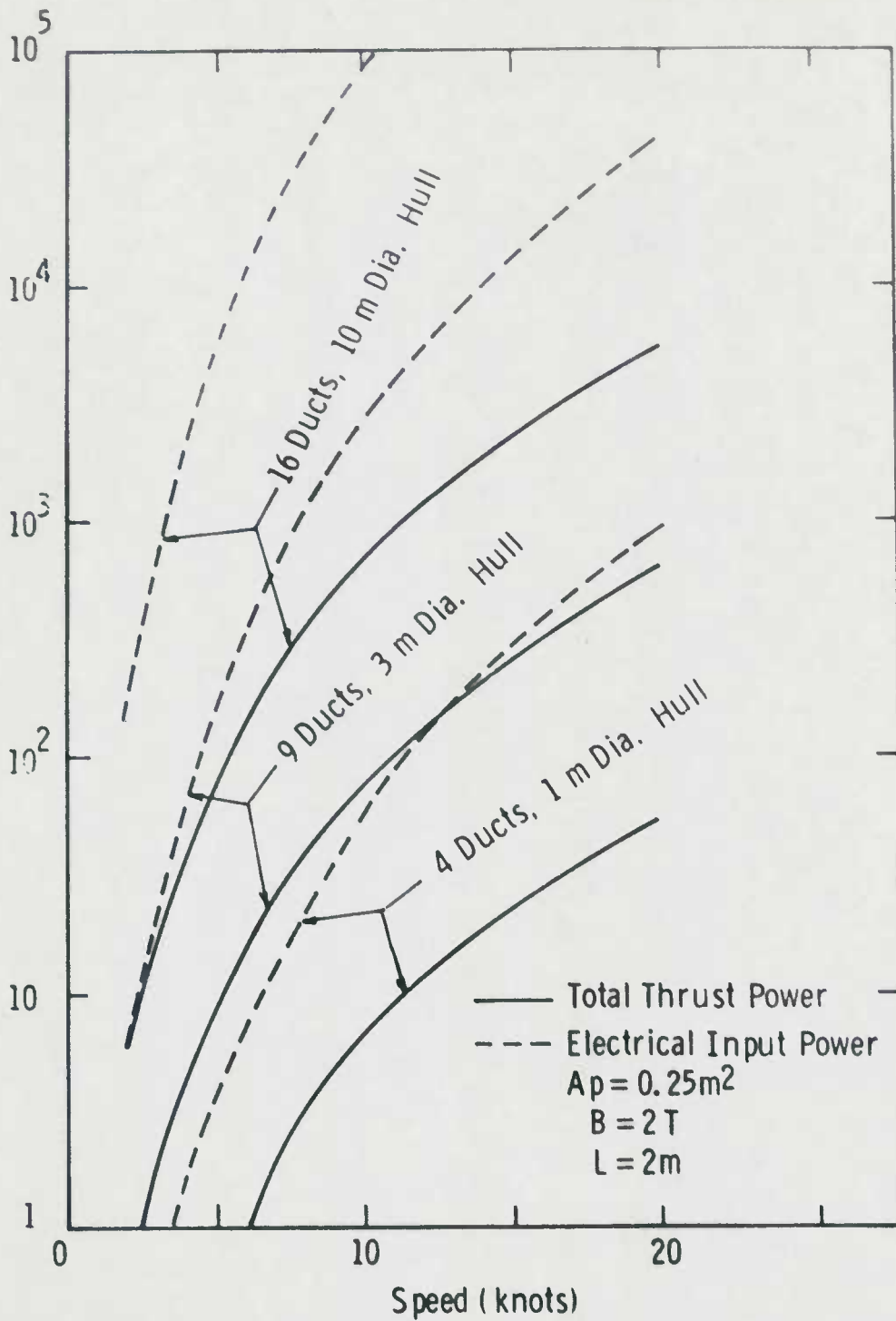


Fig. 31 — Power requirements vs. speed for selected number of ducts and hull sizes

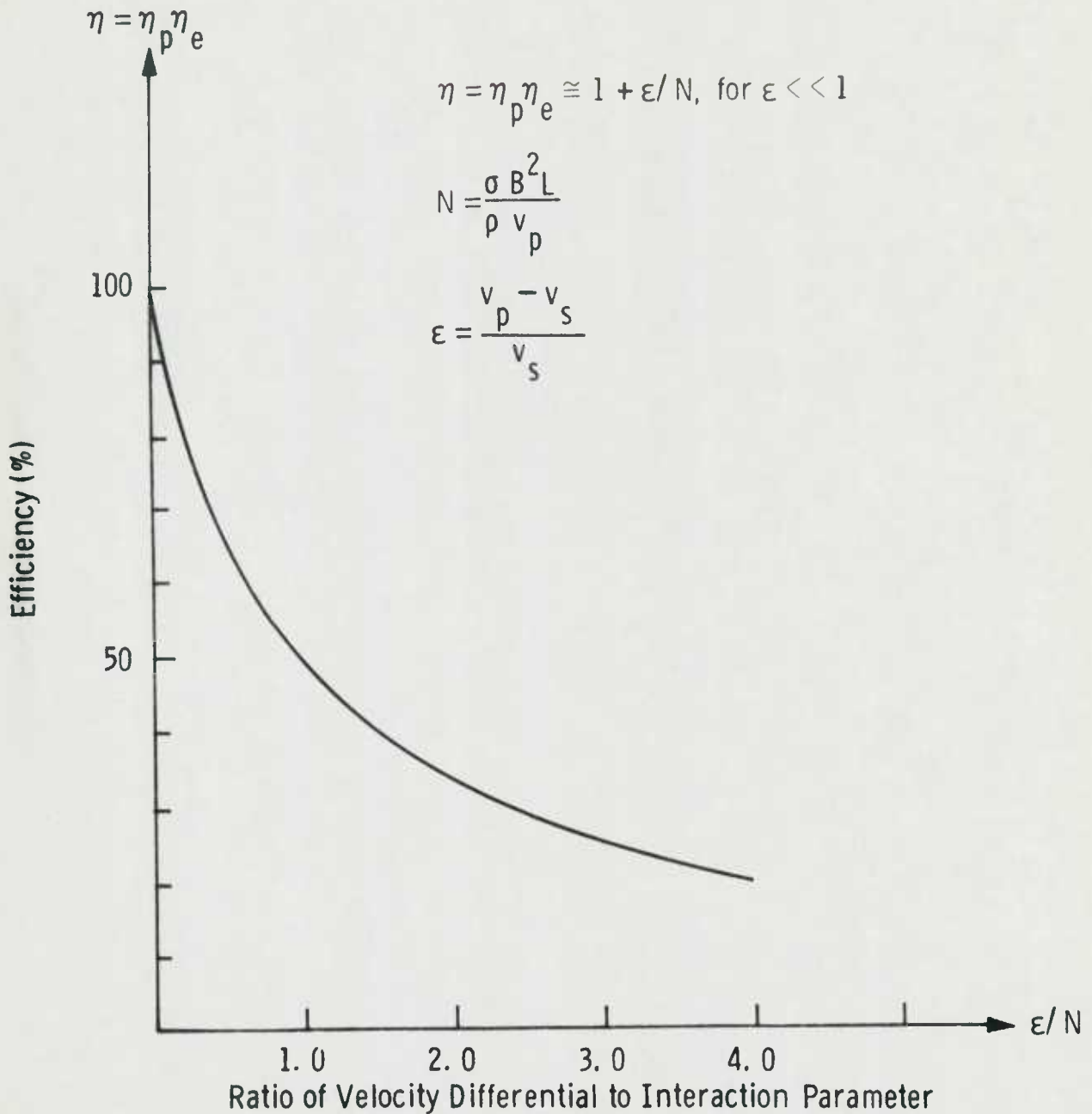


Fig. 32 — Sensitivity of ideal pump efficiency to velocity differential ÷ interaction parameter

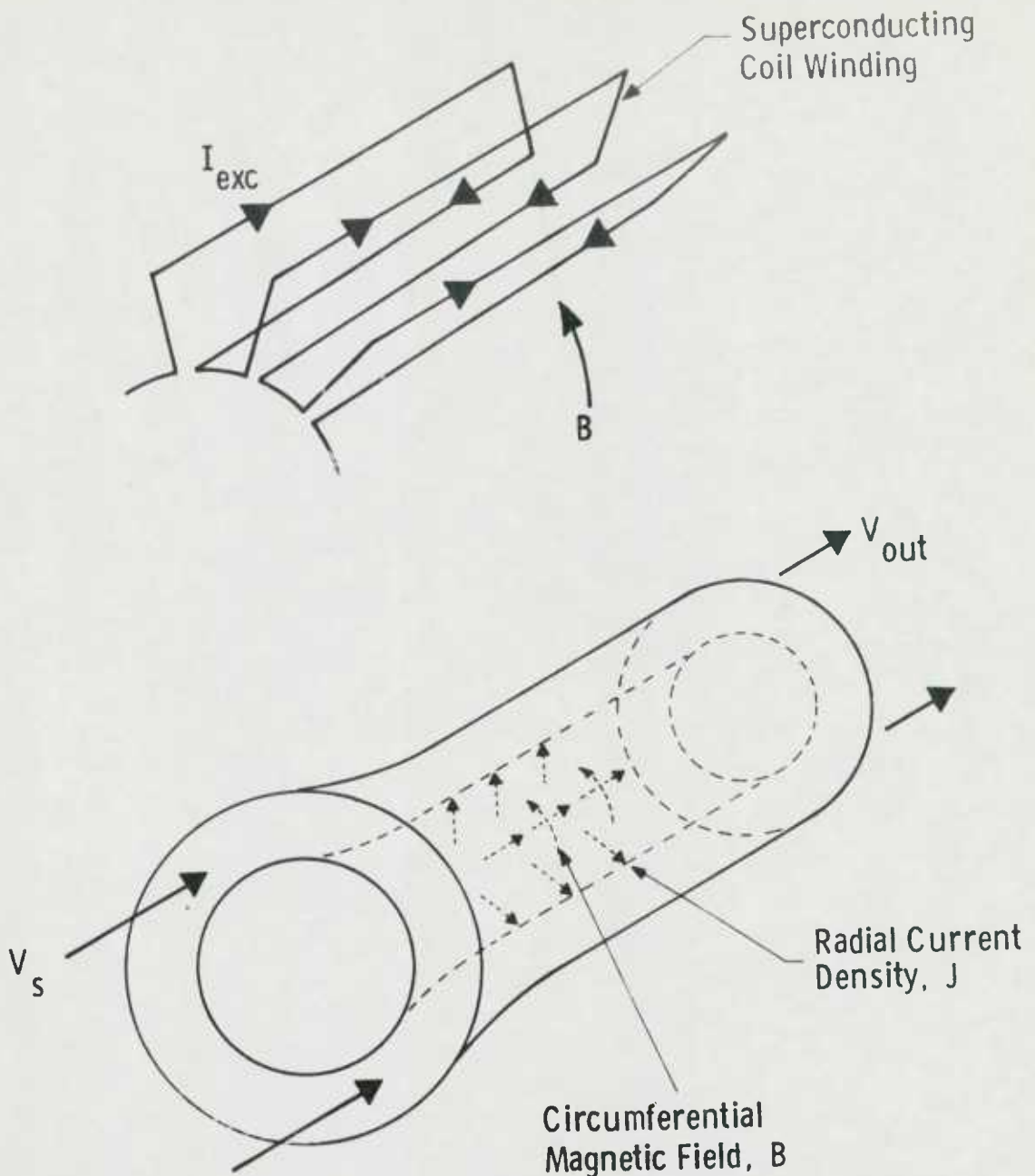


Fig. 33 — Annular pump configuration utilizing superconducting excitation. The toroidal winding establishes a high circumferential field in the pump region with low external flux leakage

## APPENDIX A-1

### SUBMERSIBLE HULL AND THRUSTER DRAG

The following calculations are presented to evaluate the frictional and total drag forces on a streamlined submersible of typical sizes and proportions moving at reasonable speeds, and to compare the frictional drag on a typical thruster to the total drag on the submersible. The frictional drags on the submersible and thruster are calculated by a standard velocity-squared formula that involves velocity-dependent parameters. However, the total drag characteristics used in Equation (5), Section 4.3, consist of a simple velocity-squared relationship and constant parameters. Therefore, discrepancies are likely to occur when comparing the total drag as given by Equation (5) to more accurate frictional drag calculations. The question is: "Are these discrepancies significant when compared to the total drag?"

#### Streamlined Hull Drag

The drag force, as used in the performance calculations in Section 4, is given by:

$$F_d = K_s v_s^2 \quad (5)$$

where  $K_s$  was determined from supplied drag vs velocity data. In order to compare this to a more accurate frictional drag, we must specify the size, shape and, hence, total submerged surface area. To do this, we assume the hull shape may be approximated by a prolate spheroid whose total surface,  $S$ , is given by:

$$S = 2 \pi a^2 + (\pi b^2/\epsilon) \cdot \ln [(1 + \epsilon)/(1 - \epsilon)] \quad (A-1.1)$$

where  $2a$  is the major axis,  $2b$  is the minor axis, and  $e$  is the eccentricity of the elliptical cross section:

$$e = \sqrt{1 - (b/a)^2} \quad (A-1.2)$$

For each hull diameter, we chose a length (and eccentricity) such that the calculated frictional drag at approximately 8 knots equals the drag given by Equation (5). The three hull sizes and shapes are summarized in the following table:

Hull Dia. (m)	Length (m)	Volume (m <sup>3</sup> )	Surface Area (m <sup>2</sup> )	Eccentricity	Displacement (Tons)
10.0	50.0	2620	4290	.980	2890
3.3	15.5	88.4	417	.977	97.4
1.0	4.35	2.28	33.2	.975	2.46

For each combination of submersible size and speed, the Reynolds' number for the resulting flow is calculated:

$$R = v_s \ell / \nu \quad (A-1.3)$$

where  $v_s$  is the free-stream speed,  $\ell$  is the length of the submersible, and  $\nu$  is the kinematic viscosity of sea water. The coefficient of friction,  $C_F$ , is interpolated from a standard table<sup>(7)</sup> that lists  $C_F$  for various values of  $R$ . (It should be noted that all of the flows are turbulent; hence, the coefficient of friction decreases for increasing Reynolds' number.) Then, the frictional drag force is calculated:

$$F_f = 1/2 \rho C_F S v_s^2 \quad (A-1.4)$$

where  $\rho$  is the density of sea water,  $C_F$  is the frictional coefficient,  $S$  is the wetted surface area (equal to the total surface area in all cases), and  $v_s$  is the free-stream speed of the submersible. Comparison between the simple velocity-squared drag used in Section 4 and the more accurate



frictional drag is shown in Figure A1-1. As shown in the figure, values of these two forces agree to within twenty percent for each of the three sizes, over a speed range of up to 20 knots. We conclude that the approximations for  $C_D$  and  $S$  incorporated in the constant  $K_S$  are reasonable.

#### Thruster Frictional Drag

The calculations for frictional drag on a thruster duct are very similar to the hull drag calculations. For the purpose of making a specific hull to thruster drag comparison, the duct length was chosen as 2 m and the cross-sectional area as  $.25 \text{ m}^2$  (this does not include inlet shroud or outlet nozzle surfaces). For these calculations the aspect ratio,  $\alpha$ , ranges from 1 to 20. The internal surface area is exactly:

$$S = 4 L a (1 + \alpha) \quad (\text{A-1.5})$$

where  $a$  is the duct half width and  $L$  is the length. The coefficient of friction is taken from the same data<sup>(7)</sup> for flow over a smooth flat plate (2-sides).

Frictional force is calculated for various speeds using Equation (A-1.4). Figure A-1.2 compares duct drag obtained using this formula to hull drag taken from Figure 1. As may be seen from the figure, an aspect ratio of 1 produces the minimum drag, and the drag per duct is less than ten percent of the total drag for the small hull and less than one percent of the total for the larger hull.

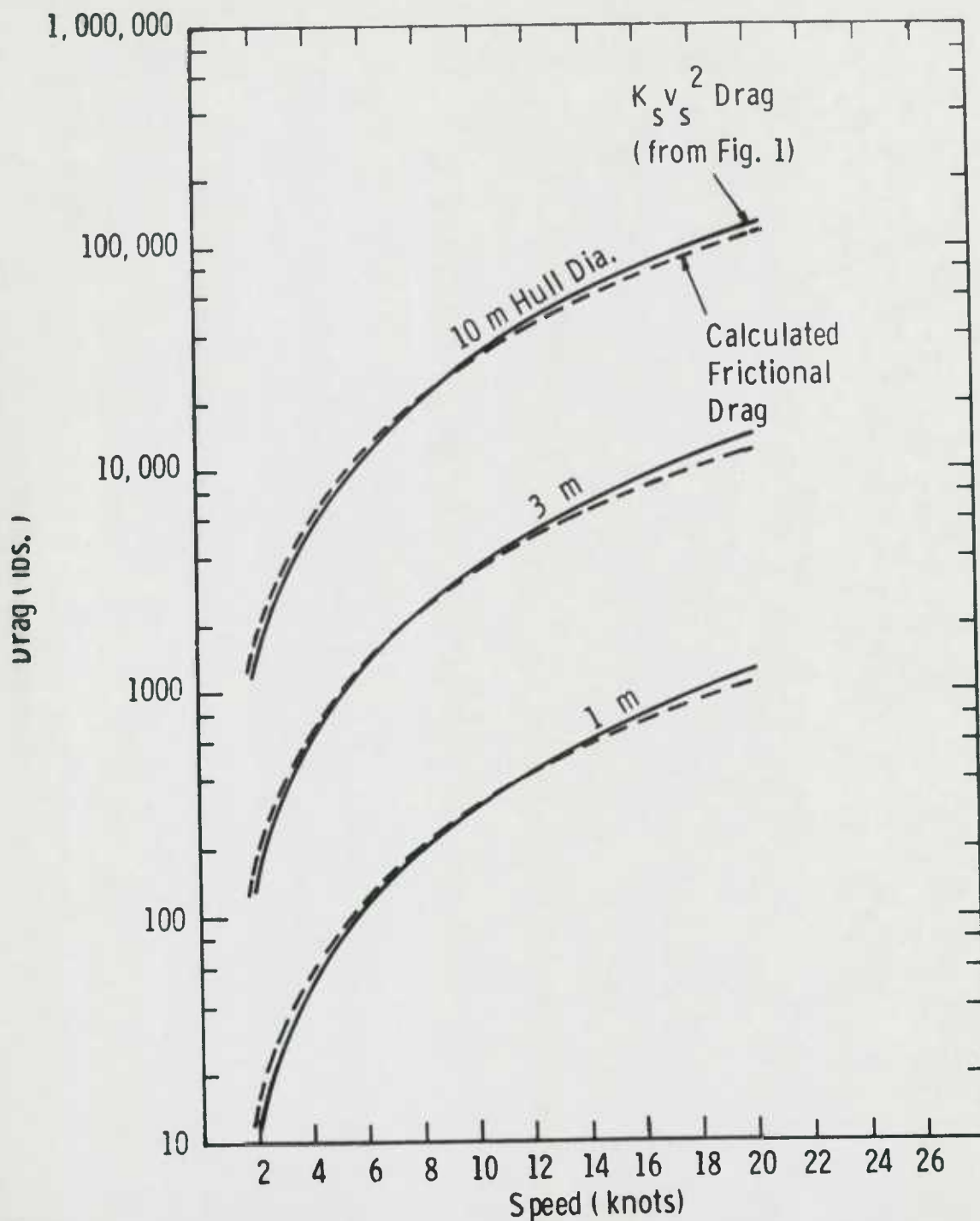


Fig. A-1.1 — Comparison of frictional hull drag to  $K_s v_s^2$  drag

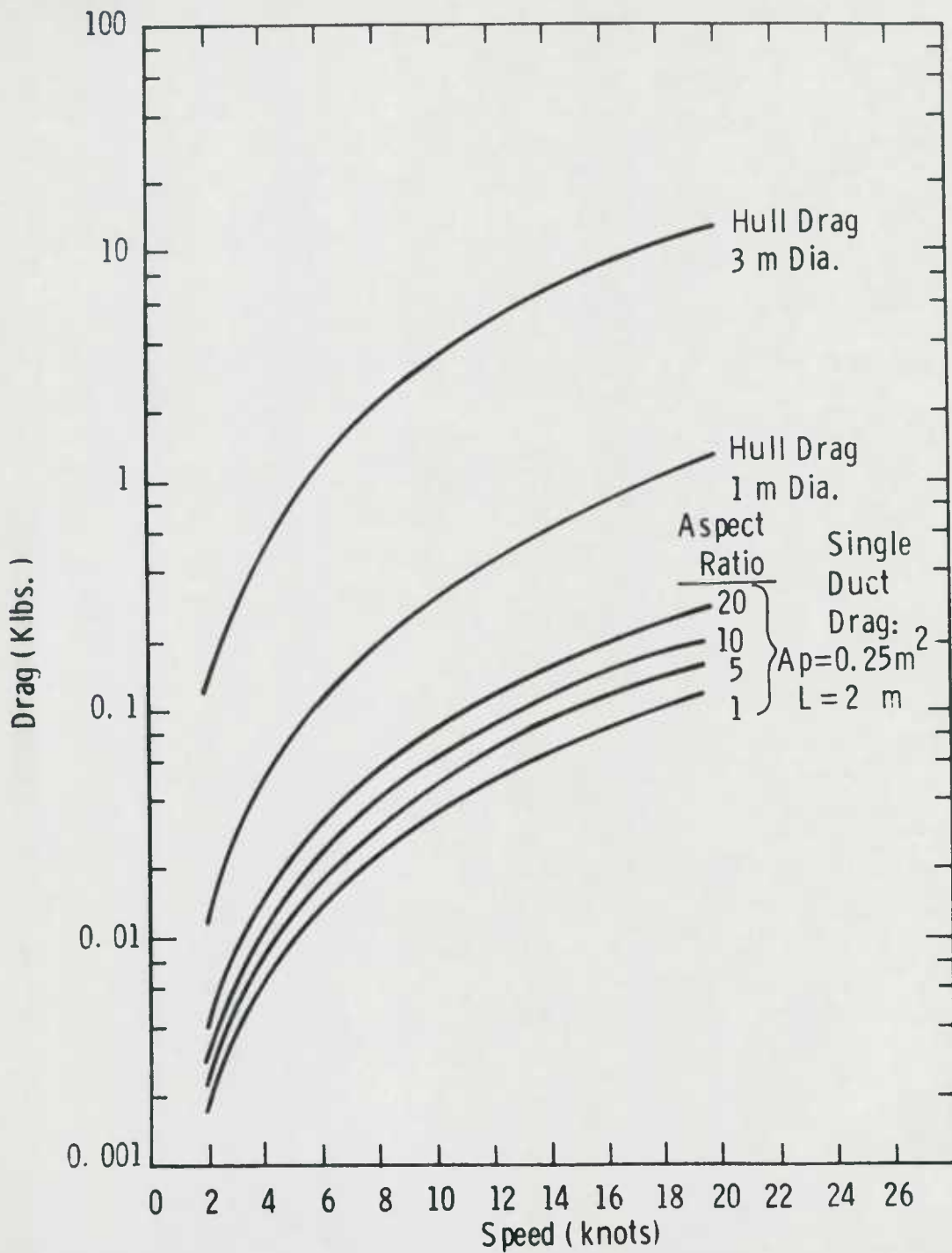


Fig. A-1. 2 — Comparison of thruster-duct drag to hull drag for selected duct size

## APPENDIX A-2

### ELECTROMAGNETIC COUPLING TO CONDUCTING FLUID FLOW

For fully developed incompressible flow, the vector equation of motion is given by:<sup>8</sup>

$$\bar{f}_b = \bar{\nabla}P - \mu_f \nabla^2 \bar{v} \quad (A-2.1)$$

where  $\bar{f}_b$  = body force

$\bar{\nabla}P$  = pressure gradient

$\mu_f \nabla^2 \bar{v}$  = viscous force density

Neglecting viscous forces and considering one-dimensional (x) motion, we have

$$\frac{\partial P}{\partial x} = (f_b)_x \quad (A-2.2)$$

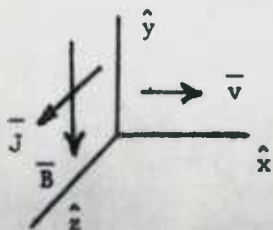
The electromagnetic body force density in a conducting fluid is given by

$$\bar{f}_b = \bar{J} \times \bar{B} \quad (A-2.3)$$

where  $\bar{J}$  = current density

$\bar{B}$  = magnetic field

If  $\bar{J}$  and  $\bar{B}$  are mutually perpendicular to the direction of fluid motion, as depicted in the sketch, where  $\bar{J} = J \hat{y}$ ,  $\bar{B} = -B \hat{z}$ , then



$$\bar{f}_b = J B \hat{x} \quad (A-2.4)$$

and from Equation (A-2.2), we have for the pressure gradient,

$$\frac{\partial P}{\partial x} = J B \quad (\text{A-2.5})$$

Assuming uniform current and magnetic field intensities, over electrode length  $L$ , we may integrate this expression to obtain for the pressure rise across the pump:

$$\Delta P_p = \int_0^L J B \, dx = J B L \quad (\text{A-2.6})$$

which is the desired expression relating pressure to current density, magnetic field, and electrode length.

Now we wish to relate current density to the difference in potential,  $V$  between the electrodes. Here we invoke Ohm's law in terms of a vector field equation for a moving medium.

$$\bar{J} = \sigma (\bar{E} + \bar{v} \times \bar{B}) \quad (\text{A-2.7})$$

where  $\sigma$  = conductivity of moving medium

$\bar{B}$  = magnetic field

$\bar{v}, \bar{E}$  = velocity and electric field as seen by stationary observer

Once again neglecting fringe effects, and separating the electrodes by a distance  $2b$  along the  $z$  axis we have:

$$\bar{E} = \hat{z} \, V/2b, \quad \bar{v} \times \bar{B} = -\hat{z} \, v_p B$$

where  $v_p$  = magnitude of velocity  $\bar{v}$  so that

$$J = \sigma (V/2b - v_p B) \quad (\text{A-2.8})$$

Finally, substituting from Equation (A-2.6), we obtain Equation (14) used in Section 4.3.3:

$$\Delta P_p = \sigma B L (V/2b - v_p B) \quad (14)$$

### APPENDIX A-3

#### A3.1 Fortran Source Listing:

Calculations of ideal efficiency, voltage and current  
as function of:

magnetic field  
area  
number of ducts  
hull size  
electrode length

#### A3.2 Sample Printout



### A3.1 Source

BRUN, /RNPT SUBCAL.09B23NSFM001.EMSUB.1.25

```

00DATA,IL TPF5.
DATA 9R1 SL74T9 08/06/79 11129154 (->0)
1. DATA LINE /6/
2. REAL KO,K1,KS
3. DIMENSION EFFARY(3,4,20),XV(21),YV(21)
4. EFFARY, XV,YV ALL USED FOR CALCOMP OUTPUT
5.
6.
7.
8. VS IN METERS/SEC
9.
10. AO IN SQ METERS
11.
12. KO IN NEWTONS/(M/S)**2
13. LBS THRUST/KNOT**2 = KS*ALPHA
14.
15. SPEED IN KNOTS = VS*BETA
16.
17. RHO = DENSITY,KG/M**3
18.
19. SIGMA = CONDUCTIVITY,MHOS
20.
21.
22. KREF = 5000.
23. AO = .25
24. SIGMA = 4.
25. RHO = 1.E3
26. VPRIME = 1.
27. VPRIME = KNOTS
28. ALPHA = ((2.57)**2)*.6973.) / ((31.E3)*.25.)
29. BETA = 5./2.57
30. VSO = VPRIME/BETA
31. VSO IN M/S
32.
33.
34. JMAX .....# OF DUCTS
35. LMAX ..... VELOCITY
36. MHAX ..... BFIELD
37. KMAX ..... DUCT AREA
38. NMAL ..... ELECRRODE LENGTH
39.
40. JMAX = 4
41. LMAX = 19
42. KMAX=4
43. MHAX=3
44. NMAL=2
45. DO 100 M= 1,MHAX
46. IF(M.EQ.1) B = .5
47. IF(M.EQ.2) B = 2.
48. IF(M.GE.3) B = 5.
49.
50. DIST IN METERS
51. DO 200 N = 1,NMAL
52. IF(N.EQ.1) DIST = 2.
53. IF(N.GE.2) DIST=10.
54.
55.
56.
57.
58. DO 300 K= 1,KMAX
59. RK =K
60. A = AO*RK
61. SIDE =SQRT(A)
62. DO 400 JSIZ = 1,3
63. IF(JSIZ.EQ.1) KO = KREF
64. IF(JSIZ.EQ.2) KO = KREF/9.
65. IF(JSIZ.EQ.3) KO = KREF/100.
66. DO 400 J=1,JMAX
67. RJ=J
68. KS = KO/(RJ*RJ)
69. ALPHA = ALPHA*KS
70. K1 = (1.+SQRT(1.+4.*KS/(RHO*A)))/2.
71. F = K1/K1 = 1.

```

```

72.      WRITE(LINE,101) KS,ALPHAK,A,K1
73.      101  FORMAT(1H,/,KS = 1E9.3, NT/(M/S)2 = 1.E9.3, LB/(KT)2 ****,
74.      1  'AREA = 1.F9.3, SQ METERS,1.000, 'K1 = 1,
75.      2F9.3, '= RATIO VIN/VS',/)
76.      WRITE(LINE,103)
77.      103  FORMAT(1H,5X,VS(M/S) VS(MTS) BITESLA) L(METERS) CUR(KAMP)
78.      1 VOLTS PRESS(PSI) TH(KNTS) TH(KLBS) EFFICIENCY(8),/)
79.      C
80.      C
81.      DO 500 L = 1,LMAX
82.      C      COMPUTE EFFICIENCY FOR VS = 2, 20 KTS
83.      RL = L*1
84.      VS = VSD*RL
85.      BETAVS = BETA*VS
86.      C
87.      C      CONVERT VS TO KNOTS
88.      C
89.      C
90.      C
91.      C      VZRO = (2.0*SIGMA*(B**2)*DIST)/RHO
92.      EFF = (2.0*KS/(A*RHO))/(F*(VS*F/VZRU +K1))
93.      C
94.      C      HERE WE ARE ASSUMING ASPECT RATIO = 1 ,THEN
95.      C
96.      C      AREA = SIDE**2
97.      C
98.      C
99.      C      CUR = SIDE*RHO*(VS**2)*((K1**2)-1.)/B
100.      C      USE SIDE/2 IN CURRENT EXPRESSION
101.      CUR = CUR/2.
102.      TH = KS*VS**2
103.      THPDS = TH*(4973./31.E3)
104.      VOLT = TH*VS/(CUR*EFF)
105.      DELP = RHO*VS*VS*(K1-K1-1.)/2.
106.      C      CONVERT DELP FROM NT/SQM TO PSI
107.      PSI = DELP*.145E-4
108.      C
109.      C      WRITE(LINE,501) VS,BETAVS,B,DIST,CUR,VOLT,
110.      1PSI,TH,THPDS,EFF
111.      501  FORMAT(1H,3X,4(F9.3,1X),-3PF9.3,1X,OPF9.3,1X,F10.2,1X
112.      12(-3PF9.3,1X),2PF9.3)
113.      C      CONTINUE
114.      500  CONTINUE
115.      400  CONTINUE
116.      C
117.      C      WRITE(LINE,301)
118.      301  FORMAT(1H,/,)
119.      300  CONTINUE
120.      200  CONTINUE
121.      100  CONTINUE
122.      STOP
123.      END
124.      END DATA. ERRORS: NONE. TIME: 0.492 SEC. IMAGE COUNT: 124

```

8FIN

$$\alpha = 4.0 \text{ mhos/m}$$

DATE 072779

PAGE 12

## ELECTROMAGNETIC THRUST PROPULSION

$K_s = .500 \cdot 04 \text{ NT/(M/S)}^2 = .297 \cdot 03 \text{ LB/(KT)}^2$  \*\*\*AREA = 1.000 SQ METERS\*\*\*K1 = 2.791= RATIO VIN/V5

VS(M/S)	VS(KTS)	B(TESLA)	L(METERS)	CUR(KAMP)	VOLTS	PRESS(PSI)	TH(KN/TS)	TH(KLBS)	EFFICIENCY(%)
1.028	2.000	.500	.000	7.177	898.550	.52	5.284	1.189	.084
1.542	3.000	.500	.000	14.148	2020.662	1.17	11.889	2.754	.056
1.542	3.000	.500	.000	28.708	591.331	2.08	21.889	4.928	.042
2.056	4.000	.500	.000	44.856	1078.324	3.25	33.024	7.428	.038
2.056	4.000	.500	.000	89.712	2156.648	4.68	47.555	10.697	.028
3.084	6.000	.500	.000	134.568	3234.972	6.37	64.728	16.040	.021
3.084	6.000	.500	.000	269.136	6469.944	8.33	87.455	24.077	.019
4.112	8.000	.500	.000	403.704	9704.916	10.54	108.999	29.714	.017
4.112	8.000	.500	.000	807.408	19409.832	13.01	132.098	35.953	.015
5.140	10.000	.500	.000	121.104	29114.748	15.74	159.839	42.787	.014
5.140	10.000	.500	.000	242.208	58229.496	21.98	223.246	50.216	.013
6.168	12.000	.500	.000	363.312	87344.244	28.50	288.710	58.655	.011
6.168	12.000	.500	.000	726.624	174688.488	37.40	378.171	76.467	.011
7.196	14.000	.500	.000	448.736	262032.732	48.59	481.763	85.872	.010
7.196	14.000	.500	.000	897.472	524065.464	64.15	642.997	96.272	.009
8.224	16.000	.500	.000	569.584	351169.708	86.06	874.874	107.266	.009
8.224	16.000	.500	.000	1139.168	702339.416	114.03	1159.748	128.534	.008
9.252	18.000	.500	.000	701.280	436708.656	152.03	1528.392	168.854	.008
9.252	18.000	.500	.000	1402.560	873417.312				
10.280	20.000	.500	.000	882.688	509725.896				
10.280	20.000	.500	.000	1765.376	1019451.792				

Full size  
1 Duct

$K_s = .125 \cdot 04 \text{ NT/(M/S)}^2 = .743 \cdot 02 \text{ LB/(KT)}^2$  \*\*\*AREA = 1.000 SQ METERS\*\*\*K1 = 1.725= RATIO VIN/V5

VS(M/S)	VS(KTS)	B(TESLA)	L(METERS)	CUR(KAMP)	VOLTS	PRESS(PSI)	TH(KN/TS)	TH(KLBS)	EFFICIENCY(%)
1.028	2.000	.500	.000	2.087	261.746	.15	1.321	.297	.249
1.542	3.000	.500	.000	4.174	523.492	.34	2.672	.669	.166
1.542	3.000	.500	.000	8.348	1046.984	.61	5.284	1.189	.125
2.056	4.000	.500	.000	12.522	1570.476	.95	8.256	1.857	.100
2.056	4.000	.500	.000	25.044	3140.952	1.36	11.889	2.674	.081
3.084	6.000	.500	.000	18.783	2398.636	1.85	16.182	3.554	.062
3.084	6.000	.500	.000	37.566	4797.272	2.42	21.136	4.607	.055
4.112	8.000	.500	.000	27.424	3477.303	3.06	24.750	5.454	.050
4.112	8.000	.500	.000	54.848	6954.606	4.58	37.024	8.228	.045
5.140	10.000	.500	.000	20.312	2590.188	5.45	39.960	8.988	.042
5.140	10.000	.500	.000	40.624	5180.376	8.30	59.920	13.077	.038
6.168	12.000	.500	.000	15.188	1936.773	8.51	64.728	14.060	.033
6.168	12.000	.500	.000	30.376	3873.546	12.26	94.505	20.917	.029
7.196	14.000	.500	.000	10.712	1377.790	9.68	84.563	18.714	.028
7.196	14.000	.500	.000	21.424	2755.580	10.93	95.461	21.468	.026
8.224	16.000	.500	.000	13.536	1732.022	12.26	106.999	24.068	.025
8.224	16.000	.500	.000	27.072	3464.044	13.62	119.218	26.816	.023
9.252	18.000	.500	.000	16.648	2094.448	15.15	132.098	29.714	.023
9.252	18.000	.500	.000	33.296	4188.896				
10.280	20.000	.500	.000	20.094	2609.448				
10.280	20.000	.500	.000	40.188	5218.896				

4 Ducts

$K_s = .556 \cdot 03 \text{ NT/(M/S)}^2 = .330 \cdot 02 \text{ LB/(KT)}^2$  \*\*\*AREA = 1.000 SQ METERS\*\*\*K1 = 1.398= RATIO VIN/V5

VS(M/S)	VS(KTS)	B(TESLA)	L(METERS)	CUR(KAMP)	VOLTS	PRESS(PSI)	TH(KN/TS)	TH(KLBS)	EFFICIENCY(%)
1.028	2.000	.500	.000	1.007	126.619	.07	.587	.132	.473
1.542	3.000	.500	.000	2.014	253.238	.16	1.174	.264	.316
1.542	3.000	.500	.000	4.028	506.476	.29	2.348	.528	.237
2.056	4.000	.500	.000	6.042	759.714	.46	3.522	.792	.185
2.056	4.000	.500	.000	12.084	1519.428	.66	5.184	1.136	.158
3.084	6.000	.500	.000	9.065	1139.258	.86	7.292	1.618	.136
3.084	6.000	.500	.000	18.130	2278.516	1.29	10.424	2.302	.119
4.112	8.000	.500	.000	12.338	1544.793	1.87	14.678	3.254	.109
4.112	8.000	.500	.000	24.676	3089.586	2.71	21.760	4.806	.096
5.140	10.000	.500	.000	9.380	1151.100	3.81	28.912	6.372	.086
5.140	10.000	.500	.000	18.760	2302.200	5.48	42.848	9.452	.079
6.168	12.000	.500	.000	36.520	4604.400	7.81	58.805	12.952	.073
6.168	12.000	.500	.000	73.040	9208.800	11.26	84.505	18.672	.068
7.196	14.000	.500	.000	24.352	3044.192	15.91	119.218	26.816	.063
7.196	14.000	.500	.000	48.704	6088.384	22.82	172.826	38.428	.059
8.224	16.000	.500	.000	16.461	2061.369	32.59	242.438	53.411	.056
8.224	16.000	.500	.000	32.922	4122.738	46.84	347.413	77.136	.053
9.252	18.000	.500	.000	22.770	2866.406	66.09	496.518	110.697	.050
9.252	18.000	.500	.000	45.540	5732.812	94.11	702.726	155.496	.048
10.280	20.000	.500	.000	30.960	3897.331	133.09	1019.748	228.454	.048
10.280	20.000	.500	.000	61.920	7794.662				

9 Ducts

$K_s = .312 \cdot 03 \text{ NT/(M/S)}^2 = .186 \cdot 02 \text{ LB/(KT)}^2$  \*\*\*AREA = 1.000 SQ METERS\*\*\*K1 = 1.250= RATIO VIN/V5

VS(M/S)	VS(KTS)	B(TESLA)	L(METERS)	CUR(KAMP)	VOLTS	PRESS(PSI)	TH(KN/TS)	TH(KLBS)	EFFICIENCY(%)
1.028	2.000	.500	.000	1.007	126.619	.07	.587	.132	.473
1.542	3.000	.500	.000	2.014	253.238	.16	1.174	.264	.316
1.542	3.000	.500	.000	4.028	506.476	.29	2.348	.528	.237
2.056	4.000	.500	.000	6.042	759.714	.46	3.522	.792	.185
2.056	4.000	.500	.000	12.084	1519.428	.66	5.184	1.136	.158
3.084	6.000	.500	.000	9.065	1139.258	.86	7.292	1.618	.136
3.084	6.000	.500	.000	18.130	2278.516	1.29	10.424	2.302	.119
4.112	8.000	.500	.000	12.338	1544.793	1.87	14.678	3.254	.109
4.112	8.000	.500	.000	24.676	3089.586	2.71	21.760	4.806	.096
5.140	10.000	.500	.000	9.380	1151.100	3.81	28.912	6.372	.086
5.140	10.000	.500	.000	18.760	2302.200	5.48	42.848	9.452	.079
6.168	12.000	.500	.000	36.520	4604.400	7.81	58.805	12.952	.073
6.168	12.000	.500	.000	73.040	9208.800	11.26	84.505	18.672	.068
7.196	14.000	.500	.000	24.352	3044.192	15.91	119.218	26.816	.063
7.196	14.000	.500	.000	48.704	6088.384	22.82	172.826	38.428	.059
8.224	16.000	.500	.000	16.461	2061.369	32.59	242.438	53.411	.056
8.224	16.000	.500	.000	32.922	4122.738	46.84	347.413	77.136	.053
9.252	18.000	.500	.000	22.770	2866.406	66.09	496.518	110.697	.050
9.252	18.000	.500	.000	45.540	5732.812	94.11	702.726	155.496	.048
10.280	20.000	.500	.000	30.960	3897.331	133.09	1019.748	228.454	.048
10.280	20.000	.500	.000	61.920	7794.662				

## ELECTROMAGNETIC THRUST PROPULSION

DATE 072779

PAGE 13

1.028	2.000	.500	2.000	.007	124.619	.07	1.587	.132	.473
1.542	3.000	.500	3.000	.007	124.619	.16	1.521	.269	.516
1.742	4.000	.500	4.000	.007	124.619	.27	1.348	.528	.537
1.842	5.000	.500	5.000	.007	124.619	.46	1.089	.889	.540
1.942	6.000	.500	6.000	.007	124.619	.68	1.022	1.018	.543
2.042	7.000	.500	7.000	.007	124.619	.97	1.022	1.113	.546
2.142	8.000	.500	8.000	.007	124.619	1.17	1.022	1.113	.549
2.242	9.000	.500	9.000	.007	124.619	1.48	1.022	1.113	.552
2.342	10.000	.500	10.000	.007	124.619	1.83	1.022	1.113	.555
2.442	11.000	.500	11.000	.007	124.619	2.21	1.022	1.113	.558
2.542	12.000	.500	12.000	.007	124.619	2.63	1.022	1.113	.561
2.642	13.000	.500	13.000	.007	124.619	3.11	1.022	1.113	.564
2.742	14.000	.500	14.000	.007	124.619	3.67	1.022	1.113	.567
2.842	15.000	.500	15.000	.007	124.619	4.31	1.022	1.113	.570
2.942	16.000	.500	16.000	.007	124.619	5.04	1.022	1.113	.573
3.042	17.000	.500	17.000	.007	124.619	5.87	1.022	1.113	.576
3.142	18.000	.500	18.000	.007	124.619	6.81	1.022	1.113	.579
3.242	19.000	.500	19.000	.007	124.619	7.87	1.022	1.113	.582
3.342	20.000	.500	20.000	.007	124.619	9.04	1.022	1.113	.585
3.442	21.000	.500	21.000	.007	124.619	10.33	1.022	1.113	.588
3.542	22.000	.500	22.000	.007	124.619	11.74	1.022	1.113	.591
3.642	23.000	.500	23.000	.007	124.619	13.27	1.022	1.113	.594
3.742	24.000	.500	24.000	.007	124.619	14.93	1.022	1.113	.597
3.842	25.000	.500	25.000	.007	124.619	16.72	1.022	1.113	.600
3.942	26.000	.500	26.000	.007	124.619	18.64	1.022	1.113	.603
4.042	27.000	.500	27.000	.007	124.619	20.70	1.022	1.113	.606
4.142	28.000	.500	28.000	.007	124.619	22.90	1.022	1.113	.609
4.242	29.000	.500	29.000	.007	124.619	25.25	1.022	1.113	.612
4.342	30.000	.500	30.000	.007	124.619	27.75	1.022	1.113	.615
4.442	31.000	.500	31.000	.007	124.619	30.40	1.022	1.113	.618
4.542	32.000	.500	32.000	.007	124.619	33.20	1.022	1.113	.621
4.642	33.000	.500	33.000	.007	124.619	36.15	1.022	1.113	.624
4.742	34.000	.500	34.000	.007	124.619	39.26	1.022	1.113	.627
4.842	35.000	.500	35.000	.007	124.619	42.53	1.022	1.113	.630
4.942	36.000	.500	36.000	.007	124.619	45.96	1.022	1.113	.633
5.042	37.000	.500	37.000	.007	124.619	49.55	1.022	1.113	.636
5.142	38.000	.500	38.000	.007	124.619	53.30	1.022	1.113	.639
5.242	39.000	.500	39.000	.007	124.619	57.21	1.022	1.113	.642
5.342	40.000	.500	40.000	.007	124.619	61.28	1.022	1.113	.645
5.442	41.000	.500	41.000	.007	124.619	65.51	1.022	1.113	.648
5.542	42.000	.500	42.000	.007	124.619	69.90	1.022	1.113	.651
5.642	43.000	.500	43.000	.007	124.619	74.45	1.022	1.113	.654
5.742	44.000	.500	44.000	.007	124.619	79.16	1.022	1.113	.657
5.842	45.000	.500	45.000	.007	124.619	84.03	1.022	1.113	.660
5.942	46.000	.500	46.000	.007	124.619	89.07	1.022	1.113	.663
6.042	47.000	.500	47.000	.007	124.619	94.38	1.022	1.113	.666
6.142	48.000	.500	48.000	.007	124.619	99.95	1.022	1.113	.669
6.242	49.000	.500	49.000	.007	124.619	105.78	1.022	1.113	.672
6.342	50.000	.500	50.000	.007	124.619	111.87	1.022	1.113	.675
6.442	51.000	.500	51.000	.007	124.619	118.22	1.022	1.113	.678
6.542	52.000	.500	52.000	.007	124.619	124.83	1.022	1.113	.681
6.642	53.000	.500	53.000	.007	124.619	131.70	1.022	1.113	.684
6.742	54.000	.500	54.000	.007	124.619	138.83	1.022	1.113	.687
6.842	55.000	.500	55.000	.007	124.619	146.22	1.022	1.113	.690
6.942	56.000	.500	56.000	.007	124.619	153.87	1.022	1.113	.693
7.042	57.000	.500	57.000	.007	124.619	161.78	1.022	1.113	.696
7.142	58.000	.500	58.000	.007	124.619	169.95	1.022	1.113	.699
7.242	59.000	.500	59.000	.007	124.619	178.38	1.022	1.113	.702
7.342	60.000	.500	60.000	.007	124.619	187.07	1.022	1.113	.705
7.442	61.000	.500	61.000	.007	124.619	196.02	1.022	1.113	.708
7.542	62.000	.500	62.000	.007	124.619	205.23	1.022	1.113	.711
7.642	63.000	.500	63.000	.007	124.619	214.70	1.022	1.113	.714
7.742	64.000	.500	64.000	.007	124.619	224.43	1.022	1.113	.717
7.842	65.000	.500	65.000	.007	124.619	234.42	1.022	1.113	.720
7.942	66.000	.500	66.000	.007	124.619	244.67	1.022	1.113	.723
8.042	67.000	.500	67.000	.007	124.619	255.18	1.022	1.113	.726
8.142	68.000	.500	68.000	.007	124.619	265.95	1.022	1.113	.729
8.242	69.000	.500	69.000	.007	124.619	276.98	1.022	1.113	.732
8.342	70.000	.500	70.000	.007	124.619	288.27	1.022	1.113	.735
8.442	71.000	.500	71.000	.007	124.619	299.82	1.022	1.113	.738
8.542	72.000	.500	72.000	.007	124.619	311.63	1.022	1.113	.741
8.642	73.000	.500	73.000	.007	124.619	323.70	1.022	1.113	.744
8.742	74.000	.500	74.000	.007	124.619	336.03	1.022	1.113	.747
8.842	75.000	.500	75.000	.007	124.619	348.62	1.022	1.113	.750
8.942	76.000	.500	76.000	.007	124.619	361.47	1.022	1.113	.753
9.042	77.000	.500	77.000	.007	124.619	374.58	1.022	1.113	.756
9.142	78.000	.500	78.000	.007	124.619	387.95	1.022	1.113	.759
9.242	79.000	.500	79.000	.007	124.619	401.58	1.022	1.113	.762
9.342	80.000	.500	80.000	.007	124.619	415.47	1.022	1.113	.765
9.442	81.000	.500	81.000	.007	124.619	429.62	1.022	1.113	.768
9.542	82.000	.500	82.000	.007	124.619	444.03	1.022	1.113	.771
9.642	83.000	.500	83.000	.007	124.619	458.70	1.022	1.113	.774
9.742	84.000	.500	84.000	.007	124.619	473.63	1.022	1.113	.777
9.842	85.000	.500	85.000	.007	124.619	488.82	1.022	1.113	.780
9.942	86.000	.500	86.000	.007	124.619	504.27	1.022	1.113	.783
10.042	87.000	.500	87.000	.007	124.619	519.98	1.022	1.113	.786
10.142	88.000	.500	88.000	.007	124.619	535.95	1.022	1.113	.789
10.242	89.000	.500	89.000	.007	124.619	552.18	1.022	1.113	.792
10.342	90.000	.500	90.000	.007	124.619	568.67	1.022	1.113	.795
10.442	91.000	.500	91.000	.007	124.619	585.42	1.022	1.113	.798
10.542	92.000	.500	92.000	.007	124.619	602.43	1.022	1.113	.801
10.642	93.000	.500	93.000	.007	124.619	619.70	1.022	1.113	.804
10.742	94.000	.500	94.000	.007	124.619	637.23	1.022	1.113	.807
10.842	95.000	.500	95.000	.007	124.619	655.02	1.022	1.113	.810
10.942	96.000	.500	96.000	.007	124.619	673.07	1.022	1.113	.813
11.042	97.000	.500	97.000	.007	124.619	691.38	1.022	1.113	.816
11.142	98.000	.500	98.000	.007	124.619	709.95	1.022	1.113	.819
11.242	99.000	.500	99.000	.007	124.619	728.78	1.022	1.113	.822
11.342	100.000	.500	100.000	.007	124.619	747.87	1.022	1.113	.825
11.442	101.000	.500	101.000	.007	124.619	767.22	1.022	1.113	.828
11.542	102.000	.500	102.000	.007	124.619	786.83	1.022	1.113	.831
11.642	103.000	.500	103.000	.007	124.619	806.70	1.022	1.113	.834
11.742	104.000	.500	104.000	.007	124.619	826.83	1.022	1.113	.837
11.842	105.000	.500	105.000	.007	124.619	847.22	1.022	1.113	.840
11.942	106.000	.500	106.000	.007	124.619	867.87	1.022	1.113	.843
12.042	107.000	.500	107.000	.007	124.619	888.78	1.022	1.113	.846
12.142	108.000	.500	108.000	.007	124.619	909.95	1.022	1.113	.849
12.242	109.000	.500	109.000	.007	124.619	931.38	1.022	1.113	.852
12.342	110.000	.500	110.000	.007	124.619	953.07	1.022	1.113	.855
12.442	111.000	.500	111.000	.007	124.619	974.92	1.022	1.113	.858
12.542	112.000	.500	112.000	.007	124.619	997.03	1.022	1.113	.861
12.642	113.000	.500	113.000	.007	124.619	1019.40	1.022	1.113	.864
12.742	114.000	.500	114.000	.007	124.619	1042.03	1.022	1.113	.867
12.842	115.000	.500	115.000	.007	124.619	1064.92	1.022	1.113	.870
12.942	116.000	.500	116.000	.007	124.619	1088.07	1.022	1.113	.873
13.042	117.000	.500	117.000	.007	124.619	1111.48	1.022	1.113	.876
13.142	118.000	.500	118.000	.007	124.619	1135.15	1.022	1.11	



## ELECTROMAGNETIC THRUST PROPULSION

DATE 072779

PAGE 14

3.084	6.000	.500	2.000	1.142	144.343	.08	.587	.132	1.098
4.118	7.000	.500	2.000	1.526	194.177	.11	.799	.180	.943
5.152	8.000	.500	2.000	2.050	255.920	.15	1.044	.232	.858
6.226	9.000	.500	2.000	2.569	331.593	.19	1.321	.292	.792
7.340	10.000	.500	2.000	3.172	427.177	.23	1.628	.367	.742
8.534	11.000	.500	2.000	3.868	547.188	.28	1.973	.444	.692
9.818	12.000	.500	2.000	4.659	697.579	.33	2.358	.528	.652
11.192	13.000	.500	2.000	5.540	879.899	.39	2.784	.620	.620
12.666	14.000	.500	2.000	6.517	1095.148	.46	3.251	.718	.592
14.240	15.000	.500	2.000	7.587	1354.737	.53	3.759	.825	.562
15.914	16.000	.500	2.000	8.753	1659.148	.60	4.313	.939	.532
17.688	17.000	.500	2.000	10.019	1999.473	.68	4.913	1.060	.502
19.562	18.000	.500	2.000	11.389	2386.473	.75	5.567	1.189	.472
21.536	19.000	.500	2.000	12.867	2820.340	.83	6.273	1.326	.442
23.710	20.000	.500	2.000	14.450	3311.340	.92	7.033	1.467	.412

$$K_s = .347 \times 10^2 \text{ NT/(M/S)}^2 = .206 \times 10^1 \text{ LB/(KT)}^2 \quad \text{--- AREA} = 1.000 \text{ SQ METERS --- K1} = 1.034 \text{--- RATIO VIN/VS}$$

VS(M/S)	VS(KTS)	B(TESLA)	L(METERS)	CUR(KAMP)	VOLTS	PRESS(PSI)	TH(KNTS)	TH(KLBS)	EFFICIENCY(%)
1.028	2.000	.500	2.000	.072	9.556	.01	.037	.008	5.468
1.542	3.000	.500	2.000	.102	21.102	.01	.083	.019	3.714
2.056	4.000	.500	2.000	.160	51.160	.02	.147	.033	2.812
2.570	5.000	.500	2.000	.231	117.731	.03	.229	.052	2.029
3.084	6.000	.500	2.000	.310	188.833	.04	.340	.074	1.489
3.598	7.000	.500	2.000	.400	274.508	.05	.480	.101	1.077
4.112	8.000	.500	2.000	.500	385.148	.06	.647	.132	.826
4.626	9.000	.500	2.000	.616	531.607	.08	.939	.167	.642
5.140	10.000	.500	2.000	.753	728.068	.11	1.321	.210	.502
5.654	11.000	.500	2.000	.914	1007.579	.13	1.810	.266	.412
6.168	12.000	.500	2.000	1.100	1386.734	.16	2.450	.337	.356
6.682	13.000	.500	2.000	1.316	1911.811	.22	3.321	.439	.288
7.196	14.000	.500	2.000	1.567	2649.498	.26	4.568	.568	.240
7.710	15.000	.500	2.000	1.844	3611.607	.33	6.273	.718	.200
8.224	16.000	.500	2.000	2.146	4949.148	.42	8.669	.896	.170
8.738	17.000	.500	2.000	2.481	6728.473	.53	11.896	.109	.140
9.252	18.000	.500	2.000	2.844	9149.498	.67	16.273	.146	.110
9.766	19.000	.500	2.000	3.240	12499.752	.83	22.284	.189	.080
10.280	20.000	.500	2.000	3.672	17111.340	.92	30.587	.232	.050

$$K_s = .500 \times 10^2 \text{ NT/(M/S)}^2 = .297 \times 10^1 \text{ LB/(KT)}^2 \quad \text{--- AREA} = 1.000 \text{ SQ METERS --- K1} = 1.048 \text{--- RATIO VIN/VS}$$

VS(M/S)	VS(KTS)	B(TESLA)	L(METERS)	CUR(KAMP)	VOLTS	PRESS(PSI)	TH(KNTS)	TH(KLBS)	EFFICIENCY(%)
1.028	2.000	.500	2.000	.103	13.447	.01	.053	.012	3.911
1.542	3.000	.500	2.000	.147	29.853	.02	.119	.027	2.643
2.056	4.000	.500	2.000	.206	67.731	.03	.211	.048	1.996
2.570	5.000	.500	2.000	.281	152.027	.05	.330	.074	1.403
3.084	6.000	.500	2.000	.372	217.706	.07	.476	.107	1.040
3.598	7.000	.500	2.000	.480	300.019	.09	.647	.140	.808
4.112	8.000	.500	2.000	.605	408.697	.12	.939	.189	.642
4.626	9.000	.500	2.000	.753	561.148	.16	1.321	.241	.502
5.140	10.000	.500	2.000	.924	772.458	.21	1.810	.307	.412
5.654	11.000	.500	2.000	1.128	1063.953	.27	2.450	.388	.356
6.168	12.000	.500	2.000	1.367	1459.498	.34	3.321	.496	.288
6.682	13.000	.500	2.000	1.644	2007.579	.42	4.568	.620	.240
7.196	14.000	.500	2.000	1.960	2749.498	.53	6.273	.761	.200
7.710	15.000	.500	2.000	2.316	3728.473	.67	8.669	.919	.170
8.224	16.000	.500	2.000	2.714	5049.148	.83	11.896	1.189	.140
8.738	17.000	.500	2.000	3.155	6977.249	.92	16.273	1.567	.110
9.252	18.000	.500	2.000	3.635	9511.340	.98	22.284	2.060	.080
9.766	19.000	.500	2.000	4.150	12966.280	.98	30.587	2.667	.050
10.280	20.000	.500	2.000	4.702	17911.340	.98	40.587	3.392	.020

$$K_s = .125 \times 10^2 \text{ NT/(M/S)}^2 = .743 \times 10^0 \text{ LB/(KT)}^2 \quad \text{--- AREA} = 1.000 \text{ SQ METERS --- K1} = 1.012 \text{--- RATIO VIN/VS}$$

VS(M/S)	VS(KTS)	B(TESLA)	L(METERS)	CUR(KAMP)	VOLTS	PRESS(PSI)	TH(KNTS)	TH(KLBS)	EFFICIENCY(%)
1.028	2.000	.500	2.000	.059	3.803	.00	.013	.003	13.600
1.542	3.000	.500	2.000	.083	8.166	.00	.030	.007	9.500
2.056	4.000	.500	2.000	.105	14.170	.00	.053	.012	7.299
2.570	5.000	.500	2.000	.134	18.115	.01	.083	.019	5.927
3.084	6.000	.500	2.000	.164	24.102	.01	.119	.027	4.988
3.598	7.000	.500	2.000	.200	32.229	.02	.162	.036	4.307
4.112	8.000	.500	2.000	.240	44.598	.03	.211	.046	3.789
4.626	9.000	.500	2.000	.284	59.808	.04	.267	.060	3.382

9 DUCTS

16 DUCTS

TENTH-  
SIZE

1 DUCT

4 DUCTS





DISTRIBUTION LIST

Office of Naval Research  
800 North Quincy St.  
Arlington, VA 22217  
LCDR H. P. Martin, Code 211

(3 copies)

Office of Naval Research  
800 North Quincy St.  
Arlington, VA 22217  
Mr. John Satkowski, Code 473

(1 copy)

Naval Sea Systems Command  
Washington, DC 20360  
CDR R. K. Watterson, Code 924A3

(1 copy)

Director  
Naval Research Laboratory  
Washington, DC 20375, Code 2627

(6 copies)

David W. Taylor Naval Ship Research  
and Development Center  
Bethesda, MD 20084  
Dr. Robert Allen, Code 012

(1 copy)

Office of Naval Research  
800 North Quincy St.  
Arlington, VA 22217, Code 102IP

(6 copies)

Naval Ship Engineering Center  
Washington, DC 20360  
Mr. D. Toffolo, Code 6157C

(1 copy)

Defense Documentation Center  
Bldg. 5 Cameron Station  
Alexandria, VA 22314

(12 copies)

Naval Material Command  
Washington, DC 20360  
Mr. O. J. Remson, MAT 08T23

(1 copy)

Office of Naval Research Branch  
Boston Branch  
495 Summer Street  
Boston, MA 02210

(1 copy)

David W. Taylor Naval Ship Research  
and Development Center  
Bethesda, MD 20084  
Mr. R. M. Stevens, Code 117

(1 copy)

Naval Sea Systems Command  
Washington, DC 20360  
Mr. C. L. Miller, Code 0331

(1 copy)

David W. Taylor Naval Ship Research  
and Development Center  
Annapolis, MD 21402  
Dr. Earl Quandt, Code 272

(1 copy)

Strategic Project Office  
NSP-200  
Washington, DC 20360  
CAPT J. P. Williamson, Jr.

(1 copy)